TITLE PAGE

A Long-Snouted Marine Bonytongue (Teleostei: Osteoglossidae) from the Early Eocene of Morocco and the Phylogenetic Affinities of Marine Osteoglossids

ALESSIO CAPOBIANCO[1,2,3,4], SAMIR ZOUHRI[5] and MATT FRIEDMAN[3,4]

[1]GeoBio-Center LMU, Ludwig-Maximilians-Universität München, Munich, Germany

[2]Department of Earth and Environmental Sciences, Palaeontology & Geobiology, Ludwig-Maximilians-Universität München, Munich, Germany

[3]Department of Earth and Environmental Sciences, University of Michigan, Ann Arbor, MI, USA

[4]Museum of Paleontology, University of Michigan, Ann Arbor, MI, USA

[5]Department of Geology and Health and Environment Laboratory, Hassan II University of Casablanca, Casablanca, Morocco

ZooBank LSID: urn:lsid:zoobank.org:pub:83110660-6D3B-438F-855A-9B50EE14F78B

ABSTRACT

Osteoglossid bonytongues (arapaimas, arowanas, and relatives) are extant tropical freshwater fishes with a relatively abundant and diverse fossil record. Most osteoglossid fossils come from a 25-million-year interval in the early Palaeogene, when these fishes were distributed worldwide in both freshwater and marine environments. Despite their biogeographic and palaeoecological relevance, and a relative abundance of well-preserved material, the evolutionary relationships between these Palaeogene forms and extant bonytongues remain unclear. Here we describe a new genus of bonytongue from early Eocene marine deposits of Morocco, represented by an articulated, three-dimensionally preserved skull with associated pectoral girdle. This taxon is characterized by an elongated snout, contrasting with the short jaws usually found in marine representatives of the clade. A revision of morphological characters in bonytongues allows us to place this new genus, together with other marine and freshwater Eocene taxa, within crown osteoglossids and closely related to extant arapaimines. The discovery of the new Moroccan taxon hints at a previously underestimated eco-morphological diversity of marine bonytongues, highlighting the diverse trophic niches that these fishes occupied in early Palaeogene seas.

ADDITIONAL KEYWORDS: computed tomography, fish, fossil evidence, Palaeogene, phylogeny, Osteoglossoidei

INTRODUCTION

The Osteoglossomorpha (bonytongue fishes) are one of the earliest diverging clades of crown teleost fishes (Arratia, 1997), with a long evolutionary history that extends to at least the Middle Jurassic (Capobianco and Friedman, 2019). The low species diversity of modern osteoglossomorphs contrasts with their remarkable diversity of form (i.e., disparity), ranging from the unassuming mooneyes to the gigantic arapaima to the electrical elephantfishes. Despite this disparity, all extant species are ecologically restricted to freshwater environments (a few species of notopterid knifefishes are occasionally found in brackish waters; Berra, 2007) in mostly tropical areas with the exception of two species of temperate-adapted mooneyes. In contrast to most groups of tropical freshwater fishes, osteoglossomorphs are known from numerous fossil species, many of which are represented by relatively well-preserved, articulated specimens. In fact, extinct bonytongue genera surpass extant ones in number (Murray and Wilson, 2008; Hilton and Lavoué, 2018).

Perhaps the most surprising feature of paleontological record of bonytongues is the presence of several fossils (including well-preserved, articulated skeletons) in marine deposits worldwide (see Capobianco *et al*., 2021 for a review of marine osteoglossomorph occurrences). The quantity and preservational quality of these specimens, as well as the range of marine environments represented by these deposits (ranging from estuarine and lagoonal to offshore pelagic), suggest that their presence in marine depositional settings is not an artifact of taphonomic processes like post-mortem transport. Remarkably, these marine occurrences are narrowly restricted to a ~25-million-year interval in the early Palaeogene (with few dubious exceptions; see Capobianco *et al*., 2021). Although fossil marine bonytongues have been known for almost two centuries (Agassiz, 1845; Woodward, 1901), their taxonomic diversity and widespread geographic distribution have become apparent only in the last two decades (Taverne, 1998; Bonde, 2008; Forey and Hilton, 2010). Several of these marine forms can be

confidently assigned to the osteoglossomorph sub-clade Osteoglossidae (*sensu* Forey and Hilton, 2010) due to the presence of anatomical features diagnostic of the family (Forey and Hilton, 2010; Hilton and Lavoué, 2018; Capobianco and Friedman, 2019).

The Osteoglossidae currently include only four genera and around 10 species, distributed in tropical freshwater areas worldwide. Within Osteoglossidae, two distinct clades can be recognized: Osteoglossinae and Arapaiminae. The former comprise the South American *Osteoglossum* Cuvier, 1829 and the Southeast Asian and northern Oceanian *Scleropages* Günther, 1864, whereas the latter comprise the South American *Arapaima* Müller, 1843 and the African *Heterotis* Rüppell, 1828. The disjunct geographic distribution of extant osteoglossids has sparked the interest of several researchers investigating underlying biogeographic processes. Time-calibrated molecular and total-evidence phylogenies suggest that the divergences between extant genera postdate major breakups of the Gondwanan supercontinent (such as the separation between West Gondwana and East Gondwana during the Late Jurassic–Early Cretaceous, or the South America–Africa breakup in the Early Cretaceous; Blakey, 2008), implying that continental vicariance is an unlikely explanation for the current distribution of osteoglossids (Lavoué, 2015; 2016). The fossil record of Osteoglossinae and Arapaiminae is consistent with these results, but caution should be applied when interpreting it at face value due to incompleteness. Fossil osteoglossines belonging to the genus *Scleropages* are known from complete articulated specimens from the early Eocene of China (Zhang and Wilson, 2017; Zhang, 2020) and putatively from fragmentary remains in the middle Paleocene of Belgium (Taverne *et al*., 2007), whereas *Osteoglossum* is unknown from the fossil record. Remains of fossil arapaimines are mostly fragmentary, with fragments of *Heterotis* found in Afro-Arabian deposits of at most Oligocene age (Otero and Gayet, 2001; Otero *et al*., 2017), and specimens of *Arapaima* known from the Miocene of Brazil (Lundberg and Chernoff, 1992). The earliest putative occurrence of arapaimines consists of jaw fragments

and squamules from the latest Cretaceous (Maastrichtian) El Molino Formation of Bolivia (Gayet and Meunier, 1998; Gayet *et al*., 2001). This material was attributed to indeterminate arapaimines, but its identity remains uncertain. These incomplete remains are potentially joined by articulated fossils of *Sinoglossus* Su, 1986 from the late Eocene–Oligocene Lushan Formation of China. This taxon has been surprisingly recovered as an arapaimine in phylogenetic analyses of bonytongues (Murray and Wilson, 2008). The presence of a freshwater arapaimine in continental Asia adds complexity to the biogeographic history of this clade, and it is difficult to interpret from a purely vicariant perspective.

In addition to the scarce record of osteoglossines and arapaimines, the fossil record of Osteoglossidae contains several taxa (including the marine forms) that cannot be easily placed in either of the two extant sub-clades. The most well-studied of these is the freshwater †*Phareodus* Leidy, 1873, known from hundreds of complete specimens from the early middle Eocene (Wasatchian–Bridgerian North American Land Mammal Ages, overlapping the Ypresian and Lutetian of the global timescale) Green River Formation of Wyoming and Utah, USA, where it is represented by two distinct species, †*P. encaustus* Cope, 1871 and †*P. testis* Cope, 1877 (Li *et al*., 1997a). Other species referred to †*Phareodus* are found in the Ypresian Yangxi Formation of China (†*P. songziensis* Zhang, 2003) and in the late Paleocene–early Eocene Redbank Plains Formation of Australia (†*P. queenslandicus* Hills, 1934; Li, 1994). Alvarado-Ortega *et al*. (2015) report a potential marine representative of †*Phareodus* in the Danian Tenejapa Formation of Mexico, but further study is needed to confirm its generic status. Several taxa similar to †*Phareodus* have been described from both freshwater and marine deposits around the world. Among these, the marine †*Brychaetus* Woodward, 1901 (Ypresian) and the freshwater †*Musperia* Sanders, 1934 (Eocene, age indeterminate) were included, together with the aforementioned †*Phareodus*, in an osteoglossid subclade coined †Phareodontinae by Taverne (1979). The diagnosis of this taxon includes several osteological

features, such as a relatively short skull and jaws, a lateral expansion of the frontal, an elongation of the occipital region of the neurocranium, the presence of a paired dorso-occipital depression or fossa, an autogenous articular and a third infraorbital smaller than the fourth one (Taverne, 1979). Other fossil bonytongues have been subsequently proposed to belong to †Phareodontinae: the freshwater †*Cretophareodus* Li, 1996 (Campanian), †*Phareodusichthys* Gayet, 1991 (Maastrichtian–Danian) and †*Taverneichthys* Kumar *et al*., 2005 (Paleocene, age indeterminate), and the marine †*Ridewoodichthys* Taverne, 2009 (Selandian) (Forey and Hilton, 2010). These are joined by a variety of marine taxa that might be included in this clade, or be closely related to it: †*Magnigena* Forey and Hilton, 2010 (Thanetian), †*Brychaetoides* Bonde, 2008 (earliest Ypresian), †*Xosteoglossid* Bonde, 2008 (earliest Ypresian), †*Monopteros* Volta, 1806 (Ypresian), †*Opsithrissops* Danil'chenko, 1968 (Paleocene–Eocene thermal maximum) and a few unnamed taxa (Forey and Hilton, 2010; Hilton and Lavoué, 2018). However, most species included in or referred to †Phareodontinae have never been added to a formal phylogenetic analysis, and their systematic placement remains dubious. Additionally, there are other marine bonytongues that might not be related to †phareodontines or even to osteoglossids (Hilton and Lavoué, 2018). Among these, †*Furichthys* Bonde, 2008 from the earliest Eocene Fur Formation of Denmark was described as a basal osteoglossiform by Bonde (2008) and is unique among marine bonytongues for its elongated preorbital region of the skull (or snout), contrasting with the short-snouted condition seen in †phareodontines as described by Taverne (1979).

The existence of several different forms of marine bonytongues in the early Palaeogene has been linked to the hypothesis of marine dispersal as main driver of the current disjunct distribution of osteoglossids (Patterson, 1975; Bonde, 2008; Hilton and Lavoué, 2018; Capobianco and Friedman, 2019). However, the lack of a robust phylogenetic framework for marine bonytongues has precluded a test of this hypothesis. Phylogenetic relationships are

uncertain even for fossil osteoglossids known from numerous well-preserved specimens, such as †*Phareodus* and †*Brychaetus*. Past studies recovered †*Phareodus* as sister-taxon to osteoglossines (Lavoué, 2016), sister-taxon to arapaimines (Wilson and Murray, 2008), as a stem osteoglossid (Murray *et al*., 2018), or closely related to the butterflyfish *Pantodon* Peters 1876 (Hilton, 2003). This uncertainty stems mainly from the peculiar mix of osteoglossine-like and arapaimine-like characters of †*Phareodus*, and the difficulty of inferring which of these are plesiomorphic for osteoglossids. Selection of taxa and characters employed in phylogenetic analyses has also been shown to have a strong influence on the position of fossil taxa in the osteoglossomorph tree (Murray *et al*., 2018). †*Brychaetus* has been interpreted as very closely related to †*Phareodus*, to the point of the former being considered a junior synonym of the latter (Li *et al*., 1997a). However, recent works on bonytongue systematics do not include †*Brychaetus* (Hilton, 2003; Wilson and Murray, 2008; Murray *et al*., 2018).

Here we describe a new genus and species of osteoglossid from early Eocene marine deposits of Morocco, based on a three-dimensionally preserved and articulated skull with pectoral girdle. This taxon bears some similarity with the Danish †*Furichthys* in having an elongated preorbital region and a long lower jaw, probably indicative of a feeding ecology very distinct from that of other short-faced marine bonytongues. New anatomical observations, as well as the reexamination of key taxa such as †*Phareodus*, †*Brychaetus*, and †*Furichthys*, strongly suggest that the new species clusters with other fossil bonytongues (both marine and freshwater) as sister-group to the arapaimines. This widely distributed and ecomorphologically diverse clade of bonytongues points to an unexpected radiation of these fishes in the early Palaeogene, possibly as a consequence of ecological opportunity and release after the Cretaceous/Palaeogene (K/Pg) mass extinction.

MATERIALS AND METHODS

Micro-computed tomography

The holotype of †*Macroprosopon hiltoni* gen. et sp. nov., as well as comparative material of extinct and extant osteoglossomorphs, was imaged using a Nikon XT H 225ST industrial µCT scanner at the University of Michigan CTEES facility (Computed Tomography in Earth & Environmental Sciences). Individual scanning parameters are given below:

†*Macroprosopon hiltoni* gen. et sp. nov., FSAC CP 330. Voltage, 215 kV, current, 109 µA; filter, 2.5 mm copper; reflection target, tungsten; effective voxel size, 122.7 µm. Additional scans were performed on smaller regions of interest of the specimen, with effective voxel sizes ranging from 40.3 to 64.0 µm. µCT data available at: [insert DOI(s) here]

†*Brychaetus muelleri* Woodward, 1901, NHMUK PV P641. Voltage, 190 kV; current, 305 µA; filter, 2.7 mm copper; reflection target, tungsten; effective voxel size, 62.9 µm. µCT data available at: https://doi.org/10.17602/M2/M582142

cf. †*Brychaetus* sp., NHMUK PV P26758. Voltage, 200 kV; current, 205 µA; filter, 2.1 mm copper; reflection target, tungsten; effective voxel size, 42.7 µm. µCT data available at: https://doi.org/10.17602/M2/M582160

†*Phareodus encaustus*, FMNH PF 11947. Voltage, 210 kV; current, 115 µA; filter, 1.0 mm copper; reflection target, tungsten; effective voxel size, 92.2 µm. µCT data available at: https://doi.org/10.17602/M2/M581465

†*Phareodus encaustus*, FMNH PF 11949. Voltage, 200 kV; current, 108 µA; filter, 1.5 mm copper; reflection target, tungsten; effective voxel size, 73.9 µm. µCT data available at: https://doi.org/10.17602/M2/M581470. Both scans of †*Phareodus encaustus* specimens were not particularly informative, as these fossils from Green River Formation are extremely

flattened and their depth is not sufficient to distinguish relevant anatomical features in tomograms.

Hiodon tergisus Lesueur, 1818, UMMZ 247425. Voltage, 110 kV; current, 165 µA; filter, none; reflection target, tungsten; effective voxel size, 40.9 µm. µCT data available at: [insert DOI here]

Chitala blanci d'Aubenton, 1965, UMMZ 232272. Voltage, 180 kV; current, 170 µA; filter, none; reflection target, tungsten; effective voxel size, 47.2 µm. µCT data available at: [insert DOI here]

Petrocephalus simus Sauvage, 1879, UMMZ 200167. Voltage, 55 kV; current, 195 µA; filter, none; reflection target, tungsten; effective voxel size, 12.5 µm. µCT data available at: [insert DOI here]

Pantodon buchholzi Peters, 1876, UMMZ 249782. Voltage, 65 kV; current, 195 µA; filter, none; reflection target, tungsten; effective voxel size, 14.9 µm. µCT data available at: [insert DOI here]

Heterotis niloticus Cuvier, 1829, UMMZ 195004. Voltage, 105 kV; current, 155 µA; filter, 0.1 mm copper; reflection target, tungsten; effective voxel size, 35.8 µm. µCT data available at: [insert DOI here]

Scans were acquired using Inspect-X and reconstructed using CT Pro 3-D (Nikon Metrology, USA). Additionally, reconstructed tomograms for *Arapaima gigas* Schinz, 1822, UF 33107 (Morphosource media M51346) and *Osteoglossum bicirrhosum* Cuvier, 1829, UF 189007 (Morphosource media M26520) were downloaded from Morphosource.

Reconstructed datasets were visualized and segmented using Mimics v. 19.0 (Materialise, Belgium). Models of segmented skeletal elements were exported as surface files (.ply) and rendered as high-quality images in Blender v. 3.5.1 (blender.org).

Fossil preparation

Mechanical preparation of FSAC CP 330 was conducted by Dr. William Sanders (chief vertebrate preparator, UMMP), using mounted carbide needles under a binocular microscope.

Specimens examined

In addition to the material listed above, the following skeletonized specimens of extant taxa and fossil specimens of extinct taxa belonging to Osteoglossomorpha were examined as comparative material:

Arapaima gigas UMMZ 177540, UMMZ 203831; †*Brychaetus muelleri* NHMUK PV 39448, NHMUK PV 39699, NHMUK PV P638, NHMUK PV P641, NHMUK PV P1748, NHMUK PV P3893, NHMUK PV P66889, SM C 21208, SM C 21209; cf. †*Brychaetus* sp. NHMD 28907, NHMUK PV P26758, NHMUK PV P66355; †*Brychaetus*? sp. NHMUK PV P73087, NHMUK PV P73088; †*Furichthys fieldsoei* Bonde, 2008, FUM-N 1440, FUM-N 1848A; *Heterotis niloticus* UMMZ 213845; *Hiodon tergisus* UMMZ 180315; *Marcusenius macrolepidotus* Peters, 1852, UMMZ 200066; *Mormyrus lacerda* Castelnau, 1861, UMMZ 200084; *Osteoglossum bicirrhosum* UF 189007, UMMZ 203832; †*Phareodus encaustus* AMNH 4587, AMNH 19441, FMNH PF 10237, FMNH PF 10255, FMNH PF 10256, FMNH PF 10257, FMNH PF 10285, FMNH PF 11946, FMNH PF 12683, FMNH PF 13321, FMNH PF 16527, FMNH PF 16528, FMNH PF 16529, FMNH PF 16538, NHMUK PV P64636I-II;

†*Phareodus testis* FMNH PF 11942, FMNH PF 16535, FMNH PF 16536, FMNH PF 16540, FMNH PF 17493, FMNH PF 17496, FMNH PF 17500, NHMUK PV P61230; *Scleropages formosus* Müller and Schlegel, 1840, UMMZ 203833, UMMZ 213853.

Phylogenetic analysis

The phylogenetic analysis performed in this study draws on the morphological character dataset by Murray *et al.* (2018), with modifications listed below. This dataset is itself the latest iteration of a character matrix first assembled by Wilson and Murray (2008) by combining the matrices of Li *et al.* (1997b) and Hilton (2003); it has been modified subsequently in several descriptive studies on fossil osteoglossomorphs (Murray *et al.*, 2010; 2016; 2018). The taxa included in this analysis are mostly the same as those included by Murray *et al.* (2018), with the following exceptions. †*Tanolepis* Jin, 1994 was excluded because of its potential synonymy with †*Paralycoptera* Chang and Chou, 1977 and because of our inability to verify the scoring of its characters in the matrix (see "*Rescoring of* †*Paralycoptera and exclusion of* †*Tanolepis*" in Results). †*Ostariostoma* Schaeffer, 1949 was also excluded from the analysis because its bonytongue affinities are questionable, as some of its anatomical features would be unique among osteoglossomorphs and its vertebral morphology is more concordant with a basal ostariophysan identification (Murray *et al.*, 2018). A broader taxonomic sampling outside Osteoglossomorpha would be needed to test the phylogenetic affinities of †*Ostariostoma*, which is beyond the scope of this paper. We added to the Murray *et al.* (2018) character matrix the recently redescribed †*Laeliichthys* Santos, 1985 from the Early Cretaceous of Brazil, using the scoring of Brito *et al.* (2020) plus the additional characters added for this study. This taxon was originally described as a close relative to arapaimines (Taverne, 1979), but it has been recently reinterpreted as the sister taxon to notopterid knifefishes (Brito *et al.*, 2020). Apart

from the new taxon described here, we included two additional marine bonytongues, †*Brychaetus* and †*Furichthys*, and based their character scoring on direct observation of specimens, literature, and μCT data (for †*Brychaetus*). Whereas Wilson and Murray (2008) and most subsequent iterations of their character matrix lumped three mormyrid genera (*Petrocephalus* Marcusen, 1854, *Gnathonemus* Gill, 1863 and *Campylomormyrus* Bleeker, 1874) into the Operational Taxonomic Unit (OTU) 'Mormyroidea' and three notopterid genera (*Chitala* Fowler, 1934, *Xenomystus* Günther, 1868 and *Papyrocranus* Greenwood, 1963) into the OTU 'Notopteridae', we decided to keep these taxa distinct at genus level in our analysis. As in Murray *et al*. (2018), we included *Amia* Linnaeus, 1766, †Ellimmichthyiformes, Clupeiformes, and *Elops* Linnaeus, 1766 as our sample of non-osteoglossomorphs. Because the character scoring for Clupeiformes in Murray *et al*. (2018) is based exclusively on the anatomy of *Dorosoma cepedianum* Lesueur, 1818 (as described and figured in Grande, 1985), we changed the name of that OTU from 'Clupeiformes' to '*Dorosoma*'. The extant holostean *Amia calva* Linnaeus, 1766 was selected as the outgroup to all other taxa included in the analysis (that is, all trees were rooted *a posteriori* on *Amia*). The data matrix, which ultimately comprised 96 characters for 34 taxa, was assembled and edited in Mesquite v. 3.61 (Maddison and Maddison, 2019).

For phylogenetic reconstruction, the character matrix was analyzed through maximum parsimony (MP), maximum likelihood (ML) and Bayesian approaches. The MP analysis was performed in PAUP* v. 4.0a169 (Swofford, 2002). All characters were designated as unweighted and unordered, except for character 96 (number of branchiostegal rays), which was ordered along a numerical morphocline. Multiple states of a character in a single taxon were treated as polymorphisms. MP trees were found with a heuristic search, using random stepwise addition (100 replicates, 10 trees held at each step) and tree-bisection-reconnection branch swapping algorithm. Support for the results of the MP analysis was evaluated by calculating

Bremer decay indices for every node. Additionally, 1000 bootstrap replicates were run and visualized with a bootstrap consensus tree including all groups compatible with the 50% majority-rule consensus tree.

The ML analysis was performed in IQ-TREE, using its dedicated web server (Trifinopoulos *et al*., 2016). The Mkv model (Markov k model with only variable characters) was used as model of character evolution. A gamma-distributed rate model with four rate categories was used to account for rate variability across characters. Node support was evaluated with 1000 ultrafast bootstrap (Hoang *et al*., 2018) replicates.

The Bayesian phylogenetic analysis was conducted in MrBayes v. 3.2.7 (Ronquist *et al*., 2012). As in the ML analysis, an Mkv model with gamma-distributed rates (four rate categories) was chosen for the analysis. Like in the MP analysis, character 96 was set as ordered. Two simultaneous analyses were run for 10 million generations, sampling every 1000 generations. Maximum standard deviation of split frequencies between the two runs reached <0.02 after 2 million generations, indicating good convergence. The first 25% of sampled trees and parameters were discarded as burn-in. Posterior probabilities were visualized on a consensus majority-rule tree showing all compatible partitions.

All phylogenetic trees were visualized using FigTree v. 1.4.4 (Rambaut, 2012).

Institutional abbreviations

FMNH, The Field Museum, Chicago, IL, USA; FSAC CP, Faculté des Sciences Aïn Chock, collection phosphates; FUM, Fur Museum, Fur, Denmark; NHMD, Natural History Museum of Denmark, Copenhagen, Demark; NHMUK, The Natural History Museum, London, UK; SM, Sedgwick Museum of Earth Sciences, Cambridge, UK; UF, Florida Museum, Gainesville,

FL, USA; UMMP, University of Michigan Museum of Paleontology, Ann Arbor, MI, USA; UMMZ, University of Michigan Museum of Zoology, Ann Arbor, MI, USA.

Dagger symbols

Following the convention of Patterson and Rosen (1977), the dagger symbol (†) precedes extinct taxa.

SYSTEMATIC PALAEONTOLOGY

TELEOSTEI MÜLLER, 1845

OSTEOGLOSSOMORPHA GREENWOOD, ROSEN, WEITZMAN AND MYERS, 1966

OSTEOGLOSSIFORMES BERG, 1940

OSTEOGLOSSIDAE BERG, 1940

†PHAREODONTINAE TAVERNE, 1979

†*MACROPROSOPON* Capobianco *et al.*, **GEN. NOV.**

ZooBank LSID: urn:lsid:zoobank.org:act:0D894681-7DF7-4892-8198-D37EFFBCA20D

Type species: †*Macroprosopon hiltoni* (monotypic)

Etymology: Generic name from the combination of the Ancient Greek *makrós* ('long') and *prósōpon* ('face'), referring to the elongated snout.

Diagnosis: As for the type species.

†***MACROPROSOPON HILTONI*** Capobianco *et al.*, **SP. NOV.**

ZooBank LSID: urn:lsid:zoobank.org:act:7F3B3C86-99CC-4D11-9997-D2408220646D

Holotype: FSAC CP 330, an almost complete and three-dimensionally preserved skull articulated with part of pectoral girdle and axial skeleton. This specimen was previously catalogued as UMMP 118216, and has been mentioned under that number by Capobianco *et al*., 2021. Reference casts are kept at the UMMP.

Etymology: Specific name in honour of Eric J. Hilton (Virginia Institute of Marine Science and College of William and Mary), in recognition of his fundamental contributions on bonytongue comparative anatomy and systematics, and ichthyology in general.

Type locality/horizon: Due to non-specialist private collection of the specimen, information on the locality for FSAC CP 330 is limited to the early Eocene (Ypresian) phosphates of the Ouled Abdoun Basin, Morocco (Fig. 1). The surrounding matrix provides two lines of corroborative evidence. First, a slightly deformed and damaged shark tooth embedded in the matrix was tentatively identified as a posterior tooth of †*Brachycarcharias atlasi* Arambourg, 1952 (Fig. 1C), which occurs in Thanetian–Ypresian strata of the Ouled Abdoun phosphates (C. Underwood, Birkbeck College, pers. comm. 2020). Secondly, the matrix includes poorly sorted peloids, and is thus lithologically consistent with Ypresian phosphates in the basin (Beds I and 0; Yans *et al*., 2014; Zouhri, S., 2017).

Diagnosis: Osteoglossiform with roughly triangular skull profile, relatively long jaws and terminal mouth; bulbous antorbital with strong ornamentation; two semicircular scleral rings; approximately 23 maxillary teeth; >26 dentary teeth; bony collars at tooth base less than half the tooth height; lower jaw more than three times longer than deep; very long posterior process of the hyomandibula; opercle with dorsally-oriented concavity above the articular facet; 18

branchiostegals. †*Macroprosopon hiltoni* differs from †*Furichthys* in having the retroarticular included in (instead of excluded from) the articulation between lower jaw and quadrate; and the posterior process of the hyomandibula longer (rather than shorter) than the dorsal articulating surface of the hyomandibula. †*Macroprosopon hiltoni* differs from both †*Phareodus* and †*Brychaetus* in having proportionally much longer lower jaws; supraorbital shelf of the frontal not extending to the anterior margin of the frontal; posterior toothless portion of maxilla not substantially deeper than toothed portion; cleithrum extending anteriorly to the level of the angular (rather than extending to just below the preopercle).

Description

The holotype is broken transversely into two blocks that meet at the level of the opercle (Figs. 2–9). It is strongly medio-laterally compressed; this compression caused the collapse of the skull roof on the left side of the specimen, which in turn resulted in several bones on the left side being crushed or completely missing. The anteriormost part of the skull is completely missing. Bones in the specimen have a widely varying state of preservation: some are heavily damaged and/or delaminated such that their surface is often missing (e.g., infraorbitals, opercular series, left angular); others are almost pristine (e.g., parts of the skull roof, branchiostegal rays). The posterior block of the holotype is covered in layered, broken scales.

Neurocranium (Figs. 3, 7). The anteriormost portion of the neurocranium (including nasals, vomer and part of the ethmoid region) is missing from the specimen. A thin, rounded bone antero-medial to the antorbital on the left side of the specimen is tentatively interpreted as the lateral ethmoid. It is slightly concave medio-laterally. Several fragments of bone located medially to the lateral ethmoid and antero-ventrally to the frontals might represent the sole exposed portion of the parasphenoid. The frontal is very long, accounting for approximately two thirds of the skull roof length when excluding the nasals. It possesses a broad supraorbital

shelf overlying the orbit and articulating antero-ventrally with the antorbital. The shelf bears a radial pattern of ornamentation on its dorsal surface, consisting of furrows and shallow pits. The anterior margin of the frontal appears to be only slightly broader than its posterior margin, as the supraorbital shelf does not seem to extend anteriorly to the articulation with the nasal. At the level of the orbit, the frontal is at least 1.5 times broader than its posterior margin. The supraorbital canal does not run throughout the whole length of the frontal. The suture between the two frontals is not visible, because the right frontal partially overlaps the left one due to taphonomic distortion of the specimen. The suture between frontal and parietal is at least partially interdigitated. The parietal is short and bears a transverse crest dividing it in two portions: the anterior one is ornamented, while the posterior one is depressed with respect to the rest of the skull roof and forms part of a dorso-occipital fossa ("dépression dorso-occipitale" or "fosse dorso-occipitale" of Taverne, 1978). This fossa is bounded antero-ventrally by the parietal, medially by the supraoccipital, and postero-laterally by the epioccipital. The central portion of the dorso-occipital fossa is occupied by an open fenestra. The external surface of the left parietal is partially broken, revealing a transverse canal-like structure that is likely the supratemporal commissure extending through the parietal. Although the temporal fossa is not exposed in the specimen and it is not possible to determine the bones that border it, the parietal clearly does not contribute to its margins. The epioccipital is a large bone forming the postero-lateral corner of the skull roof; it bears a strong ridge in continuity with the dorsal ridge of the pterotic that terminates posteriorly with a marked thickening. The antero-lateral margin of the epioccipital sutures with the pterotic. The supraoccipital bears a crest that is partially broken in the specimen, such that its full extent cannot be determined. A broken and flattened piece of tubular, canal-bearing bone overlying the medial part of epioccipital and dorso-occipital fossa is interpreted as the extrascapular. The sphenotic is relatively short and has a marked lateral projection (partially broken in the specimen) perpendicular to the antero-posterior axis of the

skull. The pterotic is very long, overlies the sphenotic anteriorly and sutures with frontal, parietal and epioccipital medially. It bears a strong dorsal ridge on its posterior half. The lateral surface of the pterotic is smooth and lacks large pits or foramina. Ventro-medial to the sphenotic and pterotic, the prootic forms at least part of the articular surface for the anterior head of the hyomandibula. Posterior to the pterotic and ventral to the epioccipital, the intercalar bears a triangle-shaped posterior projection.

Orbital region (Figs. 3, 5, 7). There is no identifiable supraorbital. The antorbital is bulbous and presents a heavily ornamented surface, with two different ornamentation fields: a postero-dorsal one with chevron-like patterns, and an antero-lateral one with radial furrows and shallow pits. The first infraorbital is slender and tapers posteriorly. It defines most of the ventral margin of the orbit and contributes partially to its anterior margin. The anterior portion of the first infraorbital is ventro-lateral to the antorbital. Posterior to the first infraorbital and lining the remaining portion of the ventral margin of the orbit there is a short and thin second infraorbital. The third and fourth infraorbitals are very large, covering most of the lateral postorbital area ('cheek') of the skull. The third and fourth infraorbitals are at least twice as long as they are deep. Their surface is ornamented with thin radial ridges. The fourth infraorbital is deeper than the third one and partially overlaps it. The infraorbital sensory canal is completely enclosed in a bony canal that extends through all the infraorbitals. Although the dermosphenotic is absent in the specimen, we interpret an elongated and roughly triangular surface postero-dorsal to the orbit as an impression left by that bone. Two semicircular ossified scleral rings (anterior and posterior) surround the eye.

Jaws (Figs. 3, 7). The premaxillae are not preserved in the specimen, except for a broken splinter of bone antero-lateral to the right maxilla. Two broken teeth appear to be associated with this premaxillary fragment. The maxilla is long and slightly curved with ventral concavity. It tapers anteriorly into an elongated, narrow, and arched anteromedial process. This process,

which articulates with the premaxilla, is missing its anterior tip. The length of the process—coupled with the length and proportions of the lower jaw—suggests that the premaxilla was a relatively long bone, especially when compared with other osteoglossids. There is no distinct dorsal swelling in the maxilla behind the anteromedial process. There are 19 maxillary teeth arranged in a single row that are visible on the right maxilla, with a complete maxillary set consisting of approximately 23 teeth when accounting for empty spaces left by tooth replacement. The teeth decrease in size from the anterior to the posterior portion of the maxilla. They are hollow, sub-conical in shape, with a short (less than a third of the tooth height) bony collar at the base and a small conical acrodin cap at the tip. The posterior, toothless portion of the maxilla, which overlies the angular, is rounded and not substantially deeper than the rest of the bone. Based on tomograms, broken pieces of bone dorsal to the posterior portion of the maxilla likely belong to the third infraorbital and potentially the maxilla itself, rather than to a supramaxilla. The lower jaws are incomplete, missing their anteriormost portions. They are straight and elongated, with a low coronoid process and a relatively long post-coronoid region. The dentary is lightly ornamented with parallel lines running along its length. Few large pores of the mandibular canal are visible on the external surface of the dentary. A complete dentary would include more than 23 teeth arranged in a single row. Dentary teeth are larger on average than the maxillary ones, and they are markedly compressed antero-posteriorly. The relative size of the bony collar at the tooth base varies from a third to half the tooth height. Dentary tooth collars are longer than maxillary tooth collars for teeth of the same size. Several replacement tooth crowns are visible on the right lower jaw. The angular is very long and extends anteriorly at the level of the anterior orbital margin. It presents a large postero-dorsal flange that laterally covers the quadrate articular condyle and the articular surface of the lower jaw. The articular and the retroarticular are not fused with the angular. They both contribute to the surface of the jaw joint (Fig. 10C).

Palate and suspensorium (Figs. 3, 5, 7, 9). Only a small part of the palate can be seen in the specimen. Anteriorly, an exposed plate-like bone with a multitude of small teeth is interpreted as either the endopterygoid or the palatine-ectopterygoid. The quadrate is approximately triangular in lateral view and likely longer than deep. The 'peg-like' head of the quadrate articulates with the articular and retroarticular of the lower jaw (Fig. 10C). Posterodorsal to its head, a strong ridge marks a portion of the posterior edge of the quadrate. The symplectic can be tentatively identified as a wedge-shaped bone overlying the posterodorsal surface of the quadrate. The hyomandibula is mostly covered by the third and fourth infraorbital and by the preopercle on both sides of the specimen. The anterior hyomandibular head is clearly distinct from the posterior one on the partially exposed left hyomandibula. The articular surface with the opercle can also be seen on the left side of the specimen. Its posterior position, distant from the heads articulating with the braincase, suggest a very long posterior (=opercular) process. This is confirmed by examination of the tomograms, which show the posterior process being slightly longer than the dorsal articulating surface of the hyomandibula.

Opercular series (Fig. 5, 7, 9). The ventral half of the right preopercle is well preserved on the right side of the specimen. It presents a curved anterior margin, with an angle larger than 90º between its vertical arm and a very short horizontal arm that does not anteriorly reach the level of the orbit. The preopercular sensory canal opens in the horizontal arm through 6 large, antero-ventrally directed pores, arranged in a straight horizontal line. It is unclear whether these were originally covered by a thin lamina of bone that might have broken off post-mortem. Smaller preopercular pores extend posteriorly back to the posterior broken margin of the bone. Two large openings for the preopercular sensory canal are visible on the vertical arm of the left preopercle. Small portions of the interopercle are visible underneath the preopercle ventrally. It contacts the subopercle posteriorly. The subopercle is partially exposed antero-ventrally to the opercle on the left side of the specimen, but its size and shape are difficult to determine.

The opercle is incompletely preserved and fractured in several pieces on both sides. Its anterior margin has a distinct dorsally-oriented concavity just above the articular facet for the hyomandibular process. In correspondence to the articular facet, the opercle bears a thickened opercular ridge on its medial side, with several small foramina on the surface. The dorsal margin of the opercle is almost flattened, with only a moderate amount of curvature. Based on its imprint on the right side of the specimen, the ventral margin of the opercle was likely straight or very slightly curved.

Branchial skeleton (Figs. 3, 5, 7, 9). The ceratohyals and the urohyal are the only exposed bones of the ventral hyoid arch. The anterior ceratohyal has a broad anterior head. The urohyal has a distinct head and a narrow ventral margin. An isolated tooth crown embedded in the sediment anterior to the ceratohyal might be part of the basibranchial toothplate dentition. There are 18 branchiostegals, with the posterior ones notably deeper than the anterior ones.

Pectoral girdle and fin (Figs. 5, 7, 9). The posttemporal can be seen on the left side of the specimen. It bears a broad and flattened dorsal arm that articulates with the back of the neurocranium. The ventral arm of the posttemporal can be identified in the tomograms; it is laterally compressed and relatively short, reaching around half the length of the dorsal arm. The supracleithrum is a slightly curved, laterally flattened bone with a thickened head antero-dorsally. Its medial surface bears a few distinct foramina anteriorly. The cleithrum and scapula are partially exposed on the right side of the specimen. However, anatomical details of these bones cannot be discerned. The coracoid extends anteriorly beyond the lower jaw joint, as inferred by its exposed ventral margin. Six pectoral rays are partially preserved. The first one is greatly enlarged and thickened. Two radials are visible ventral to the first two pectoral rays.

Postcranial axial skeleton (Figs. 5, 7, 9). The first fourteen vertebrae (or at least their centra) are preserved in the specimen, as evaluated from the tomograms. All the vertebrae are

amphicoelous and much deeper than long. Examination of the tomograms reveals the presence of a paired autogenous structure ventral to the first vertebra that extends anteriorly few centimeters below the occipital region of the neurocranium. We interpret this structure as a greatly expanded first parapophysis that is wedge-shaped in lateral view (see 'Modified coding and scoring of characters' on Character 88 for further discussion of this feature). The second and third vertebrae are partially exposed on the left side of the specimen, and clearly illustrate the autogenous nature of the neural arches (Fig. 10B). Nine abdominal ribs are partially exposed on the right side of the specimen (Fig. 5).

Scales. Scales are poorly preserved in the specimen, with small scale fragments including their surface texture found in the anterior block, and whole scales (often fractured and delaminated) in the right side of the posterior block, posterior to the pectoral girdle. Scales appear to be subcycloid, few centimeters in diameter and partially overlapping. They seem to lack reticulate furrows; instead, small tubercles ornament their surface.

RESULTS

Modified coding and scoring of characters

Character (2): Shape of extrascapular. This character has been scored for †*Sinoglossus* as '0' (expanded) by Wilson and Murray (2008), who adapted the scoring by Li *et al*. (1997b) to the coding of this character by Hilton (2003). However, many of the taxa scored by Li *et al*. (1997b) as possessing an expanded extrascapular have a reduced extrascapular according to the coding of Hilton (2003; see Hilton 2003:30 for an in-depth discussion of this character). Although we were not able to examine any specimen of †*Sinoglossus* first-hand, the original description of this taxon (Su, 1986) does not suggest the presence of an extrascapular expanded in a similar way to the extrascapulars of hiodontids and mormyrids. Given the uncertainty on the state of

this character for this taxon, we changed the scoring of †*Sinoglossus* from '0' (expanded) to '?'.

Character (8): Parasphenoid teeth. The ventral surface of the parasphenoid of †*Phareodus* is almost devoid of teeth, with the exception of one large conical tooth (sometimes joined by two smaller ones) between the basipterygoid processes (Li *et al*., 1997a). We changed the scoring of †*Phareodus* for this character from '?' to '3' (large and restricted to the basal portion of the parasphenoid).

Character (9): Basipterygoid process. Hilton (2003) coded this character with two possible scores, absent (state 0) and present (state 1). However, the scores in Hilton's (2003) character matrix are inverted, with taxa possessing a basipterygoid process (such as *Osteoglossum* and *Pantodon*) scored as '0' and taxa lacking a basipterygoid process (such as *Hiodon* Lesueur, 1818 and *Chitala*) scored as '1'. This mis-scoring has been repeated in all successive versions of the character matrix. We maintain the original definition and coding of the character, but we fixed the scoring such that '0' indicates absence and '1' indicates presence of the basipterygoid process.

Character (13): Basisphenoid. The basisphenoid has been identified in †*Phareodus* by Li *et al.* (1997a) as being one of the cartilaginous bones forming the dorso-medial wall of the orbit, located ventromedial to the orbitosphenoid. However, it is difficult to establish whether the ventral portion of the orbital wall in †*Phareodus* (as seen, for example, in FMNH PF 10237, FMNH PF 10285, FMNH PF 16536) represents a basisphenoid or rather a medial vertical lamina of the parasphenoid. Because of the uncertainty in interpreting this feature in †*Phareodus*, we changed the scoring for this character from '0' (present) to '?'.

Character (20): Supraorbital bone. Several non-osteoglossomorph teleosts possess a supraorbital bone anterodorsal to the orbit. Among these, *Elops* (Forey, 1973) and *Dorosoma*

Rafinesque, 1820 (Grande, 1985) are included in the character matrix and were previously scored as lacking the supraorbital (state 1) by Murray *et al*. (2018). Thus, we changed the scoring for *Elops* and *Dorosoma* from '1' (absent) to '0' (present). Additionally, †Ellimmichthyiformes were also scored as lacking the supraorbital (state 1) by Murray *et al*. (2018). Because the supraorbital is present in several †ellimmichthyiforms and secondarily lost in the sub-clade †Paraclupeinae (Murray and Wilson, 2013), we changed the scoring for †Ellimmichthyiformes to '0' (present), reflecting the likely ancestral state of this character within this clade.

Character (22): Number of bones in the infraorbital series, not including the dermosphenotic or the antorbital if present. We changed the scoring for *Pantodon*, which is unique among osteoglossomorphs in having five (instead of four) infraorbitals (Hilton, 2003), from '1' (four) to '0' (five). The previous scoring was likely an accidental error in the Wilson and Murray (2008) matrix, which carried on to the Murray *et al*. (2018) matrix.

Character (23): First infraorbital. This character, as defined by Hilton (2003), distinguishes a condition in which the first infraorbital does not contribute or only partially contributes to the anterior margin of the orbit (state 0) from a condition in which the first infraorbital is the only bone that contributes to the anterior margin of the orbit (state 1). Based on this definition, we changed the scoring of this character for *Dorosoma* from '1' to '0' (Grande, 1985); for †*Xixiaichthys* Zhang, 2004 from '1' to '0' (Zhang, 2004); for †*Joffrichthys tanyourus* Murray *et al*., 2018 from '?' to '0' (Murray *et al*., 2018); and for †*Paralycoptera* from '?' to '0' (Xu and Chang, 2009). It should be noted that redefining this character by including more states that distinguish between a condition in which the first infraorbital does not contribute at all to the anterior margin of the orbit and another one in which the first infraorbital contributes to the ventral portion of the anterior margin of the orbit might better capture the range of

morphologies and topological relationships observed for the first infraorbital of osteoglossomorphs.

Character (26): Dermosphenotic. Li and Wilson (1996) defined this character to distinguish the triradiate condition found exclusively in Hiodontiformes from other osteoglossomorphs, which were assigned the plesiomorphic state (defined as 'irregularly triangular'). Hilton (2003) added a third state (tubular) to describe the condition seen in some notopterids and mormyrids, and changed the definition of the plesiomorphic state to simply 'triangular'. Several taxa scored as having a 'triangular' dermosphenotic have a quadrangular or irregularly shaped dermosphenotic (e.g., *Heterotis*, *Notopterus* Lacepède, 1800, †*Lycoptera* Müller, 1848; Hilton, 2003). To avoid future ambiguities in scoring and highlight the distinction from a tubular or triradiate state, we changed the definition of the plesiomorphic state (state 0) to 'flattened, plate-like.'

Character (28): Neurocranial heads of the hyomandibula. †*Phareodus* has been previously described as having one continuous hyomandibular head, corresponding to state 0 (one head or two heads but continuous) of this character (Wilson and Murray, 2008). However, we observed two clearly distinct hyomandibular heads in †*Phareodus encaustus* (e.g., FMNH PF 10237, FMNH PF 10285) and †*Phareodus testis* (e.g., FMNH PF 11942, FMNH PF 17493). We changed the scoring for †*Phareodus* from '0' to '1' (two heads, separate). We also changed the scoring for †*Wilsonichthys* Murray *et al*., 2016 from '1' (two heads, separate) to '?', because Murray *et al*. (2016: 7) report that the hyomandibula "[...] has two articular heads, but the bone is not well preserved, and whether or not the heads might have had a bony connection cannot be determined". As the condition of having two hyomandibular heads bridged by a bony connection would correspond to state 2 of this character, it is more conservative to score †*Wilsonichthys* as uncertain for this character.

Character (31): Autopalatine bone. A bony autopalatine is absent in osteoglossomorphs, with the only reported exceptions in *Heterotis* and possibly *Scleropages leichardti* Günther, 1864 (Arratia and Schultze, 1991; Hilton, 2003). Reexamination of †*Phareodus encaustus* (e.g., FMNH PF 10237, FMNH PF 16529) reveals the presence of a bony autopalatine in this species as well. We changed the scoring of this character for †*Phareodus* from '?' to '0' (present). Some non-osteoglossid osteoglossomorphs (†*Joffrichthys tanyourus*, †*Shuleichthys* Murray *et al*., 2010 and †*Xixiaichthys*) have been scored as '0' (present) in previous versions of the data matrix (Wilson and Murray, 2008; Murray *et al*., 2010, 2018). Since there is no mention of an autopalatine in the descriptions of those taxa (Zhang, 2004; Murray *et al*., 2010, 2018) and an autopalatine cannot be identified in specimen photographs and interpretative drawings, we changed the scoring of †*Joffrichthys tanyourus*, †*Shuleichthys* and †*Xixiaichthys* for this character from '0' (present) to '?'.

Character (40): Supramaxillae. †*Joffrichthys tanyourus* is scored as state 0 (present) in the Murray *et al*. (2018) character matrix. However, the description clearly states that there are no supramaxillae in this taxon (Murray *et al*., 2018). Hence, we changed the scoring for †*Joffrichthys tanyourus* from '0' to '1' (absent).

Character (42): Posterior bones of the lower jaw. †*Lopadichthys* Murray *et al*., 2018 is scored as state 2 (all separate) in the Murray *et al*. (2018) character matrix. However, the description and figures clearly indicate the angular and the articular as indistinguishably fused with each other (Murray *et al*., 2018). Hence, we changed the scoring for †*Lopadichthys* to '1' (angular and articular fused).

Character (75): Intestine. One of the few synapomorphies shared by all extant osteoglossomorphs is having an intestine that passes to the left of the stomach, instead of passing to the right like in the vast majority of ray-finned fishes (Nelson, 1972). Although this

character is particularly difficult—if not impossible—to evaluate in fossil taxa, due to the low preservation potential of soft tissues like the gastrointestinal tract, it is nonetheless valuable in supporting the monophyly of Osteoglossomorpha on the basis of morphological characters. We changed the scoring of several extant taxa that were listed as uncertain ('?') according to whether their intestine coils to the right of the stomach ('0') or to the left of the stomach ('1'), based on relevant literature (Nelson, 1972; Banan Khojasteh, 2012): *Amia* ('?' ⟶ '0'), *Elops* ('?' ⟶ '0'), *Gnathonemus* ('?' ⟶ '1'), *Chitala* ('?' ⟶ '1'), *Xenomystus* ('?' ⟶ '1'), and *Papyrocranus* ('?' ⟶ '1').

Character (78): Second infraorbital shape and size. †*Joffrichthys tanyourus* was scored as state 1 (triangular or rectangular and smaller than third infraorbital) in the Murray *et al*. (2018) character matrix. However, in this taxon the second infraorbital is probably fused to the third (Murray *et al*., 2018). Thus, we consider this character to be not applicable in †*J. tanyourus*. The second infraorbital of †*Sinoglossus* is approximately rectangular in shape and relatively deep, yet substantially smaller than the third infraorbital (Su, 1986; Li and Wilson, 1996). Accordingly, we changed the scoring of †*Sinoglossus* for this character from '2' (expanded and equivalent in size to or larger than third infraorbital) to '1' (triangular or rectangular and smaller than third infraorbital). *Pantodon* has five infraorbitals instead of the usual condition of four infraorbitals seen in extant osteoglossomorphs, complicating the assessment of their homology. However, the neuromast pattern of the infraorbitals of *Pantodon* suggests that, in this taxon, the first two infraorbital bones correspond to the first infraorbital of other osteoglossomorphs (Nelson, 1969; Hilton, 2003). Thus, the third infraorbital of *Pantodon*, which is substantially deeper than the first two and smaller than the fourth, is homologous to the second infraorbital of other bonytongues. Following this identification, we changed the scoring of *Pantodon* for this character from '0' (more or less slender or tubular and small in size) to '1' (triangular or rectangular and smaller than third infraorbital).

Character (86): Anal fin sexual dimorphism. We changed the scoring for *Pantodon*, which is characterized by extreme sexual dimorphism in the anal fin (Lastein and Van Deurs, 1973), from '0' (absent) to '1' (present).

Character (88): Parapophysis on the first centrum. The parapophysis of the first vertebral centrum is expanded or hypertrophied in several osteoglossids, as first noted by Forey and Hilton (2010) in *Arapaima*, *Osteoglossum*, and †*Phareodus*. Murray *et al*. (2018) included this information in their character matrix by adding a two-state character where one state indicates a non-expanded or hypertrophied first parapophysis, and the other state indicates an expanded or hypertrophied first parapophysis that reaches under the occiput. However, the enlarged first parapophysis in osteoglossids can exist in two very different conditions. In *Osteoglossum* and *Scleropages* (and maybe †*Singida* Greenwood and Patterson, 1967; Murray *et al*., 2018), the first parapophysis is rounded in lateral and ventral views, it touches the basioccipital but does not contact the parasphenoid. In *Arapaima* and several fossil taxa (including †*Phareodus*, †*Brychaetus* and †*Macroprosopon*), the first parapophysis is greatly hypertrophied, it appears wedge-shaped in lateral view, reaches anteriorly below the occipital region of the neurocranium and contacts (or even interdigitates with) the parasphenoid (Fig. 11). Thus, we changed the coding of this character to encompass its observed variability among bonytongues: parapophysis on the first centrum not expanded or hypertrophied (state 0); expanded and rounded, barely reaching below the occiput and not touching the parasphenoid (state 1); greatly hypertrophied and extending anteriorly to touch the parasphenoid, wedge-shaped in lateral view (state 2).

This character is difficult to score for *Heterotis*, because in this taxon the first vertebra is completely fused to the occipital region of the neurocranium (Taverne, 1977; Forey and Hilton, 2010). Ontogenetic studies suggest that *Heterotis* has completely lost the parapophysis on the first centrum, as it cannot be identified in young specimens where the first vertebra is not yet

fused to the basioccipital (Britz and Johnson, 2010). Hence, we considered the scoring of character 88 to be not applicable for *Heterotis*.

Rescoring of †*Paralycoptera* and exclusion of †*Tanolepis*

We rescored 33 characters for the Early Cretaceous †*Paralycoptera wui* Chang and Chou, 1977 based on the redescription of this genus and species by Xu and Chang (2009). Most of these changes replace previously missing data. The following list indicates the number of the updated character, the state of that character in the Murray *et al*. (2018) matrix and the new state scored in this study: (2) ?⟶0; (5) ?⟶0&1; (6) ?⟶2; (7) ?⟶3; (8) ?⟶2; (12) ?⟶0; (20) ?⟶1; (21) ?⟶0; (24) ?⟶0; (25) ?⟶1; (29) ?⟶0; (32) 0⟶2; (33) 0⟶1; (35) 1⟶0; (36) ?⟶1; (38) ?⟶0; (42) ?⟶1; (43) ?⟶1; (44) ?⟶1; (47) 0⟶?; (51) ?⟶1; (55) ?⟶0; (56) ?⟶0; (60) ?⟶0; (61) ?⟶1; (63) ?⟶0; (64) ?⟶0; (67) 0⟶1; (68) ?⟶2; (78) ?⟶0; (82) 1⟶0; (83) ?⟶0; (87) ?⟶1.

†*Tanolepis ningjiagouensis* Jin, 1991 from the Late Jurassic–?Early Cretaceous Fenshuiling Formation has been included in several phylogenetic analyses of Osteoglossomorpha alongside †*Paralycoptera*, always falling as sister taxa to each other (Li *et al*., 1997*b*; Wilson and Murray, 2008; Murray *et al*., 2018). †*Tanolepis* has been synonymized with †*Paralycoptera* by Jin *et al*. (1995). This decision is supported by Xu and Chang (2009) in their redescription of †*Paralycoptera*, whereas Li *et al*. (1997*b*) listed a few characters differentiating the two taxa and rejected the synonymization. Because we were not able to visually examine any specimen of †*Tanolepis* and check the state of the characters we rescored for †*Paralycoptera* in this taxon, we decided to exclude †*Tanolepis* from our character matrix and phylogenetic analysis.

Newly defined characters

Character (89): Dorso-occipital fossa: absent [0]; present [1]. The dorso-occipital fossa, a large paired depression on the posterior portion of the skull roof bordered by parietal, supraoccipital, and epioccipital, was proposed by Taverne (1979) as a diagnostic characteristic of †Phareodontinae. Among the taxa included in this study, only †*Phareodus*, †*Brychaetus*, and †*Macroprosopon* present a dorso-occipital fossa. The presence or absence of this depression cannot be determined from available specimens of †*Furichthys*.

Character (90): Contact between dermosphenotic and anteriormost bone of the infraorbital series: absent [0]; present [1]. A contact between the dermosphenotic and the anteriormost bone of the infraorbital series (either the antorbital or the first infraorbital, in cases where the antorbital is absent) is seen only in *Osteoglossum*, *Scleropages*, and *Arapaima* among osteoglossomorphs. It should be noted that this character is partially correlated to some extent with character 4 (supraorbital shelf of frontal bone), as taxa that have a supraorbital shelf of the frontal will likely lack a contact between the dermosphenotic and the antorbital (or first infraorbital). However, several taxa in which the dermosphenotic does not contact the antorbital (or first infraorbital) lack a supraorbital shelf of the frontal.

Character (91): Depth of dorsal posterior infraorbital compared to ventral posterior infraorbital: shallower [0]; equal [1]; deeper [2]. The two most posterior infraorbitals in osteoglossomorphs are usually identified (*sensu* Hilton, 2003) as infraorbitals 3 (ventral) and 4 (dorsal). Exceptions are found in *Pantodon* (infraorbitals 4 and 5, as there is one more element in the infraorbital series), some species of †*Lycoptera* (e.g., †*L. middendorffi* Müller, 1848 and †*L. davidi* Gaudant, 1968, with three posterior elements of the infraorbital series identified as infraorbitals 3, 4 and 5; Greenwood, 1970; Ma, 1987), *Gymnarchus* Cuvier, 1829 (with more than 10 small tubular elements in the infraorbital series; Taverne, 1972), and potentially †*Phareodus testis*

and †*Brychaetus*, in which there are apparently only three elements of the infraorbital series (excluding antorbital and dermosphenotic; Roellig, 1974; Li *et al.*, 1997a). This character captures the relative depth proportions of the two posteriormost infraorbitals. †*Lycoptera* was scored as '?', due to the difficulty in defining the identity and homology of the three posteriormost elements of its infraorbital series.

Character (92): Scleral ossicles: absent [0]; present [1]. Scleral ossicles are supportive bony structures found in the eyes of some teleost fishes. The phylogenetic distribution of scleral ossicles within teleosts is complex, with multiple clades losing or gaining scleral ossicles independently (Franz-Odendaal, 2008; 2020). However, presence or absence of scleral ossicles tends to be conserved within family-level taxa (Mok and Liu, 2012). Among extant osteoglossomorphs, two scleral ossicles forming a thin ring around the eye are only found in large specimens of *Hiodon* (Hilton, 2002; contrary to Taverne, 1977). Scleral ossicles seem to be absent in the majority of fossil osteoglossomorphs. However, at least two extinct taxa (†*Brychaetus* and †*Macroprosopon*) have a robust, well-developed scleral ring. Remarkably, the scleral ring of †*Brychaetus* appears to be made of one single circular ossicle (Casier, 1966; Roellig, 1974), whereas the scleral ring of †*Macroprosopon* is made of two ossicles (anterior and posterior). The variability in the number of ossicles making up the scleral ring could be included in future phylogenetic analyses, especially if this feature is discovered in more fossil taxa.

Character (93): Postero-dorsal flange of the angular: absent [0]; present [1] (Fig. 12). This character captures the presence (or absence) of a raised flange in the postero-dorsal portion of the angular (or angulo-articular, or angulo-retroarticular, when this bone is fused to other bones of the lower jaw), which covers the articular surface of the quadrate in lateral view. Most osteoglossomorphs do not present this anatomical feature, and in these taxa the articular condyle of the quadrate can be clearly seen in lateral view (when it is not covered by

infraorbitals or by the preopercular). A postero-dorsal flange of the angular covering the articular condyle of the quadrate is present in most osteoglossids (*Arapaima*, *Heterotis*, *Scleropages*, †*Macroprosopon*, †*Phareodus* and †*Brychaetus*), but not in *Osteoglossum*.

Character (94): Posterior process of the hyomandibula: short (less than half the length of the dorsal articulating surface of the hyomandibula) [0]; long (more than half the length of the dorsal articulating surface of the hyomandibula) [1]; absent or extremely reduced [2] (Fig. 13). The posterior [= opercular] process of the hyomandibula is short in extant and fossil holosteans (Grande and Bemis, 1998; Grande, 2010), stem teleosts such as †pholidophorids (Arratia, 2013) and †ichthyodectiforms (Cavin *et al*., 2013), and several crown teleost clades (e.g. elopomorphs, clupeomorphs, osmeriforms, galaxiids, salmonids; Forey, 1973; Grande, 1985; Sanford, 2000; McDowall and Burridge, 2011), suggesting that a short posterior process is the ancestral state for crown teleosts and for osteoglossomorphs. Within Osteoglossomorpha, there is great variability in the relative length of the posterior process of the hyomandibula. In †*Lycoptera*, the posterior process is more strongly developed than in most teleosts, but it reaches at most half the length of the dorsal articulating surface of the hyomandibula (Greenwood, 1970; Jin *et al*., 1995; Zhang, 2002). Hiodontids are characterized by a long and deep opercular process, with dorsomedial and ventrolateral flanges (Hilton, 2002; Hilton and Grande, 2008). Mormyroids present an extremely modified hyomandibula that lacks a distinct posterior process and articulates with the opercle through a deep condyle (Taverne, 1972). The opercular process varies considerably within notopterids, with *Notopterus*, *Chitala*, and *Xenomystus* having strongly developed but relatively short processes, and *Papyrocranus* showing a very long posterior process connected with the dorsal articulating surface of the hyomandibula by a bony wing (Taverne, 1978). Most of the non-osteoglossid fossil taxa examined here, as well as the extant *Pantodon*, display the plesiomorphic condition of having a short posterior process of the hyomandibula. An exception to this is represented by

†*Paralycoptera*, which has a strongly developed posterior process. Among extant Osteoglossidae, the hyomandibulae of *Osteoglossum*, *Scleropages* and *Heterotis* have a short posterior process, whereas the hyomandibula of *Arapaima* has a very long and pillar-like posterior process. †Phareodontines also possess a very long posterior process of the hyomandibula, being even longer than its dorsal surface in †*Phareodus encaustus*. However, in contrast to *Arapaima*, the posterior process in †phareodontines points slightly ventrally rather than just extending posteriorly.

Character (95): Endopterygoid dentition: patch of shagreen-like fine teeth or small conical teeth [0]; few rows of large conical teeth [1]; one or more medio-dorsal rows of large conical teeth, bordered laterally by a patch of shagreen-like fine teeth [2]; teeth absent or extremely reduced [3] (Fig. 14). The oral surface of the endopterygoid bears a patch of shagreen-like fine teeth in extant and fossil holosteans (Grande and Bemis, 1998; Grande, 2010) and in several stem and crown teleosts (Forey, 1973; Arratia, 2013, 2016; Cavin *et al*., 2013). The dentition of the endopterygoid varies greatly within osteoglossomorphs. Among extant bonytongues, an endopterygoid with a patch of fine teeth can be seen in *Hiodon*, *Arapaima* and most notopterids. The extension of this tooth patch on the endopterygoid varies greatly between these taxa, from the small tooth patch of *Hiodon* restricted to the ventrolateral area near the ectopterygoid (Hilton, 2002), to the tooth patch of *Arapaima* that covers the whole medial surface of the bone. The endopterygoids of *Pantodon* and *Heterotis* bear instead few rows of relatively large conical teeth dorso-mesially. Extant osteoglossines (*Osteoglossum* and *Scleropages*) have one or two rows of large teeth on the dorso-mesial margin of the endopterygoid, bordered laterally by a patch of fine teeth that covers the whole medial surface of the bone. Teeth are completely absent from the endopterygoid in mormyrids, *Gymnarchus*, and *Xenomystus* (in mormyrids and *Gymnarchus,* the endopterygoid is fused with the ectopterygoid in a single bone; Taverne, 1998). Among fossil osteoglossomorphs for which the medial side of the endopterygoid can be

observed, a patch of shagreen-like fine teeth is present in †*Lycoptera* (Ma, 1987), †*Paralycoptera*, †*Shuleichthys*, †*Laeliichthys*, †*Chauliopareion* Murray and Wilson, 2005, and †*Brychaetus*. †*Phareodus* has a single row of very large conical teeth in the dorso-mesial margin of the bone, bordered laterally by a few rows of teeth decreasing progressively in size until they become a shagreen-like tooth patch that covers the rest of the bone (a condition very similar to extant osteoglossines). Teeth are apparently absent from the endopterygoid of †*Singida* (Murray and Wilson, 2005).

Character (96): Number of branchiostegal rays: 8 or fewer [0]; between 9 and 13 [1]; 14 or more [2]. Branchiostegal rays are long paired struts of dermal bone that form the floor of the gill chamber and are involved in ventilatory functions by being part of the buccal pump (Hughes, 1960; Farina *et al*., 2015). The number of branchiostegal rays varies widely within teleosts, but tends to not vary much within species and is conserved among closely related species (McAllister, 1968; Ascarrunz *et al*., 2019). Extant *Hiodon* species have 7–9 branchiostegal rays (8 as modal value; Hilton, 2002). The butterflyfish *Pantodon* has 10 branchiostegals (Taverne, 1978). Despite their great taxonomic and morphological diversity, all mormyrids have either 7 or 8 branchiostegal rays (Taverne, 1968; 1969; 1971; 1972), while their sister taxon *Gymnarchus* is characterized by a reduced set of 4 branchiostegals. All notopterids have 8 or less branchiostegals (extremely reduced to only 3 rays in *Xenomystus*; Taverne, 1978). Extant osteoglossids show a large variance in number of branchiostegal rays, with *Heterotis* on the lower end of the spectrum (7–8 rays) and *Scleropages* on the higher end (14–16). In fossil specimens, the count of branchiostegal rays (when preserved) is relatively straightforward, but we acknowledge that this might not always reflect the true number of branchiostegals in extinct taxa, due to lack of preservation of loosely attached rays or to difficulty in distinguishing left and right branchiostegal series in two-dimensionally preserved specimens. Most fossil taxa considered in this analysis have between 8 and 13 branchiostegal

rays. Notable outliers include †*Wilsonichthys* with only 5 branchiostegals (Murray *et al*., 2016), and †*Brychaetus* and †*Macroprosopon* with 15–18 and 18 branchiostegals, respectively. After discretizing the number of branchiostegal rays into three states designed to minimize the number of taxa scored as polymorphic, this character was designated as ordered to reflect its underlying meristic nature and its relative phylogenetic conservatism.

Phylogenetic analysis

The maximum parsimony (MP) phylogenetic analysis (Fig. 15A) recovered six most parsimonious trees, with tree length = 375, consistency index (CI) = 0.4080, retention index (RI) = 0.6487, and rescaled consistency index (RC) = 0.2647. The most parsimonious trees differ in the relative positions of †*Shuleichthys*, †*Wilsonichthys*, and the hiodontid clade (†*Eohiodon* Cavender, 1966 + *Hiodon*), in the positions of †*Xixiaichthys*, †*Paralycoptera*, †*Chauliopareion* and the †*Joffrichthys* Li and Wilson, 1996 clade (†*J. symmetropterus* Li and Wilson, 1996 + †*J. tanyourus*) with respect to the rest of Osteoglossiformes, and in the relationships of the three notopterid genera included in the analysis (*Chitala*, *Xenomystus* and *Papyrocranus*). †*Macroprosopon* is consistently recovered as an osteoglossid most closely related to †*Brychaetus*. †*Macroprosopon*, †*Brychaetus* and †*Phareodus* form a phareodontine clade to the exclusion of other osteoglossids. †*Furichthys* is reconstructed as sister taxon to a crown Arapaiminae clade formed by *Arapaima*, *Heterotis* and †*Sinoglossus*. A close relationship between phareodontines and arapaimines to the exclusion of Osteoglossinae (*Osteoglossum* + *Scleropages*) is strongly supported (Bremer index = 4). A crown Osteoglossidae clade that excludes *Pantodon* and †*Singida* is also strongly supported by the MP analysis (Bremer index = 4).

Maximum likelihood (ML) and Bayesian phylogenetic analyses recovered identical tree topologies (Figs. 15B, 16). They differ from the MP strict consensus tree in having *Pantodon* (rather than †*Singida*) as sister taxon to crown Osteoglossidae, and in recovering †*Furichthys* as sister taxon to †*Macroprosopon* (instead of being more closely related to crown arapaimines). Statistical support in both analyses is relatively high for the node uniting arapaimines and phareodontines (posterior probability = .97, ML bootstrap = 96%), for crown Arapaiminae (posterior probability = 1, ML bootstrap = 99%) and for crown Osteoglossidae (posterior probability = 1, ML bootstrap = 98%).

DISCUSSION

Phylogenetic position of †*Macroprosopon* with remarks on osteoglossomorph phylogeny

In every phylogenetic analysis performed here, †*Macroprosopon* is a member of Osteoglossidae closely related to the freshwater †*Phareodus* and to the marine †*Brychaetus*. Additionally, in the maximum likelihood topology it is recovered as sister taxon to †*Furichthys*, another long-snouted marine bonytongue. †*Macroprosopon*, †*Phareodus* and †*Brychaetus* (possibly together with †*Furichthys*) form a distinct osteoglossid clade that corresponds to the †Phareodontinae coined by Taverne (1979; see Hilton and Lavoué (2018) for the taxonomic history of †Phareodontinae). Besides being characterized by a series of unique anatomical features such as the presence of a dorso-occipital fossa and of a lateral expansion of the frontal (see "Comparison between other extinct and extant osteoglossids" below), †Phareodontinae can be defined operationally as the clade including every taxon most closely related to †*Phareodus* than either *Arapaima* or *Osteoglossum*. Contrary to most previous phylogenetic analyses (e.g., Li *et al*., 1997a; Hilton, 2003; Lavoué, 2016), †*Phareodus* (together with other †phareodontines) is here found to be more closely related to Arapaiminae than to

Osteoglossinae. In fact, every extinct osteoglossid included in this analysis is either an arapaimine or lies on the arapaimine stem. Remarkably, phylogenetic relationships within Osteoglossidae (except for the position of the incompletely known †*Furichthys*) seem robust to the different methods of phylogenetic analysis used here, and nodes within this group have stronger statistical support than most other nodes in osteoglossomorph phylogeny as indicated by Bremer decay indices, ML bootstrap values, and Bayesian posterior probabilities.

Outside of Osteoglossidae, the phylogenetic hypotheses supported in this study are topologically compatible with previously published osteoglossomorph phylogenies. The only exception is presented by †*Paralycoptera*, which is recovered as an osteoglossiform (possibly a crown-member of the group) instead of a stem osteoglossomorph as in previous studies (e.g., Murray and Wilson, 2008; Lavoué, 2016). This is due to the rescoring of this taxon based on a recent redescription (Xu and Chang, 2009). Whereas all major extant clades (Osteoglossidae, Mormyridae and Notopteridae) are relatively well-supported, the backbone of osteoglossomorph phylogeny is highly unstable. Previous work has shown that there are few or no characters supporting several relationships found in the more basal portions of the osteoglossomorph tree, and that exclusion of just one character or one taxon from the morphological matrix has the potential to substantially change the position of some fossil taxa (Murray *et al*., 2018). Although a more uncertain placement of extinct taxa in comparison to extant ones should be generally expected based on loss of information in fossils, this problem is exacerbated by the state of preservation of most Cretaceous and Paleocene osteoglossomorphs. These are known from flattened and approximately two-dimensional specimens often lacking any information about highly informative anatomical regions, such as hyoid and branchial skeletons and some parts of the neurocranium. Exceptions are represented by the Paleocene osteoglossids †*Taverneichthys* and †*Magnigena*, which are known from three-dimensional articulated cranial material, thus being key taxa for future investigation of

the evolutionary history of bonytongues. Inclusion of molecular data in a total-evidence (morphology + molecules) approach might at least help to stabilize deep nodes subtended by extant taxa, and possibly increase the statistical support for the placement of some fossil taxa.

Comparison with other extinct and extant osteoglossids

The phylogenetic position of †*Macroprosopon* as a member of Osteoglossidae closely related to arapaimines is supported by several characters. †*Macroprosopon* shares with other osteoglossids the presence of a postero-dorsal flange of the angular, a character that is uniquely present in osteoglossids among Osteoglossomorpha and has been secondarily lost in *Osteoglossum*. Additionally, in †*Macroprosopon*, like in other osteoglossids (except †*Phareodus*), the supratemporal canal passes through the parietals. This feature evolved independently several times within Osteoglossomorpha, as it is present also in †*Joffrichthys symmetropterus*, †*Chauliopareion*, and notopterids. We were not able to determine the presence or absence of other synapomorphies of Osteoglossidae in †*Macroprosopon*, including: a foramen for cranial nerve V + anteroventral lateral line nerve in the prootic (also observed in *Hiodon* and secondarily modified in *Arapaima*); an anterior process of the hyomandibula contacting the endopterygoid; a small subopercle anterior to the opercle (also seen in †*Chauliopareion* and secondarily modified in †*Furichthys*); the lateral line piercing the supracleithrum (independently evolved in notopterids as well); and a dorsal fin with long base and rounded outline.

†*Macroprosopon* shares exclusively with arapaimines and with other †phareodontines an autogenous articular (thus having angular, articular, and retroarticular all separate from each other) and a greatly hypertrophied parapophysis on the first vertebra. Additional characters link †*Macroprosopon* and other †phareodontines to arapaimines, but they also evolved

independently in more distantly related osteoglossomorphs. These are the presence of two separate neurocranial heads of the hyomandibula (also seen in †*Lopadichthys*), and a dorsal posterior infraorbital deeper than the ventral one (also seen in †*Paralycoptera*, *Xenomystus* and some specimens of †*Eohiodon*). A long posterior process of the hyomandibula also appears to be a synapomorphy of the Arapaiminae + †Phareodontinae clade, as it is present in *Arapaima*, †*Macroprosopon*, †*Brychaetus*, †*Phareodus* and †*Furichthys* (*Heterotis* possesses a short posterior process of the hyomandibula instead). This state evolved independently in hiodontids and †*Paralycoptera*. Similarly to arapaimines but unlike †*Phareodus* and †*Furichthys*, the retroarticular of †*Macroprosopon* takes part in the articulation between lower jaw and quadrate. Other synapomorphies of arapaimines, such as a third infrapharyngobranchial divided into two elements (one of which entirely cartilaginous), are very unlikely to be observed in fossil taxa because they involve non-mineralized or poorly mineralized tissues.

†*Macroprosopon*, †*Phareodus*, and †*Brychaetus* uniquely share the presence of a dorso-occipital fossa and of a supraorbital shelf of the frontal. We were not able to ascertain the state of these characters in †*Furichthys*. †*Macroprosopon* also shares with †*Brychaetus* the presence of a scleral ring formed by scleral ossicles, which is absent in †*Phareodus* and apparently in †*Furichthys* – although for the latter it is difficult to establish whether the absence of a scleral ring in the only specimen with preserved orbital region is due to true absence or to an artifact of preservation. The presence of a well-developed scleral ring in both †*Macroprosopon* and †*Brychaetus* is intriguing from an ecomorphological perspective, as scleral ossicles tend to be more common in fish clades with an active lifestyle (Franz-Odendaal, 2008) and they are more robust and forming a complete ring in fast pelagic predators such as scombrids and istiophorids (Nakamura and Yamaguchi, 1991; Franz-Odendaal, 2008). †*Macroprosopon* and †*Brychaetus* are also characterized by a high branchiostegal ray count (18 and 15–18, respectively). Among all other osteoglossomorphs, only *Scleropages* bears a similarly high count (between 14 and

16). The number of branchiostegal rays is unknown in †*Furichthys*. While it has been historically suggested that higher numbers of branchiostegals are found in marine fishes (Hubbs, 1919), recent phylogenetic comparative studies do not find statistical support for this proposed pattern (Ascarrunz *et al*., 2019).

The scales of †*Macroprosopon* seem to lack the reticulate furrows that are characteristic of osteoglossid scales. Instead, they present an ornamentation of small tubercles, similar to the scales of †*Furichthys* and of †*Monopteros*—a marine bonytongue with uncertain phylogenetic affinities from the early Eocene Bolca Lagerstätte (Taverne, 1998). Interestingly, these tubercles resemble the ones found on the external surface of posterior squamules (scale fragments) of extant osteoglossids, and in particular of *Heterotis* (pers. obs. of UMMZ 213845), except for their larger size.

Diversity of early Palaeogene marine osteoglossids and biogeographic remarks

The discovery of †*Macroprosopon* not only increases the known taxonomic diversity of marine bonytongues, but highlights how these fishes diversified in a wide range of morphologies that likely reflect a previously underappreciated ecological variety. Unlike other coeval marine bonytongues characterized by short and robust snouts, such as †*Brychaetus* and several other †*Phareodus*-like forms, *Macroprosopon* and the potentially closely related †*Furichthys* are long-snouted bonytongues, with elongated straight lower jaws and an extensive preorbital region of the skull (Fig. 17). The long snout and sub-conical tooth tips of †*Macroprosopon* indicate a predatory—and likely piscivorous—feeding ecology for this taxon. The aspect ratio of its lower jaw (relatively moderate height compared to length) suggests that †*Macroprosopon* had fast-closing jaws and probably a weaker bite relative to †*Brychaetus* and †*Phareodus* (Westneat, 2004). Although elongated lower jaws capable of fast-bite strikes are also found in

some extant osteoglossids (*Osteoglossum* and *Scleropages*), these taxa have a short preorbital region of the skull and their mouth is superior (strongly oblique), suggesting that modern bonytongues are not direct trophic analogues for the early Palaeogene long-snouted forms. Strikingly, long-snouted and short-snouted predatory bonytongues likely co-existed in the same marine habitats. This is implied by the occurrence of several osteoglossid jaw fragments and isolated teeth found in Ypresian Moroccan phosphates that do not correspond to the morphology of †*Macroprosopon* and are instead referable to †*Brychaetus* or a †*Brychaetus*-like form—characterized by more robust jaw bones and teeth and by a taller bony collar at the tooth base (Arambourg, 1952; Forey and Hilton, 2010). Similarly, in the Danish Fur Formation †*Furichthys* is found alongside †*Brychaetus*-like jaw fragments (plus several other bonytongue species; Bonde, 2008). Thus, at least in the western Tethys and North Sea, during the earliest Eocene osteoglossids occupied different trophic niches within the guild of large carnivorous fishes.

†*Macroprosopon* joins a great diversity of early Palaeogene marine bonytongues, which are now known from more than 10 different genera—a striking contrast with the depauperate taxonomic richness of extant osteoglossids. Several of these marine taxa, such as †*Monopteros*, †*Heterosteoglossum* Bonde, 2008, †*Brychaetoides*, †*Xosteoglossid*, and †*Thrissopterus* Heckel, 1856, remain poorly known with uncertain phylogenetic affinities (Taverne, 1998; Bonde, 2008; Hilton and Lavoué, 2018; Capobianco *et al.*, 2021). Although some of them are known from fragmentary or poorly preserved remains (thus complicating efforts to elucidate their relationships), they hint at a much higher degree of ecomorphological disparity of Palaeogene osteoglossids relative to extant representatives of this clade, including forms with durophagous dentition and others with broad pectoral fins and very elongated bodies (Capobianco *et al.*, 2021).

The phylogenetic placement of the marine †*Macroprosopon*, †*Furichthys* and †*Brychaetus* as stem arapaimines suggests that marine dispersal might have played a role in the present-day disjunct geographic distribution of this clade, with *Arapaima* endemic to South America and *Heterotis* endemic to Africa. Model-based ancestral state reconstruction and biogeographic inference might provide a way to test whether arapaimines were ancestrally marine, thus making extant *Arapaima* and *Heterotis* secondarily freshwater taxa. We point out that the phylogenetic hypotheses derived in this study are also compatible with one or two freshwater-to-marine transitions not involving the lineage leading directly to crown arapaimines. However, the presence of †*Phareodus*-like and †*Brychaetus*-like fossils in freshwater and marine deposits worldwide (Capobianco *et al*., 2021) lends some credibility to the scenario of long-distance marine dispersals followed by multiple marine-to-freshwater transitions. Inclusion of additional fossil osteoglossids within the phylogenetic framework laid out in this study will be paramount to paint a clearer picture of the biogeographic history of bonytongue fishes.

The diversity of early Palaeogene bonytongues and their worldwide presence in a variety of depositional environments hints at an unexpected evolutionary radiation of this group of fishes. This radiation might have been triggered or facilitated by the K/Pg mass extinction, which decimated large predatory fishes and other trophic specialists in marine settings, opening up new ecological opportunities for surviving taxa (Cavin, 2002; Friedman, 2009; Capobianco et al., 2021). The inclusion of fossil bonytongues in a 'tip-dated' phylogenetic analysis could help to better constrain the time of origin of the early Palaeogene bonytongue radiation and would be an important step towards clarifying the role of the K/Pg mass extinction in the evolutionary history of osteoglossomorphs.

Future efforts to resolve the phylogenetic affinities of Palaeogene marine bonytongues will be instrumental in elucidating some of the outstanding questions about osteoglossomorph evolution that remain unanswered. These include when and how many times bonytongues

transitioned from freshwater to marine environments (and vice-versa); how these environmental transitions affected the biogeographic history of the group; and the role of the K/Pg mass extinction in the diversification dynamics of bonytongues. We believe that the well-supported close relationship between arapaimines and †phareodontines found in this study is a promising first step towards answering these questions.

CONFLICT OF INTEREST

The authors declare that they have no conflict of interest.

DATA AVAILABILITY STATEMENT

The data underlying this article are available in Deep Blue Repositories of the University of Michigan Library, at [[insert link address]], and in Morphosource. These include: µCT for the holotype of †*Macroprosopon hiltoni* and for newly scanned comparative material; 3D surface models of the holotype of †*Macroprosopon hiltoni*; and high-resolution photographs and line drawings combining Figs. 2 and 4, Figs. 3 and 5, Figs. 6 and 8, and Figs. 7 and 9 into large-format figures.

ACKNOWLEDGMENTS AND FUNDING

The authors would like to give many thanks to Carol Abraczinskas (University of Michigan Museum of Paleontology) for making the weighted-line drawings of the †*Macroprosopon hiltoni* holotype, for figure design, and for very helpful discussion on the anatomy of the specimen. We thank Sky Jung for the artistic reconstruction of the complete skull of †*Macroprosopon*. We also thank William Sanders (University of Michigan Museum of

Paleontology) for the mechanical preparation of the †*Macroprosopon hiltoni* holotype. We thank Kyle Kramer (Undergraduate Research Opportunity Program at the University of Michigan) for great help with segmentation of CT data. We also thank for specimen access Douglas Nelson and Randy Singer at the University of Michigan Museum of Zoology, William F. Simpson at the Field Museum of Natural History, Chicago, Bo Schultz and René L. Sylvestersen at the Fur Museum, Bent E. K. Lindow at the Natural History Museum of Denmark, Emma Bernard at the Natural History Museum, London, Matt Riley at the Sedgwick Museum of Earth Sciences, Cambridge, Mariagabriella Fornasiero at the Istituto Geologico dell'Università di Padova, the late Anna Vaccari and Roberta Salmaso at the Museo Civico di Storia Naturale, Verona, Gaël Clement at the Muséum National d'Histoire Naturelle, Paris and Florias Mees at the Musée Royal de l'Afrique Centrale. We would like to thank Zach Randall and the Florida Museum of Natural History, University of Florida for permission to use CT data stored on Morphosource. We thank Charlie Underwood for his identification of the embedded shark tooth. We thank Alison Murray for providing the Nexus file of the morphological matrix used in Murray *et al*. (2018). We finally would like to thank the Friedman Lab students and postdocs for helpful discussion and comments on this manuscript. This study includes data produced in the CTEES facility at University of Michigan, supported by the Department of Earth & Environmental Sciences and College of Literature, Science, and the Arts. This work was supported by funding from the Department of Earth and Environmental Sciences of the University of Michigan (Scott Turner Student Research Grant Award 2017, to A.C.), by the Rackham Graduate School of the University of Michigan (Rackham Predoctoral Fellowship Award 2020-2021, to A.C.), by the Society of Systematic Biologists (2017 SSB Graduate Student Research Award, to A.C.), and by the Palaeontological Association (Palaeontological Association Career Development Grant PA-CD202102, to A.C.). This work was also supported by the European Union (ERC, MacDrive, GA 101043187). Views and

opinions expressed are however those of the authors only and do not necessarily reflect those of the European Union or the European Research Council Executive Agency. Neither the European Union nor the granting authority can be held responsible for them. This work was also supported by the National Science Foundation (NSF DEB 2017822 to Friedman).

SUPPORTING INFORMATION

Additional Supporting Information may be found in the online version of this article at the publisher's web-site:

File S1. List of morphological characters and states.

File S2. Morphological data matrix in Nexus format.

REFERENCES

Agassiz L. 1845. Report on the fossil fishes of the London Clay, *Report of the British Association for the Advancement of Science* 14: 279–310.

Alvarado-Ortega J, Cuevas-García M, del Pilar Melgarejo-Damián M, Cantalice KM, Alaniz-Galvan A, Solano-Templos G, Than-Marchese BA. 2015. Paleocene fishes from Palenque, Chiapas, southeastern Mexico, *Palaeontologia Electronica* 18: 1–22.

Arambourg C. 1952. Les vertébrés fossiles des gisements de phosphates (Maroc-Algérie-Tunisie), *Notes et Mémoires du Service Géologique du Maroc* 92: 1–372.

Arratia G. 1997. Basal teleosts and teleostean phylogeny, *Palaeo Ichthyologica* 7: 5–168.

Arratia G. 2013. Morphology, taxonomy, and phylogeny of Triassic pholidophorid fishes (Actinopterygii, Teleostei), *Journal of Vertebrate Paleontology* 33 (supplement 1): 1–138.

Arratia G. 2016. New remarkable Late Jurassic teleosts from southern Germany: Ascalaboidae n. fam., its content, morphology, and phylogenetic relationships, *Fossil Record* 19: 31–59.

Arratia G, Schultze HP. 1991. Palatoquadrate and its ossifications: development and homology within osteichthyans, *Journal of Morphology* 208: 1–81.

Ascarrunz E, Sánchez-Villagra MR, Betancur-R R, Laurin M. 2019. On trends and patterns in macroevolution: Williston's law and the branchiostegal series of extant and extinct osteichthyans, *BMC Evolutionary Biology* 19: 1–11.

Banan Khojasteh SM. 2012. The morphology of the post-gastric alimentary canal in teleost fishes: a brief review, *International Journal of Aquatic Science* 3: 71–88.

Bell MA, Lloyd GT. 2015. strap: an R package for plotting phylogenies against stratigraphy and assessing their stratigraphic congruence, *Palaeontology* 58: 379–389.

Berg L. 1940. *Classification of fishes both recent and fossil*. Travaux de l'Institut Zoologique de l'Académie des Sciences de l'URSS, Moscow, 517 pp. [Translated and reprinted in English, 1947, Ann Arbor]

Berra TM. 2007. *Freshwater Fish Distribution*. Chicago: The University of Chicago Press.

Blakey RC. 2008. Gondwana paleogeography from assembly to breakup—A 500 my odyssey, *Geological Society of America Special Papers* 441: 1–28.

Bleeker P. 1874. Typi nonnuli generici piscium neglecti, *Verslagen en Mededeelingen der Koninklijke Akademie van Wetenschappen. Afdeeling Natuurkunde (Ser. 2)* 8: 367–371.

Bonde N. 2008. Osteoglossomorphs of the marine Lower Eocene of Denmark – with remarks on other Eocene taxa and their importance for palaeobiogeography, *Geological Society of London, Special Publications* 295: 253–310.

Brito PM, Figueiredo FJ, Leal MEC. 2020. A revision of *Laeliichthys ancestralis* Santos, 1985 (Teleostei: Osteoglossomorpha) from the Lower Cretaceous of Brazil: Phylogenetic relationships and biogeographical implications, *PLOS One* 15: e0241009.

Britz R, Johnson GD. 2010. Occipito-vertebral fusion in actinopterygians: conjecture, myth and reality. Part 1: non-teleosts. In: Nelson JS, Schultze HP, Wilson MVH, eds. *Origin and Phylogenetic Interrelationships of Teleosts. Honoring Gloria Arratia*, München: Verlag Dr. F. Pfeil, 77–95.

Capobianco A, Friedman M. 2019. Vicariance and dispersal in southern hemisphere freshwater fish clades: a palaeontological perspective, *Biological Reviews* 94: 662–699.

Capobianco A, Beckett HT, Steurbaut E, Gingerich PD, Carnevale G, Friedman M. 2020. Large-bodied sabre-toothed anchovies reveal unanticipated ecological diversity in early Palaeogene teleosts, *Royal Society Open Science* 7: 192260.

Capobianco A, Foreman E, Friedman M. 2021. A Paleocene (Danian) marine osteoglossid (Teleostei, Osteoglossomorpha) from the Nuussuaq Basin of Greenland, with a brief review of Palaeogene marine bonytongue fishes, *Papers in Palaeontology* 7: 625–640.

Casier E. 1966. *Faune Icthyologique du London Clay: Atlas Edition* (Volume 2). London: British Museum (Natural History).

Castelnau FL. 1861. *Mémoire sur les poissons de l'Afrique australe*. Paris.

Cavender T. 1966. Systematic position of the North American Eocene fish, "*Leuciscus*" *rosei* Hussakof, *Copeia* 1966: 311–320.

Cavin L. 2002. Effects of the Cretaceous-Tertiary boundary event on bony fishes. In: Buffetaut E, Koeberl C, eds. *Geological and biological effects of impact events*. Berlin, Heidelberg: Springer, 141–158.

Cavin L, Forey PL, Giersch S. 2013. Osteology of *Eubiodectes libanicus* (Pictet & Humbert, 1866) and some other ichthyodectiformes (Teleostei): phylogenetic implications, *Journal of Systematic Palaeontology* 11: 115–177.

Chang MM, Chou CC. 1974. On Late Mesozoic fossil fishes from Zhejiang Province, China, *Vertebrata PalAsiatica* 12: 183–186.

Cope ED. 1871. On the fishes of the Tertiary shales of Green River, Wyoming Territory. In: Hayden FV, ed. *Sixth Annual Report of the United States Geological Survey of the Territories*. Washington: Government Printing Office, 545–643.

Cope ED. 1877. New fossil fishes from Wyoming, *American Naturalist* 11: 570.

Cuvier G. 1829. *Le Règne Animal, distribué d'après son organisation, pour servir de base à l'histoire naturelle des animaux et d'introduction à l'anatomie comparée*. Edition 2. v. 2

d'Aubenton F. 1965. *Notopterus blanci* n. sp., nouvelle espèce de poisson Notopteridae du haut Mékong cambodgien. *Bulletin du Muséum National d'Histoire Naturelle (Série 2)* 37, 261–264.

Danil'chenko PG. 1968. Fishes of the Upper Paleocene of Turkmenia. In: Obruchev DV, ed. *Essays on the phylogeny and systematics of fossil fishes and agnathans*. Moscow: Nauka Press. [In Russian].

Farina SC, Near TJ, Bemis WE. 2015. Evolution of the branchiostegal membrane and restricted gill openings in Actinopterygian fishes, *Journal of Morphology* 276: 681–694.

Forey PL. 1973. A revision of the Elopiformes fishes, fossil and recent, *Bulletin of the British Museum of Natural History (Geology)* 10: 1–222.

Forey PL, Hilton EJ. 2010. Two new Tertiary osteoglossid fishes (Teleostei: Osteoglossomorpha) with notes on the history of the family. In: Elliott DK, Maisey JG, Yu

X, Miao D, eds. *Morphology, phylogeny and paleobiogeography of fossil fishes*. München: Verlag Dr. F. Pfeil, 215– 246.

Fowler HW. 1934. Descriptions of new fishes obtained 1907 to 1910, chiefly in the Philippine Islands and adjacent seas, *Proceedings of the Academy of Natural Sciences of Philadelphia* 85: 233–367.

Franz-Odendaal TA. 2008. Scleral ossicles of teleostei: evolutionary and developmental trends, *The Anatomical Record* 291: 161–168.

Franz-Odendaal TA. 2020. Skeletons of the eye: An evolutionary and developmental perspective, *The Anatomical Record* 303: 100–109.

Friedman M. 2009. Ecomorphological selectivity among marine teleost fishes during the end-Cretaceous extinction, *Proceedings of the National Academy of Sciences* 106: 5218–5223.

Gaudant J. 1968. Recherches sur l'anatomie et la position systématique du genre *Lycoptera* (poisson téléostéen), *Mémoires de la Société géologique de France* 40: 1–41.

Gayet M. 1991. Holostean and teleostean fish from Bolivia. In: Suárez-Soruco R, ed. *Fósiles y Facies de Bolivia, I. Revista Técnica YPFB* 12: 453–494.

Gayet M, Meunier FJ. 1998. Maastrichtian to early late Paleocene freshwater Osteichthyes of Bolivia: additions and comments. In: Malabarba LR, Reis RE, Vari RP, Lucena ZM, Lucena CAS, eds. *Phylogeny and classification of neotropical fishes*. Porto Alegre: EdiPUCRS, 85–110.

Gayet M, Marshall LG, Sempere T, Meunier FJ, Cappetta H, Rage JC. 2001. Middle Maastrichtian vertebrates (fishes, amphibians, dinosaurs and other reptiles, mammals) from Pajcha Pata (Bolivia). Biostratigraphic, palaeoecologic and palaeobiogeographic implications, *Palaeogeography, Palaeoclimatology, Palaeoecology* 169: 39–68.

Gill TN. 1863. Description of a new generic type of mormyroids and note on the arrangement of the genus, *Proceedings of the Academy of Natural Sciences of Philadelphia* 14: 443–445.

Grande L. 1985. Recent and fossil clupeomorph fishes with materials for revision of the subgroups of clupeoids, *Bulletin of the American Museum of Natural History* 181: 231–372.

Grande L. 2010. An empirical synthetic pattern study of gars (Lepisosteiformes) and closely related species, based mostly on skeletal anatomy. The resurrection of Holostei, *Copeia* 2010 (Supplement 2A): 1– 871.

Grande L, Bemis WE. 1998. A comprehensive phylogenetic study of amiid fishes (Amiidae) based on comparative skeletal anatomy. An empirical search for interconnected patterns of natural history, *Journal of Vertebrate Paleontology* 18 (Supplement 1): 1–696.

Greenwood PH. 1963. The swimbladder in African Notopteridae (Pisces) and its bearing on the taxonomy of the family, *Bulletin of the British Museum (Natural History) Zoology* 11: 377–412.

Greenwood PH. 1970. On the genus *Lycoptera* and its relationship with the family Hiodontidae (Pisces, Osteoglossomorpha), *Bulletin of the British Museum of Natural History (Zoology)* 19: 259–285.

Greenwood PH, Patterson C. 1967. A fossil osteoglossoid fish from Tanzania (E. Africa), *Zoological Journal of the Linnean Society* 47: 211–223.

Greenwood PH, Rosen DE, Weitzman SH, Myers GS. 1966. Phyletic studies of teleostean fishes, with a provisional classification of living forms, *Bulletin of the American Museum of Natural History* 131: 339–456.

Günther A. 1864. On a new generic type of fishes discovered by the late Dr. Leichardt in Queensland, *Annals and Magazine of Natural History (Series 3)* 14: 195–197.

Günther A. 1868. *Catalogue of the fishes in the British Museum. Catalogue of the Physostomi, containing the families Heteropygii, Cyprinidae, Gonorhynchidae, Hyodontidae, Osteoglossidae, Clupeidae,... [thru]... Halosauridae, in the collection of the British Museum* 7: 1–512.

Heckel JJ. 1856. *Beiträge zur Kenntniss der fossilen Fische Österreichs*. Aus der Kaiserlich-Königlichen Hof-und Staatsdruckerei.

Hills ES. 1934. Tertiary fresh water fishes from southern Queensland, *Memoirs of the Queensland Museum* 10: 157–174.

Hilton EJ. 2002. Osteology of the extant north American fishes of the genus *Hiodon* Lesueur, 1818 (Teleostei: Osteoglossomorpha: Hiodontiformes), *Fieldiana Zoology* 100: 1–142.

Hilton EJ. 2003. Comparative osteology and phylogenetic systematics of fossil and living bony-tongue fishes (Actinopterygii, Teleostei, Osteoglossomorpha), *Zoological Journal of the Linnean Society* 137: 1–100.

Hilton EJ, Grande L. 2008. Fossil mooneyes (Teleostei: Hiodontiformes, Hiodontidae) from the Eocene of western North America, with a reassessment of their taxonomy, *Geological Society of London, Special Publications* 295: 221–251.

Hilton EJ, Lavoué S. 2018. A review of the systematic biology of fossil and living bony-tongue fishes, Osteoglossomorpha (Actinopterygii: Teleostei), *Neotropical Ichthyology* 16: e180031.

Hoang DT, Chernomor O, Von Haeseler A, Minh BQ, Vinh LS. 2018. UFBoot2: improving the ultrafast bootstrap approximation, *Molecular Biology and Evolution* 35: 518–522.

Hubbs CL. 1919. A comparative study of the bones forming the opercular series of fishes, *Journal of Morphology* 33: 60–71.

Hughes GM. 1960. A comparative study of gill ventilation in marine teleosts, *Journal of Experimental Biology* 37: 28–45.

Jin F. 1991. A new genus and species of Hiodontidae from Xintai, Shandong, *Vertebrata PalAsiatica* 29: 46–54.

Jin F. 1994. A nomen novum for *Tanichthys* Jin, 1991, *Vertebrata PalAsiatica* 32: 70.

Jin F, Zhang J, Zhou Z. 1995. Late Mesozoic fish fauna from western Liaoning, China, *Vertebrata PalAsiatica* 33: 169–193.

Kumar K, Rana RS, Paliwal BS. 2005. Osteoglossid and lepisosteid fish remains from the Paleocene Palana Formation, Rajasthan, India, *Palaeontology* 48: 1187–1210.

Lacepède BGE. 1800. *Histoire naturelle des poissons* 2: 1–632.

Lastein U, Van Deurs B. 1973. The copulatory organ of *Pantodon buchholzi* Peters (Teleostei), *Acta Zoologica* 54: 153–160.

Lavoué S. 2015. Testing a time hypothesis in the biogeography of the arowana genus *Scleropages* (Osteoglossidae), *Journal of Biogeography*: 42, 2427–2439.

Lavoué S. 2016. Was Gondwanan breakup the cause of the intercontinental distribution of Osteoglossiformes? A time-calibrated phylogenetic test combining molecular, morphological, and paleontological evidence, *Molecular Phylogenetics and Evolution* 99: 34–43.

Leidy J. 1873. Notice of remains of fishes in the Bridger Tertiary Formation of Wyoming, *Proceedings of the Academy of Natural Sciences of Philadelphia* 25: 97–99.

Lesueur CA. 1818. Descriptions of several new species of North American fishes. *Journal of the Academy of Natural Sciences, Philadelphia* 1: 222–235, 359–368.

Li GQ. 1994. Systematic position of the Australian fossil osteoglossid fish †*Phareodus* (= *Phareoides*) *queenslandicus* Hills, *Memoirs of the Queensland Museum* 37: 287–300.

Li GQ. 1996. A new species of Late Cretaceous osteoglossid (Teleostei) from the Oldman Formation of Alberta, Canada, and its phylogenetic relationships. In: Arratia G, Viohl G, eds. *Mesozoic Fishes. Systematics and Paleoecology*. München: Verlag Dr. F. Pfeil, 285–298.

Li GQ, Wilson MVH. 1996. Phylogeny of Osteoglossomorpha. In: Stiassny MLJ, Parenti LR, Johnson GD, eds. *Interrelationships of Fishes*. San Diego: Academic Press,163–174.

Li GQ, Grande L, Wilson MVH. 1997a. The species of †*Phareodus* (Teleostei: Osteoglossidae) from the Eocene of North America and their phylogenetic relationships, *Journal of Vertebrate Paleontology* 17: 487–505.

Li GQ, Wilson MVH, Grande L. 1997b. Review of *Eohiodon* (Teleostei: Osteoglossomorpha) from western North America, with a phylogenetic reassessment of Hiodontidae. *Journal of Paleontology* 71: 1109–1124.

Linnaeus C. 1766. *Systema naturae sive regna tria naturae, secundum classes, ordines, genera, species, cum characteribus, differentiis, synonymis, locis*. Holmiae: Laurentii Salvii.

Lundberg JG, Chernoff B. 1992. A Miocene fossil of the Amazonian fish *Arapaima* (Teleostei, Arapaimidae) from the Magdalena River region of Colombia--Biogeographic and evolutionary implications, *Biotropica* 24: 2–14.

Ma FZ. 1987. Review of *Lycoptera davidi*, *Vertebrata PalAsiatica* 25: 8–19.

Maddison WP, Maddison DR. 2019. Mesquite: a modular system for evolutionary analysis. Version 3.61. http://www.mesquiteproject.org

Marcusen J. 1854. Vorläufige Mittheilung aus einer Abhandlung über die Familie der Mormyren, *Bulletin de la Classe Physico-Mathématique de l'Académie Impériale des Sciences de St. Pétersbourg* 12: 1–14.

McAllister DE. 1968. Evolution of branchiostegals and classification of teleostome fishes, *Bulletin of the National Museum of Canada* 221: 1–237.

McDowall RM, Burridge CP. 2011. Osteology and relationships of the southern freshwater lower euteleostean fishes, *Zoosystematics and Evolution* 87: 7–185.

Mok HK, Liu SH. 2012. Morphological variations in the scleral ossicles of 172 families of actinopterygian fishes with notes on their phylogenetic implications, *Zoological Studies* 51: 1490–1506.

Müller J. 1843. Beiträge zur Kenntniss der natürlichen Familien der Fische, *Archiv für Naturgeschichte* 9: 292–330.

Müller J. 1845. Uber den Bau und die Grenzen der Ganoiden, und uber das naturliche System der Fische, *Physikalisch-Mathematische Abhandlungen der koniglichen Akademie der Wissenschaften zu Berlin* 1845: 117–216.

Müller J. 1848. Fossil Fische. In: Middendorf AT, ed. *Klimatologie Geognosie*. St. Petersburg: 259–263.

Müller S, Schlegel H. 1840. Beschrijving van een' nieuwen Zoetwater-visch van Borneo, *Osteoglossum formosum*. *Verhandelingen over de natuurlijke geschiedenis der Nederlandsche overzeesche bezittingen / door de Leden der Natuurkundige Commissie in Indië en andere schrijvers; uitgegeven ... door C. J. Temminck* 2: 1–7.

Murray AM, Wilson MVH. 2005. Description of a new Eocene osteoglossid fish and additional information on †*Singida jacksonoides* Greenwood and Patterson, 1967 (Osteoglossomorpha),

with an assessment of their phylogenetic relationships, *Zoological Journal of the Linnean Society* 144: 213–228.

Murray AM, Wilson MVH. 2013. Two new paraclupeid fishes (Clupeomorpha: Ellimmichthyiformes) from the Upper Cretaceous of Morocco. In: Arratia G, Schultze HP, Wilson MVH, eds. *Mesozoic Fishes 5 - Global Diversity and Evolution*. München: Verlag Dr. F. Pfeil, 267–290.

Murray AM, You HL, Peng C. 2010. A new Cretaceous osteoglossomorph fish from Gansu Province, China, *Journal of Vertebrate Paleontology* 30: 322–332.

Murray AM, Newbrey MG, Neuman AG, Brinkman DB. 2016. New articulated osteoglossomorph from Late Cretaceous freshwater deposits (Maastrichtian, Scollard Formation) of Alberta, Canada, *Journal of Vertebrate Paleontology* 36: e1120737.

Murray AM, Zelenitsky DK, Brinkman DB, Neuman AG. 2018. Two new Palaeocene osteoglossomorphs from Canada, with a reassessment of the relationships of the genus †*Joffrichthys*, and analysis of diversity from articulated versus microfossil material, *Zoological Journal of the Linnean Society* 183: 907–944.

Nakamura K, Yamaguchi H. 1991. Distribution of scleral ossicles in teleost fishes, *Memoirs of Faculty of Fisheries, Kagoshima University* 40: 1–20.

Nelson GJ. 1972. Observations on the gut of the Osteoglossomorpha, *Copeia* 17: 325–329.

Otero O, Gayet M. 2001. Palaeoichthyofaunas from the Lower Oligocene and Miocene of the Arabian Plate: palaeoecological and palaeobiogeographical implications, *Palaeogeography, Palaeoclimatology, Palaeoecology* 165: 141–169.

Otero O, Garcia G, Valentin X, Lihoreau F, Manthi FK, Ducrocq S. 2017. A glimpse at the ectotherms of the earliest fauna from the East African Rift (Lokone, Late Oligocene of Kenya), *Journal of Vertebrate Paleontology* 37: e1312691.

Patterson C. 1975. The distribution of Mesozoic freshwater fishes. *Memoires du Museum national d'Histoire naturelle de Paris, serie A* 88: 156–174.

Patterson C, Rosen DE. 1977. Review of ichthyodectiform and other Mesozoic teleost fishes, and the theory and practice of classifying fossils, *Bulletin of the American Museum of Natural History* 158: 81–172.

Peters WCH. 1852. Diagnosen von neuen Flussfischen aus Mossambique. *Monatsberichte der Königlichen Preussischen Akademie der Wissenschaften zu Berlin* 1852: 275–276, 681–685.

Peters WCH. 1876. Über eine merkwürdige von Hrn. Professor Dr. Buchholz entdeckte neue Gattung von Süsswasserfischen, Pantodon Buchholzi, welche zugleich eine neue, den Malacopterygii abdominales angehörige Gruppe von Fischen, Pantodontes, repräsentirt. *Monatsberichte der Königlichen Preussischen Akademie der Wissenschaften zu Berlin* 1876: 195–200.

Rafinesque CS. 1820. Fishes of the Ohio River, *Western Review and Miscellaneous Magazine: a monthly publishing, devoted to literature and science, Lexington, KY* 2: 169–177.

Rambaut A. 2012. Figtree v 1.4.0. http://tree.bio.ed.ac.uk/software/figtree/

Roellig HF. 1974. The cranial osteology of *Brychaetus muelleri* (Pisces Osteoglossidae) Eocene, Isle of Sheppey, *Journal of Paleontology* 48: 947–951.

Ronquist F, Teslenko M, Van Der Mark P, Ayres DL, Darling A, Höhna S, Larget B, Liu L, Suchard MA, Huelsenbeck JP. 2012. MrBayes 3.2: efficient Bayesian phylogenetic inference and model choice across a large model space, *Systematic Biology* 61: 539–542.

Rüppell WPES. 1828. *Atlas zu der Reise im nördlichen Afrika. Fische des Rothen Meers*. Frankfurt am Main: Heinrich Ludwig Brönner.

Sanders M. 1934. Die fossilen Fische der Alttertiären Süsswasserablagerungen aus Mittel-Sumatra. *Verhandelingen van het Geologisch-Mijnbouwkundig Genootschap voor Nederland en Koloni'n Geologische Series* 11: 1–144.

Sanford CPJ. 2000. Salmonoid fish osteology and phylogeny (Teleostei: Salmonoidei), *Theses Zoologicae* 33: 1–264.

Santos RS. 1985. *Laeliichthys ancestralis*, novo gênero e espécie de osteoglossiformes do Aptiano da Formaçâo, Estado de Minas Gerais, Brasil, *Coletânea de Trabalhos Paleontológicos, Congresso Brasileiro de Paleontologia. Departamento Nacional de Produção Mineral* 8: 161–167.

Sauvage HE. 1879. Notice sur la faune ichthyologique de l'Ogôoué. *Bulletin de la Société philomathique de Paris (7th Série)* 3: 90–103.

Schaeffer B. 1949. A teleost from the Livingston Formation of Montana. *American Museum Novitates* 1427: 1–16.

Schinz HR. 1822. *Das Thierreich eingetheilt nach dem Bau der Thiere als Grundlage ihrer Naturgeschichte und der vergleichenden Anatomie. Mit vielen Zusätzenversehen von H. R. Schinz*, 2. Cotta, Stuttgart & Tübingen.

Su D. 1986. The discovery of a fossil osteoglossid fish in China, *Vertebrata PalAsiatica* 24: 10–19.

Swofford DL. 2002. PAUP: Phylogenetic Analysis Using Parsimony (and Other Methods), Version 4.0 Beta 10. Sunderland: Sinauer Associates.

Taverne L. 1968. Ostéologie du genres *Gnathonemus* Gill sensu stricto, *Gnathonemus petersii* (Gthr.) et espèces voisines, *Annales du Musée Royal de l'Afrique Centrale, Sciences Zoologiques* 170: 1–91.

Taverne L. 1969. Etude ostéologique des genres *Boulengeromyrus* Taverne et Géry, *Genyomyrus* Boulenger, *Petrocephalus* Marcusen (Pisces Mormyriformes), *Annales du Musée Royal de l'Afrique Centrale, Sciences Zoologiques* 174: 1–85.

Taverne L. 1971. Ostéologie des genres *Marcusenius* Gill, *Hippopotamyrus* Pappenheim, *Cyphomyrus* Myers, *Pollimyrus* Taverne et *Brienomyrus* Taverne (Pisces, Mormyriformes), *Annales du Musée Royal de l'Afrique Centrale, Série In-8°, Sciences Zoologiques* 188: 1–143.

Taverne L. 1972. Ostéologie des genres *Mormyrus* Linné, *Mormyrops* Müller, *Hyperopisus* Gill, *Isichthys* Gill, *Myomyrus* Boulenger, *Stomatorhinus* Boulenger et *Gymnarchus* Cuvier: considérations générales sur la systématique des poissons de l'ordre des Mormyriformes, *Musée royal de l'Afrique centrale—Tervuren, Belgique Annales—Serie in-8°—Sciences Zoologiques* 200: 1–198.

Taverne L. 1977. Ostéologie, phylogénèse et systématique des Téléostéens fossiles et actuels du super-ordre des Ostéoglossomorphes, Première partie. Ostéologie des genres *Hiodon*, *Eohiodon*, *Lycoptera*, *Osteoglossum*, *Scleropages*, *Heterotis* et *Arapaima*, *Ac adémie Royale de Belgique, Mémoires de la Classe des Sciences, Collection in-8° - 2e série* 42: 1– 235.

Taverne L. 1978. Osteologie, phylogénèse et systématique des Téléostéens fossiles et actuels de super–ordre des Ostéoglossomorphes. Deuxième partie. Ostéologie des genres *Phareodus*, *Phareoides*, *Brychaetus*, *Musperia*, *Pantodon*, *Singida*, *Notopterus*, *Xeno mystus* et *Papyrocranus*, *Mémoires de la Classe des Sciences, Académie Royale de Belgique, Collection in–8°, 2e Série* 42: 1–213.

Taverne L. 1979. Osteologie, phylogénèse et systématique des Téléostéens fossiles et actuels de super-ordre des Ostéoglossomorphes. Troisième partie. Evolution des structures ostéologiques et conclusions générales relatives à la phylogénèse et à la systématique du super-ordre. Addendum, *Mémoires de la Classe des Sciences, Académie Royale de Belgique, Collection in-8°, 2e Série* 43: 1–168.

Taverne L. 1998. Les Ostéoglossomorphes marins de l'Eocène du Monte Bolca (Italie): *Monopteros* Volta, 1796, *Thrissopterus* Heckel, 1856 et *Foreyichthys* Taverne, 1979. Considérations sur la phylogénie des Téléostéens ostéoglossomorphes, *Studi e ricerche sui giacimenti Terziari di Bolca*, *Miscellanea Paleontologica* 7: 67–158.

Taverne L. 2009. *Ridewoodichthys*, a new genus for *Brychaetus caheni* from the marine Paleocene of Cabinda (Africa): re-description and comments on its relationships within the Osteoglossidae (Teleostei, Osteoglossomorpha), *Bulletin de l'Institut Royal des Sciences Naturelles de Belgique, Sciences de la Terre* 79: 147–153.

Taverne L, Nolf D, Folie A. 2007. On the presence of the osteoglossid fish genus *Scleropages* (Teleostei, Osteoglossiformes) in the continental Paleocene of Hainin (Mons Basin, Belgium), *Belgian Journal of Zoology* 137: 89–97.

Trifinopoulos J, Nguyen LT, von Haeseler A, Minh BQ. 2016. W-IQ-TREE: a fast online phylogenetic tool for maximum likelihood analysis, *Nucleic Acids Research* 44: W232–W235.

Volta GS. 1806. *Ittiolitologia veronese del Museo Bozziano ora annesso a quello del Conte Giovambattista Gazola e di altri gabinetti di fossili veronesi*, part 2: 53–236.

Westneat MW. 2004. Evolution of levers and linkages in the feeding mechanisms of fishes, *Integrative and Comparative Biology* 44: 378–389.

Wilson MVH, Murray AM. 2008. Osteoglossomorpha: phylogeny, biogeography, and fossil record and the significance of key African and Chinese fossil taxa, *Geological Society of London, Special Publications* 295: 185–219.

Woodward AS. 1901. *Catalogue of fossil fishes in the British Museum (Natural History). Part IV*. London: Longmans and Co.

Xu GH, Chang MM. 2009. Redescription of †*Paralycoptera wui* Chang & Chou, 1977 (Teleostei: Osteoglossoidei) from the Early Cretaceous of eastern China, *Zoological Journal of the Linnean Society* 157: 83–106.

Yans J, Amaghzaz MB, Bouya B, Cappetta H, Iacumin P, Kocsis L, Mouflih M, Selloum O, Sen S, Storme JY, Gheerbrant E. 2014. First carbon isotope chemostratigraphy of the Ouled Abdoun phosphate Basin, Morocco; implications for dating and evolution of earliest African placental mammals, *Gondwana Research* 25: 257–269.

Zhang JY. 2002. A new species of *Lycoptera* from Liaoning, China, *Vertebrata PalAsiatica* 40: 257–266.

Zhang JY. 2003. First *Phareodus* (Osteoglossomorpha: Osteoglossidae) from China, *Vertebrata PalAsiatica* 41: 327–334.

Zhang JY. 2004. New fossil osteoglossomorph from Ningxia, China, *Journal of Vertebrate Paleontology* 24: 515–524.

Zhang JY. 2020. A new species of *Scleropages* (Osteoglossidae, Osteoglossomorpha) from the Eocene of Guangdong, China, *Vertebrata PalAsiatica* 58: 100–119.

Zhang JY, Wilson MVH. 2017. First complete fossil *Scleropages* (Osteoglossomorpha), *Vertebrata PalAsiatica* 55: 1–23.

Zouhri S. (ed.) 2017. *Paléontologie des vertébrés du Maroc: état des connaissances*. Mémoires de la Société géologique de France, 180.

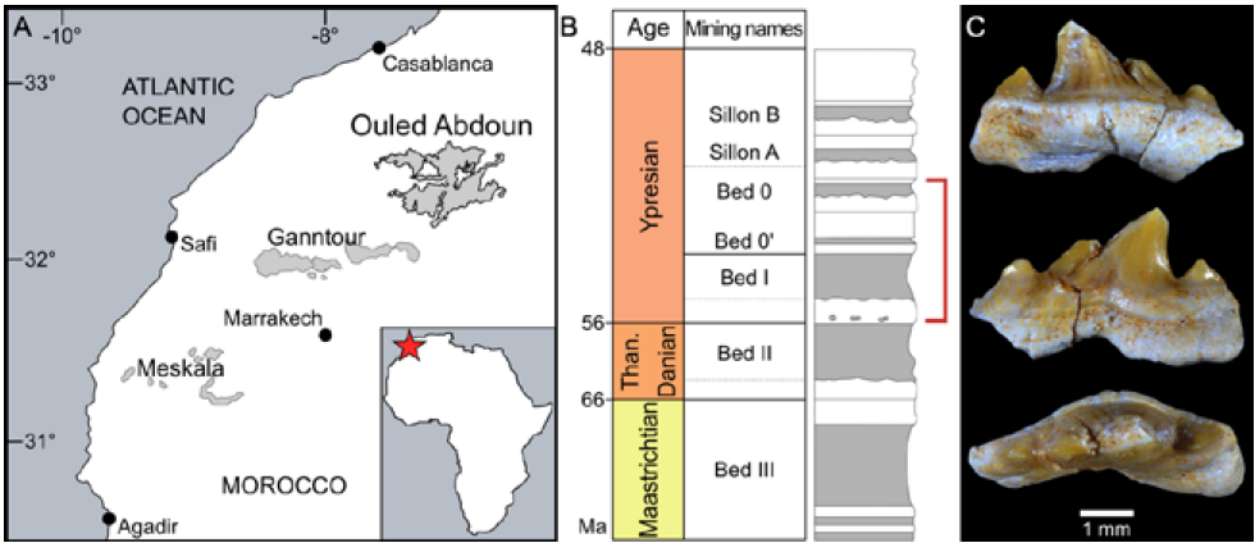

Figure 1. Geographic and stratigraphic context for the holotype of †*Macroprosopon hiltoni* (FSAC CP 330). A, geographic distribution of phosphorite deposits (in grey) in Morocco (modified from Yans *et al*., 2014); B, simplified stratigraphic chart of the Ouled Abdoun Basin deposits, with phosphorite sands in grey (modified from Yans *et al*., 2014). Red bracket indicates possible range of FSAC CP 330, based on lithology and ichthyoliths associated with the specimen. C, posterior tooth of ?*Brachycarcharias atlasi* found embedded in the matrix of FSAC CP 330, in labial, lingual and occlusal views (from top to bottom). Scale bar: 1 mm.


5 cm

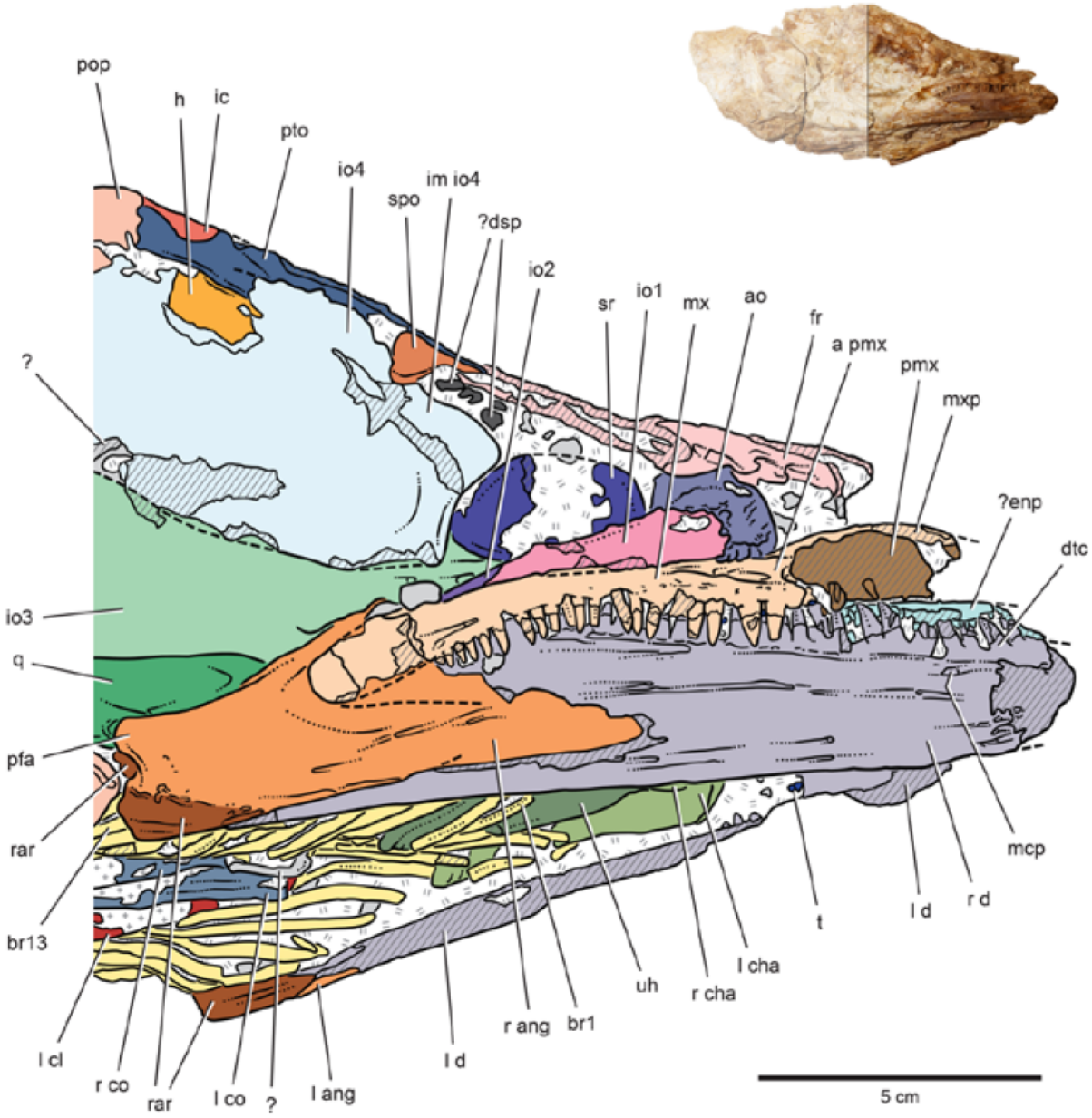

Figure 2. †*Macroprosopon hiltoni* (holotype, FSAC CP 330). Photograph in right lateral view, anterior portion of the specimen. Inset at top right shows highlighted portion compared to the whole specimen. Scale bar: 50 mm.

Figure 3. †*Macroprosopon hiltoni* (holotype, FSAC CP 330). Interpretative weighted-line drawing in right lateral view, anterior portion of the specimen. Inset at top right shows highlighted portion

compared to the whole specimen. Parallel lines indicate broken bone surface; plus-sign pattern indicates scales; double-line pattern indicates matrix. Dashed lines indicate a missing margin. Scale bar: 50 mm. Abbreviations: a pmx, articular surface for the premaxilla; ang, angular; ao, antorbital; br1, branchiostegal ray 1; br13, branchiostegal ray 13; cha, anterior ceratohyal; cl, cleithrum; co, coracoid; d, dentary; dsp, dermosphenotic; dtc, dentary tooth collar; enp, endopterygoid; fr, frontal; h, hyomandibula; ic, intercalar; im, impression of; io1–io4, infraorbitals 1–4; l, left; mcp, mandibular canal pore; mx, maxilla; mxp, anterior process of maxilla; pfa, posterodorsal flange of the angular; pmx, premaxilla; pop, preopercle; pto, pterotic; q, quadrate; r, right; rar, retroarticular; spo, sphenotic; sr, sclerotic ring; t, tooth; uh, urohyal; ?,uncertain or unidentified bone.

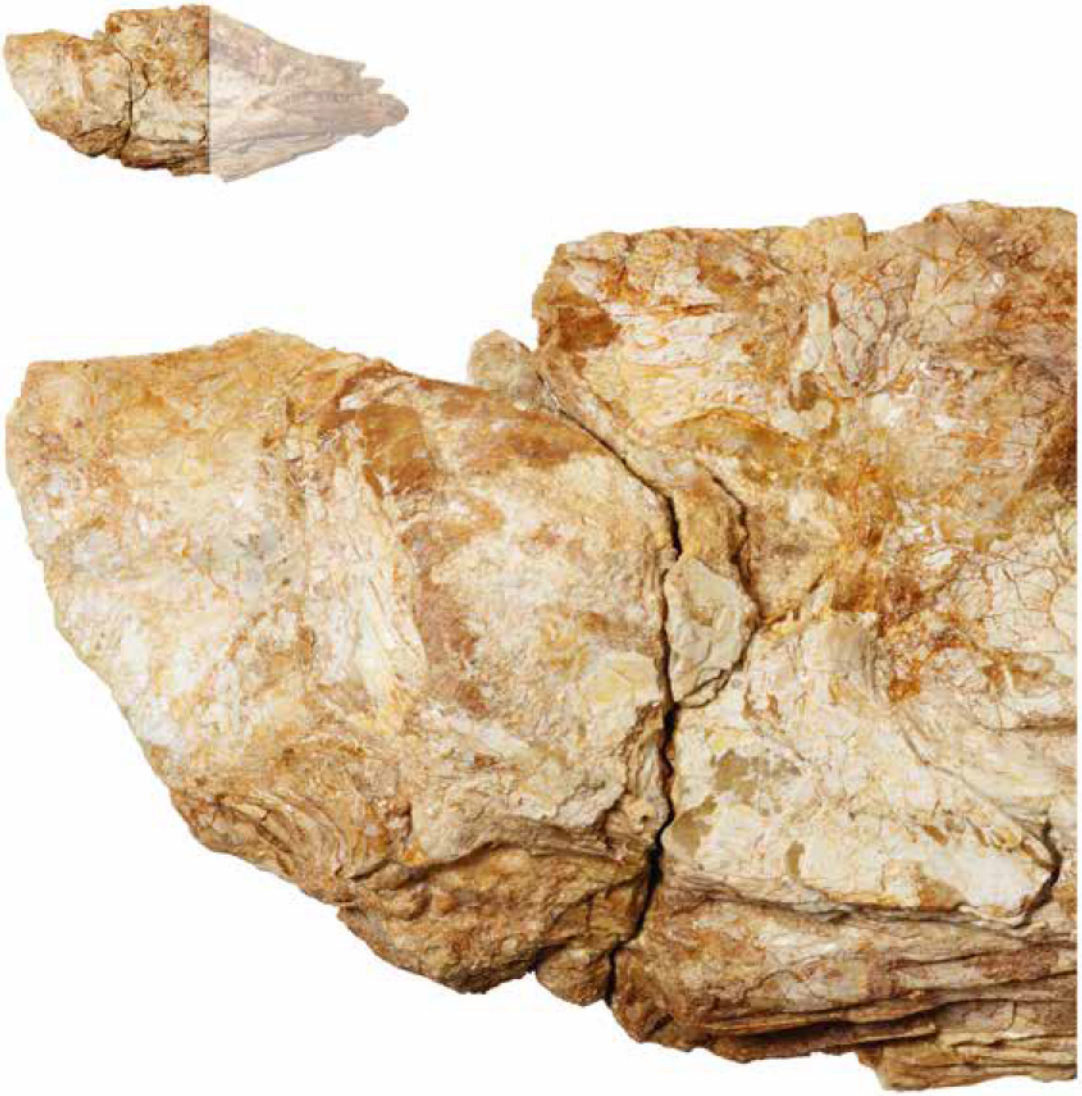
5 cm

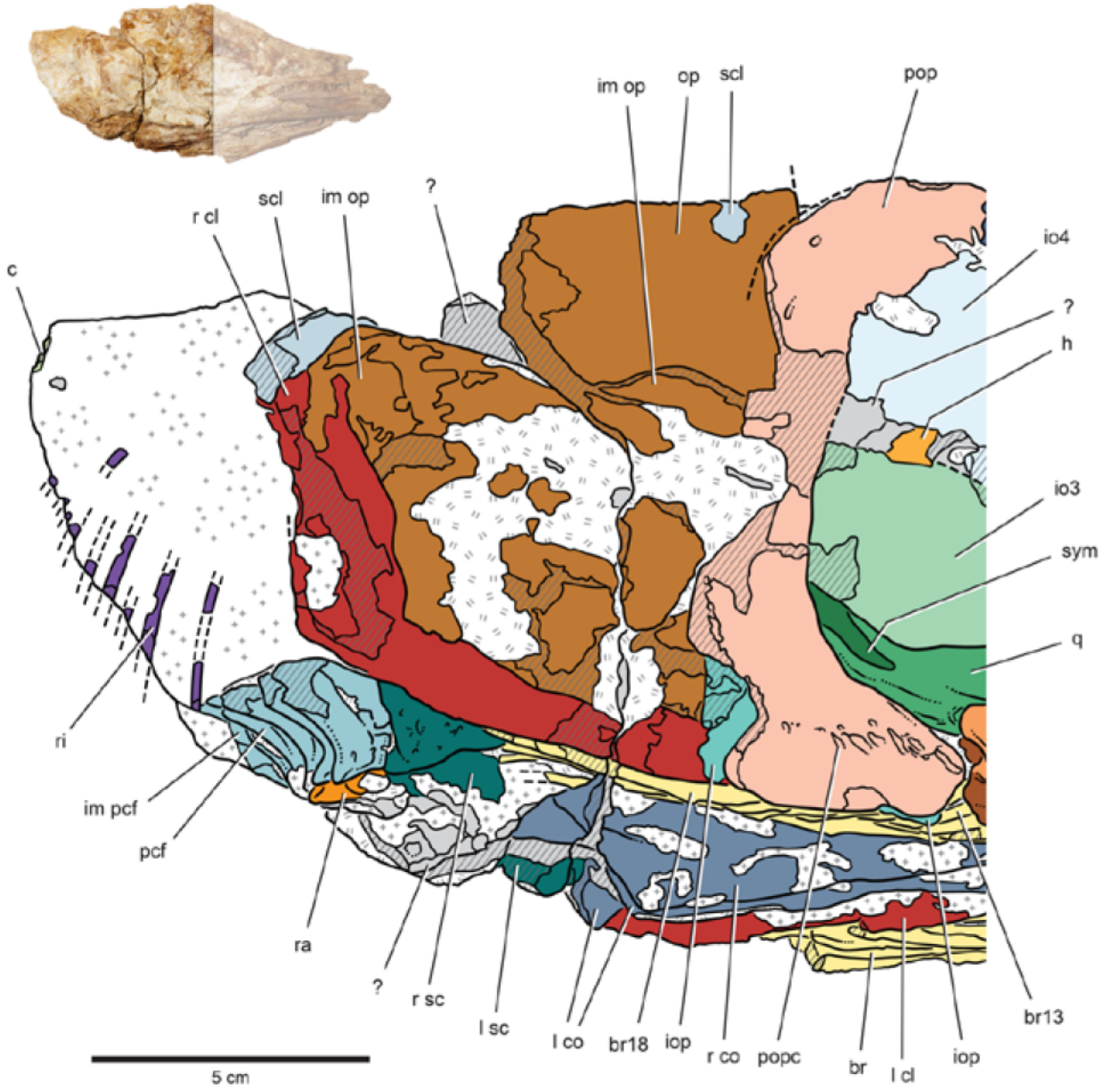

Figure 4. †*Macroprosopon hiltoni* (holotype, FSAC CP 330). Photograph in right lateral view, posterior portion of the specimen. Inset at top left shows highlighted portion compared to the whole specimen. Scale bar: 50 mm.

Figure 5. †*Macroprosopon hiltoni* (holotype, FSAC CP 330). Interpretative weighted-line drawing in right lateral view, posterior portion of the specimen. Inset at top left shows highlighted portion

compared to the whole specimen. Parallel lines indicate broken bone surface; plus-sign pattern indicates scales; double-line pattern indicates matrix. Dashed lines indicate a missing margin. Scale bar: 50 mm. Abbreviations: a pfa, articular surface for the posterodorsal flange of the angular; br, branchiostegal ray; br13, branchiostegal ray 13; br18, branchiostegal ray 18; c, centrum; cl, cleithrum; co, coracoid; h, hyomandibula; im, impression of; io3, infraorbital 3; io4, infraorbital 4; iop, interopercle; l, left; op, opercle; pcf, pectoral fin ray; pop, preopercle; popc, opening of preopercular sensory canal; q, quadrate; r, right; ra, radial; ri, rib; sc, scapula; scl, supracleithrum; sym, symplectic; ?, unidentified bone.

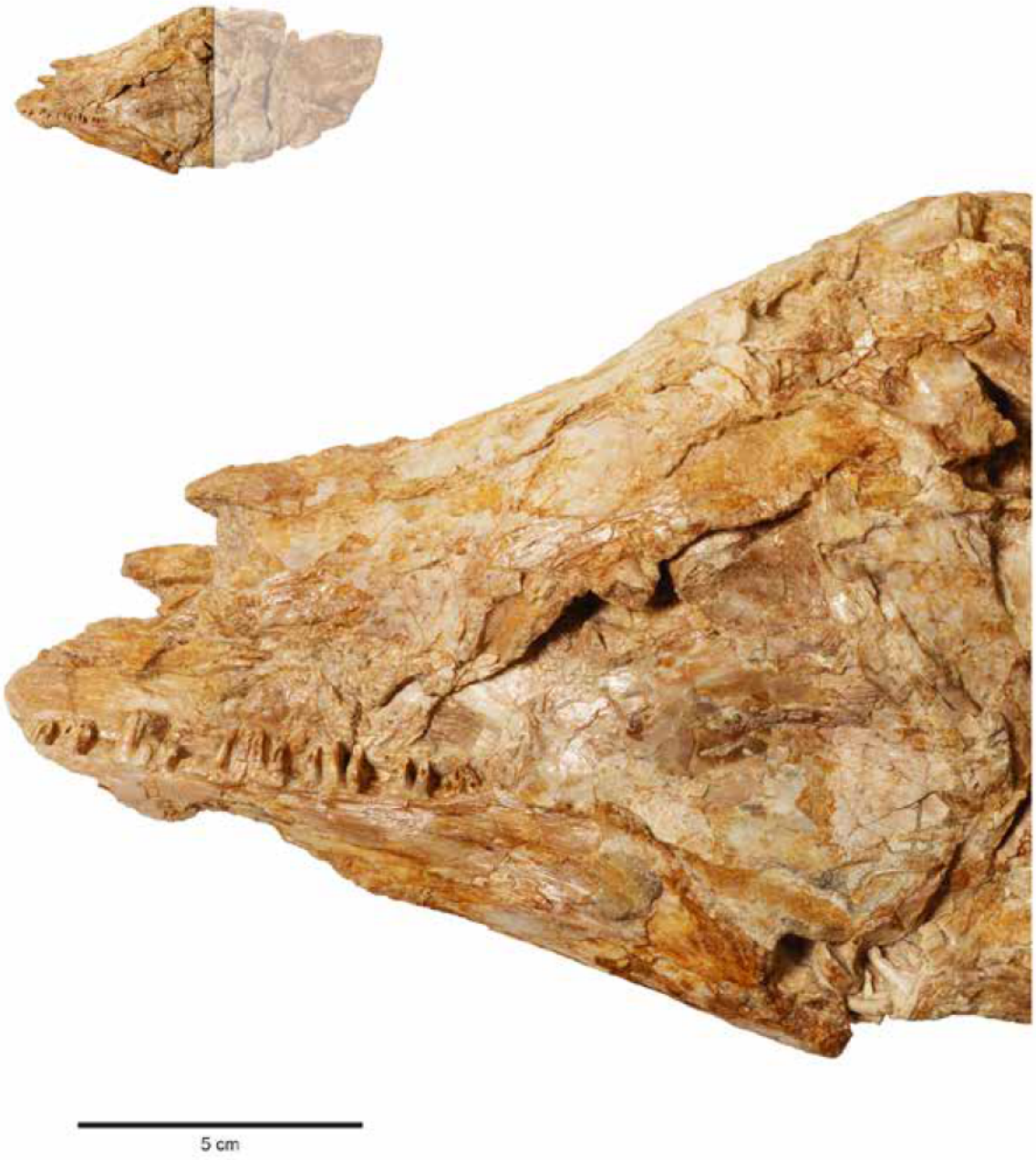
5 cm

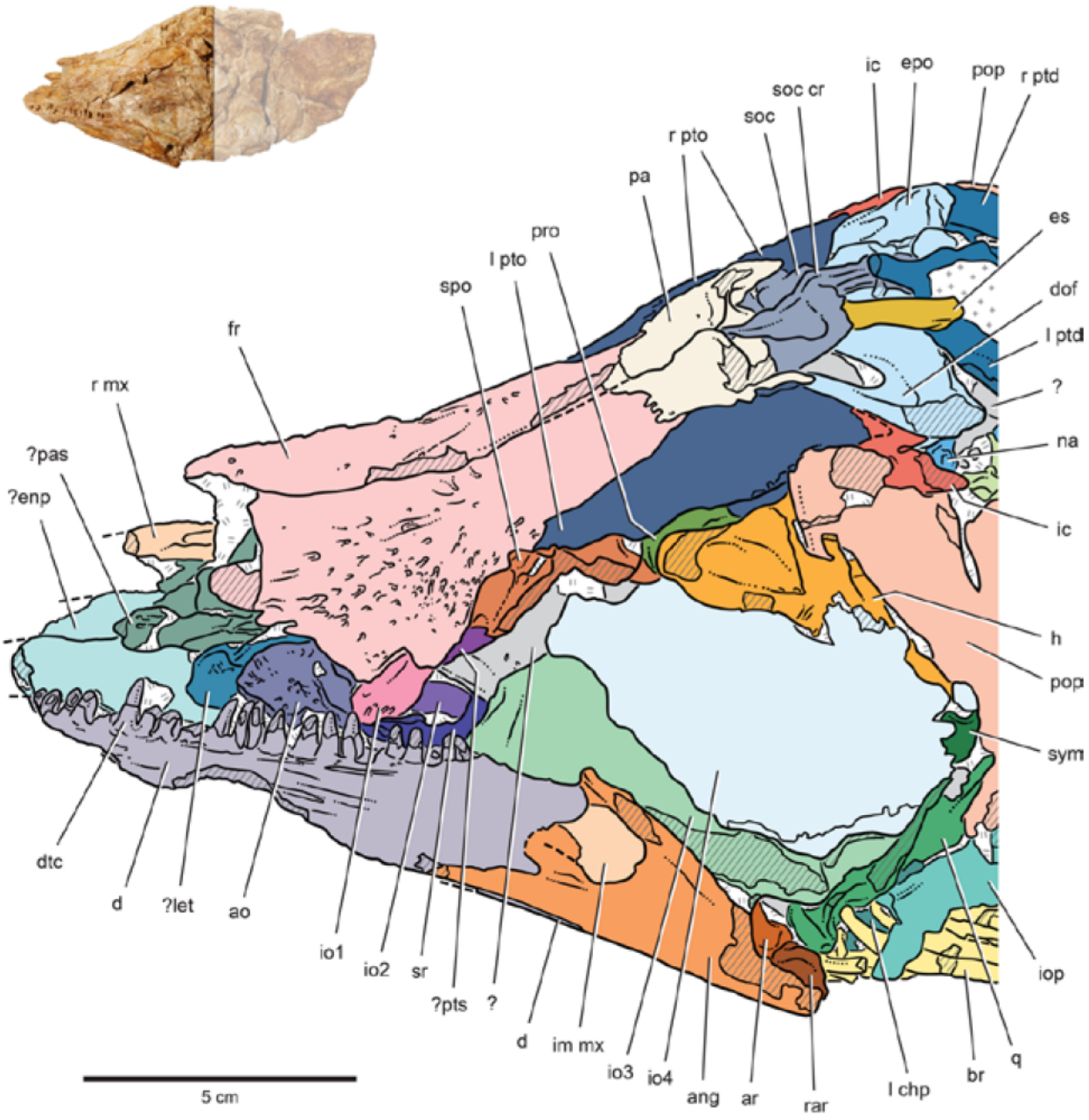

Figure 6. †*Macroprosopon hiltoni* (holotype, FSAC CP 330). Photograph in left lateral view, anterior portion of the specimen. Inset at top right shows highlighted portion compared to the whole specimen. Scale bar: 50 mm.

Figure 7. †*Macroprosopon hiltoni* (holotype, FSAC CP 330). Interpretative weighted-line drawing in left lateral view, anterior portion of the specimen. Inset at top right shows highlighted portion compared

to the whole specimen. Parallel lines indicate broken bone surface; plus-sign pattern indicates scales; double-line pattern indicates matrix. Dashed lines indicate a missing margin. Scale bar: 50 mm. Abbreviations: ang, angular; ao, antorbital; ar, articular; br, branchiostegal ray; chp, posterior ceratohyal; d, dentary; dof, dorso-occipital fossa; dsp, dermosphenotic; dtc, dentary tooth collar; enp, endopterygoid; epo, epioccipital; es, extrascapular; fr, frontal; h, hyomandibula; ic, intercalar; im, impression of; io1–io4, infraorbitals 1–4; iop, interopercle; l, left; le, lateral ethmoid; mx, maxilla; na, neural arch; pa, parietal; pas, parasphenoid; pop, preopercle; pro, prootic; ptd, dorsal arm of posttemporal; pto, pterotic; q, quadrate; r, right; rar, retroarticular; sc, scapula; soc, supraoccipital; soc cr, supraoccipital crest; spo, sphenotic; sr, sclerotic ring; sym, symplectic; ?, uncertain or unidentified bone.


5 cm

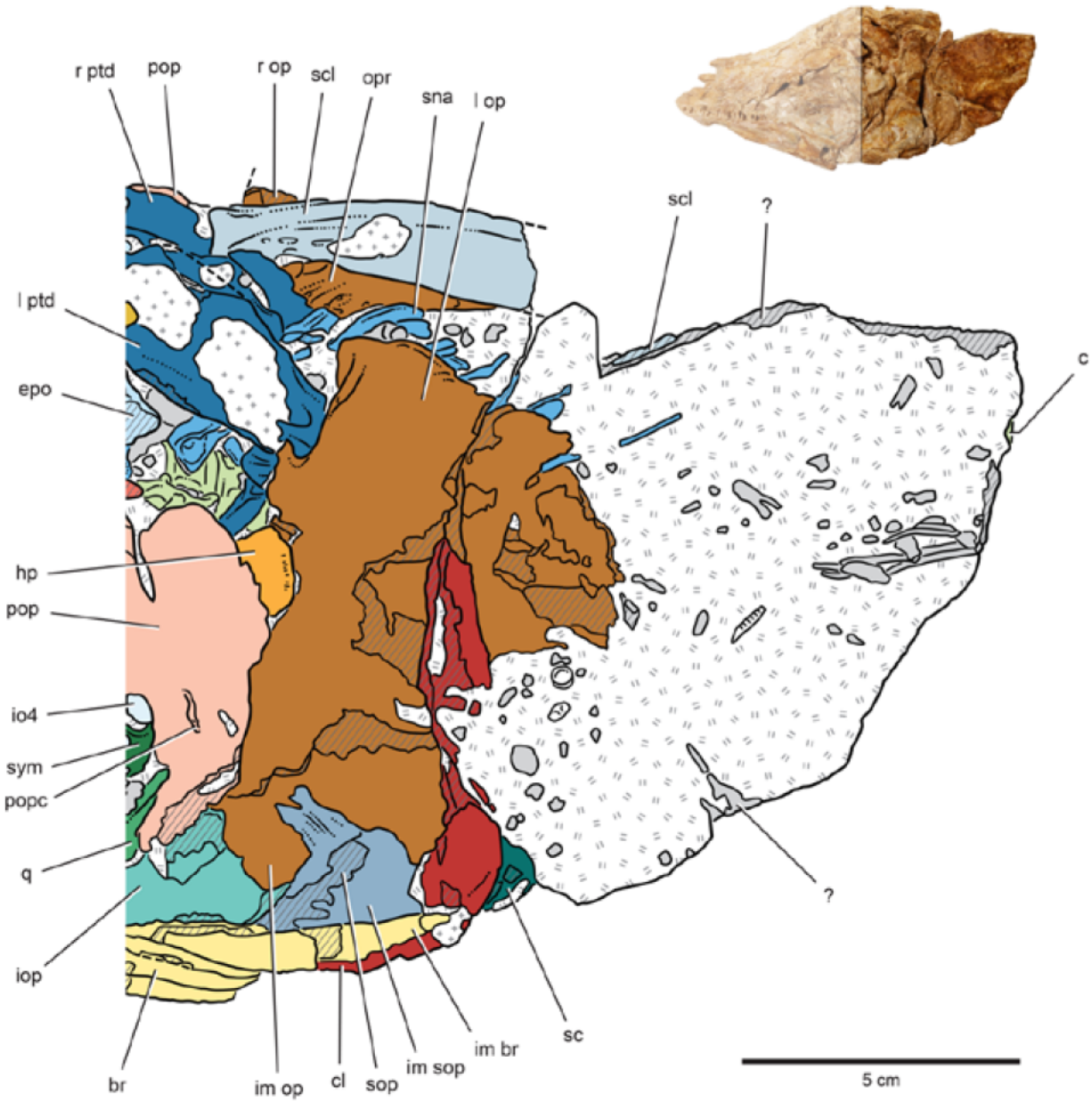

Figure 8. †*Macroprosopon hiltoni* (holotype, FSAC CP 330). Photograph in left lateral view, posterior portion of the specimen. Inset at top left shows highlighted portion compared to the whole specimen. Scale bar: 50 mm.

Figure 9. †*Macroprosopon hiltoni* (holotype, FSAC CP 330). Interpretative weighted-line drawing in left lateral view, posterior portion of the specimen. Inset at top left shows highlighted portion compared

to the whole specimen. Parallel lines indicate broken bone surface; plus-sign pattern indicates scales; double-line pattern indicates matrix. Dashed lines indicate a missing margin. Scale bar: 50 mm. Abbreviations: br, branchiostegal ray; c, centrum; cl, cleithrum; epo, epioccipital; hp, opercular head of hyomandibula; im, impression of; io4, infraorbital 4; iop, interopercle; l, left; op, opercle; opr, opercular ridge; pop, preopercle; popc, opening of the preopercle sensory canal; ptd, dorsal arm of posttemporal; q, quadrate; r, right; sc, scapula; scl, supracleithrum; sna, spine of neural arch; sop, subopercle; sym, symplectic; ?, unidentified bone.

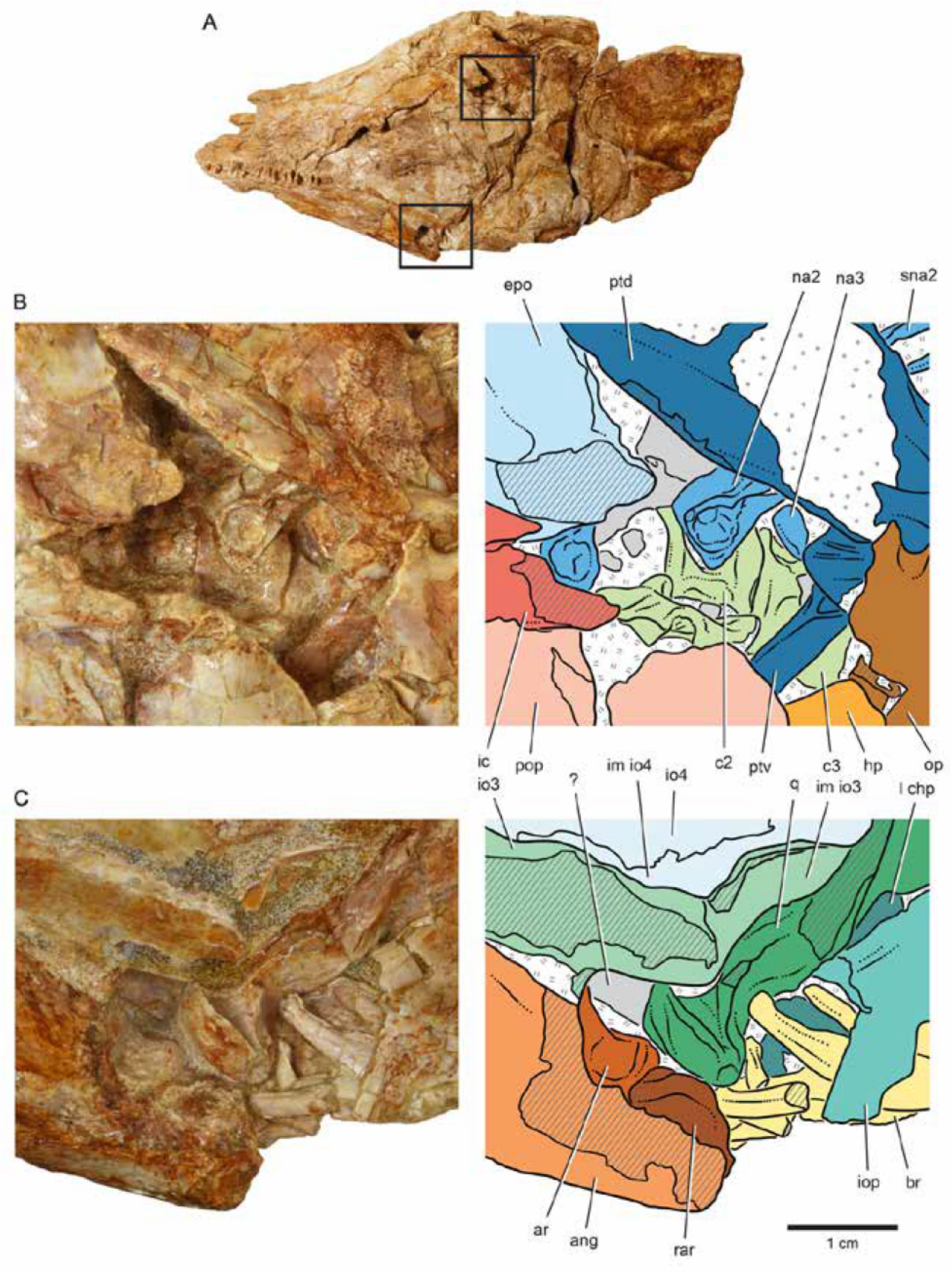

Figure 10. †*Macroprosopon hiltoni* (holotype, FSAC CP 330), anatomical details. A, holotype in left lateral view, with rectangles highlighting areas of interest depicted in panels B and C; B, photograph

and weighted-line drawing of post-occipital region, showing exposed portions of the vertebral column; C, photograph and weighted-line drawing of the articulation between quadrate and lower jaw. Parallel lines indicate broken bone surface; plus-sign pattern indicates scales; double-line pattern indicates matrix. Scale bar: 10 mm. Abbreviations: ang, angular; ar, articular; br, branchiostegal ray; c2, second vertebral centrum; c3, third vertebral centrum; chp, posterior ceratohyal; epo, epioccipital; hp, posterior (=opercular) process of the hyomandibula; ic, intercalar; im, impression of; io3, infraorbital 3; io4, infraorbital 4; iop, interopercle; l, left; na2, neural arch of the second vertebra; na3, neural arch of the third vertebra; op, opercle; pop, preopercle; ptd, dorsal arm of posttemporal; ptv, ventral arm of the posttemporal; q, quadrate; rar, retroarticular; sna2, spine of the second neural arch; ?, unidentified bone.

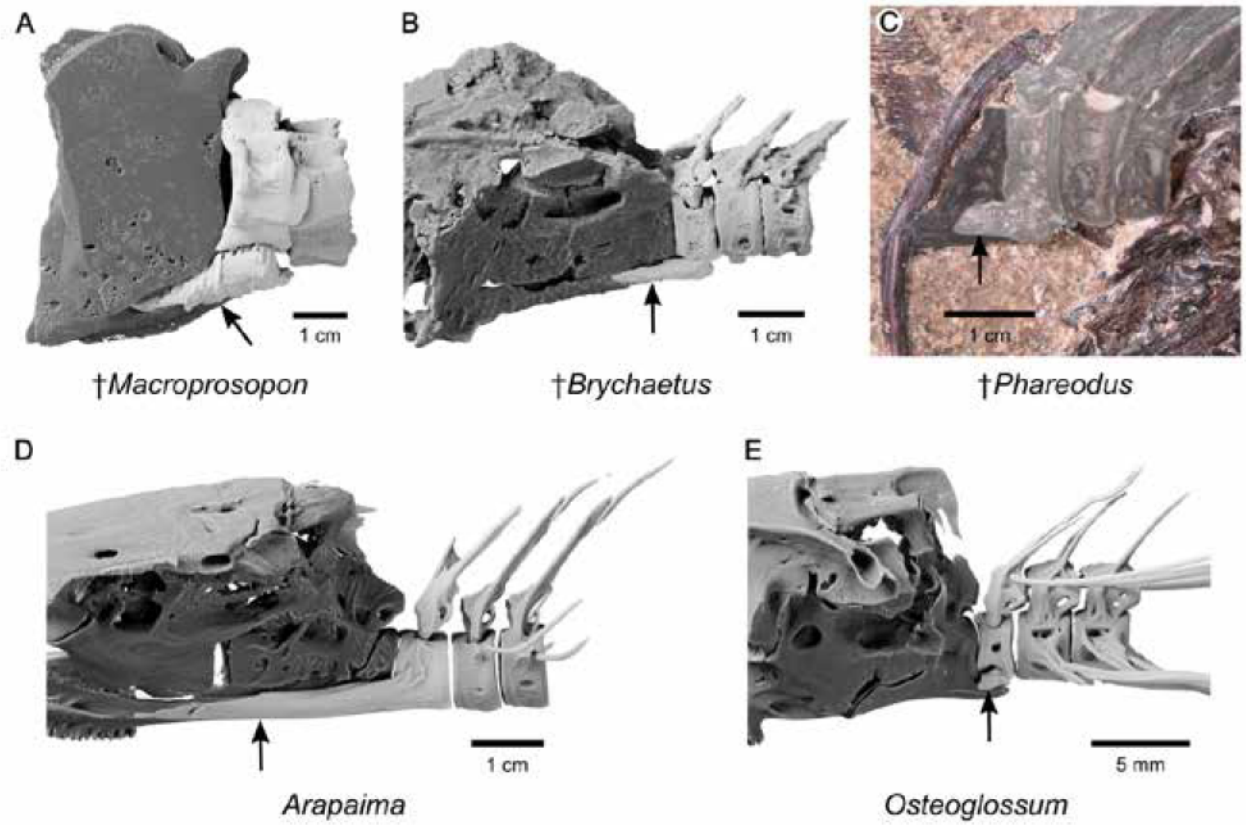

Figure 11. Left lateral view of the occipital region of the braincase and the first few vertebrae in Osteoglossidae. Arrows point to the enlarged parapophysis ventral to the first vertebral centrum

(character 88). Notice that in *Arapaima* and in the fossil taxa shown here, the first parapophysis is greatly hypertrophied and extends anteriorly below the braincase (state 2). A, †*Macroprosopon hiltoni* (FSAC CP 330; braincase model approximate due to insufficient contrast in tomography data); B, †*Brychaetus muelleri* (NHMUK PV P641); C, †*Phareodus encaustus* (FMNH PF 10257); D, *Arapaima gigas* (UF 33107); E, *Osteoglossum bicirrhosum* (UF 189007). Shades of grey indicate different anatomical regions: neurocranium (dark grey); first, second and third vertebrae (lighter shades of grey). Scale bars: 10 mm (A, B, C, D); 5 mm (E).

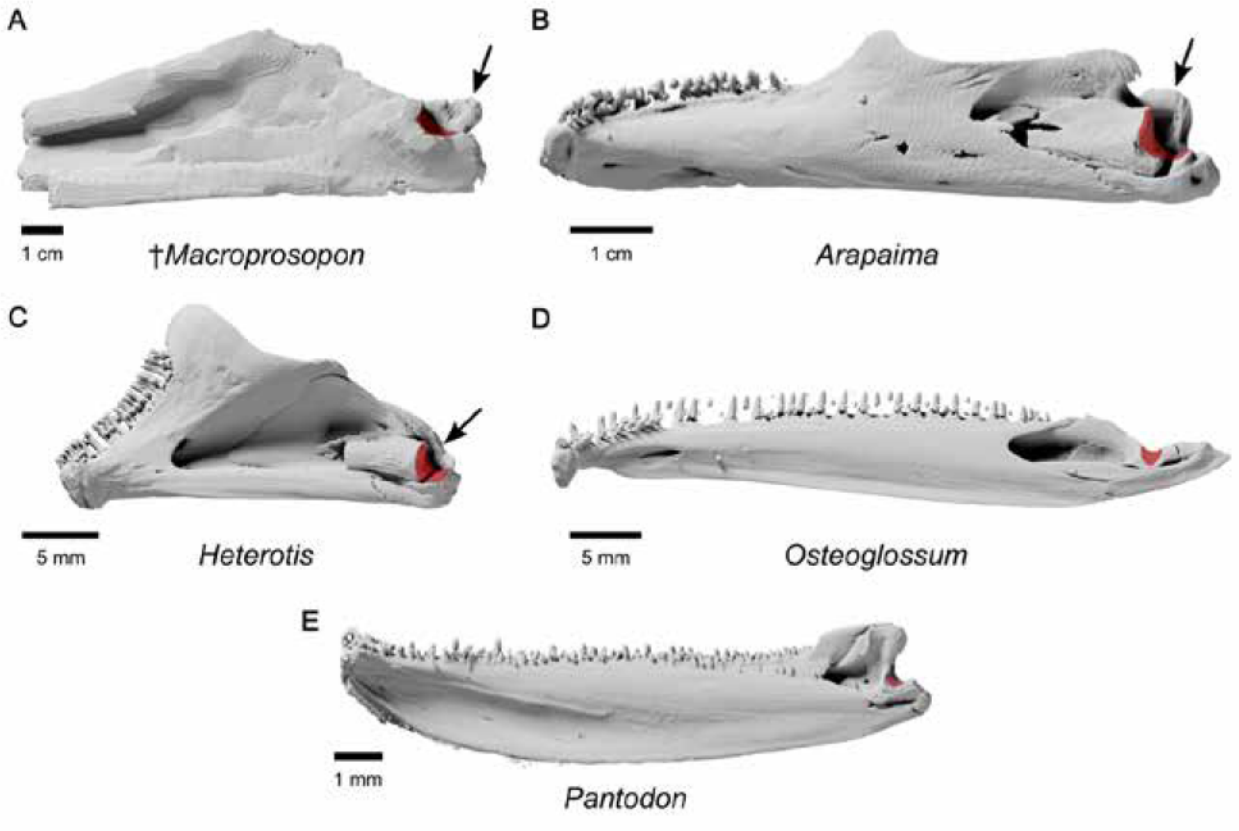

Figure 12. Right lower jaws of osteoglossomorphs in medial view (digital renderings). The red shade indicates the articular surface of the quadrate-lower jaw articulation. The arrows point to the postero-dorsal flange of the angular, when present (character 93, state 1). A, †*Macroprosopon hiltoni* (FSAC CP 330; partial lower jaw); B, *Arapaima gigas* (UF 33107); C, *Heterotis niloticus* (UMMZ 195004);

D, *Osteoglossum bicirrhosum* (UF 189007); E, *Pantodon buchholzi* (UMMZ 249782). Scale bars: 10 mm (A, B); 5 mm (C, D); 1 mm (E).

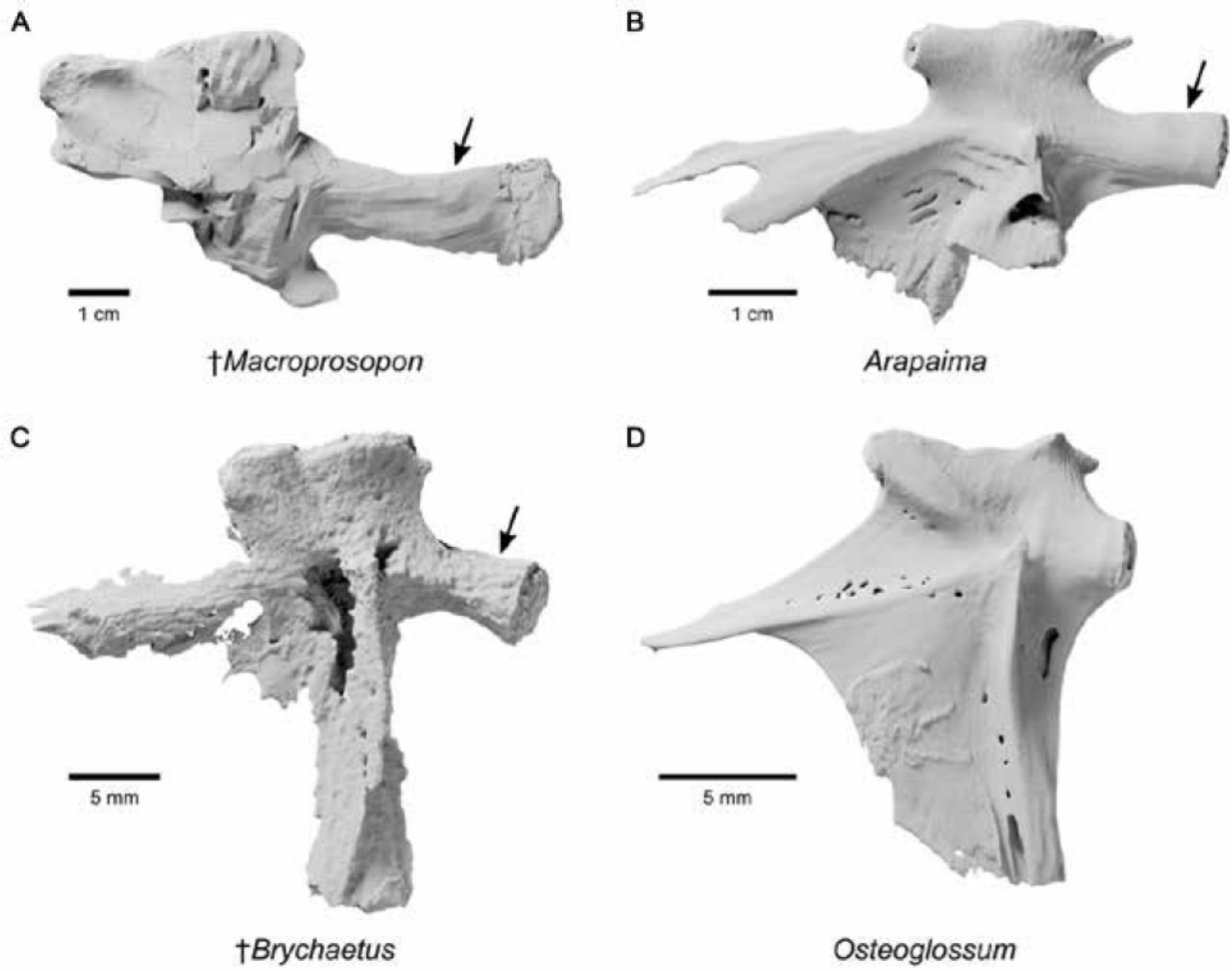

Figure 13. Posterior process of the hyomandibula in osteoglossomorphs. Lateral views of left hyomandibulae (digital renderings). Arrows point to a long (more than half the length of the dorsal articulating surface of the hyomandibula) posterior process (character 94, state 1). A, †*Macroprosopon hiltoni* (FSAC CP 330; partial hyomandibula); B, *Arapaima gigas* (UF 33107); C, cf. †*Brychaetus* sp. (NHMUK PV P26758); D, *Osteoglossum bicirrhosum* (UF 189007). Scale bars: 10 mm (A, B); 5 mm (C, D).

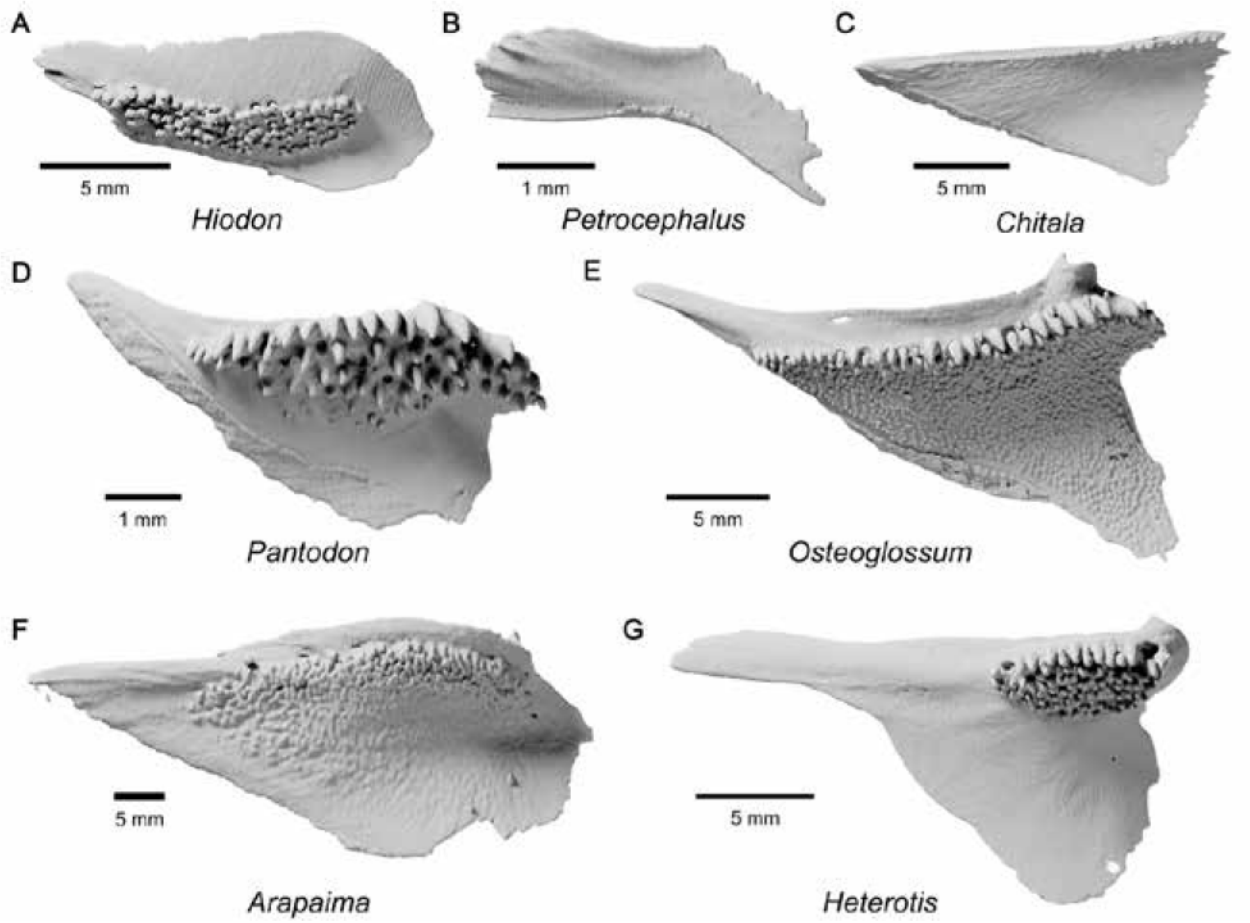

Figure 14. Endopterygoid dentition (character 95) in extant osteoglossomorphs. Medial views of right endopterygoids (digital renderings). State 0 (patch of shagreen-like fine teeth or small conical teeth) is represented by *Hiodon*, *Chitala*, and *Arapaima*; state 1 (few rows of large conical teeth) by *Pantodon* and *Heterotis*; state 2 (one or more medio-dorsal rows of large conical teeth, bordered laterally by a patch of shagreen-like fine teeth) by *Osteoglossum*; state 3 (teeth absent or extremely reduced) by *Petrocephalus*. A, *Hiodon tergisus* (UMMZ 247425); B, *Petrocephalus simus* (UMMZ 200167); C, *Chitala blanci* (UMMZ 232272); D, *Pantodon buchholzi* (UMMZ 249782); E, *Osteoglossum bicirrhosum* (UF 189007); F, *Arapaima gigas* (UF 33107); G, *Heterotis niloticus* (UMMZ 195004). Scale bars: 5 mm (A, C, E, F, G); 1 mm (B, D).

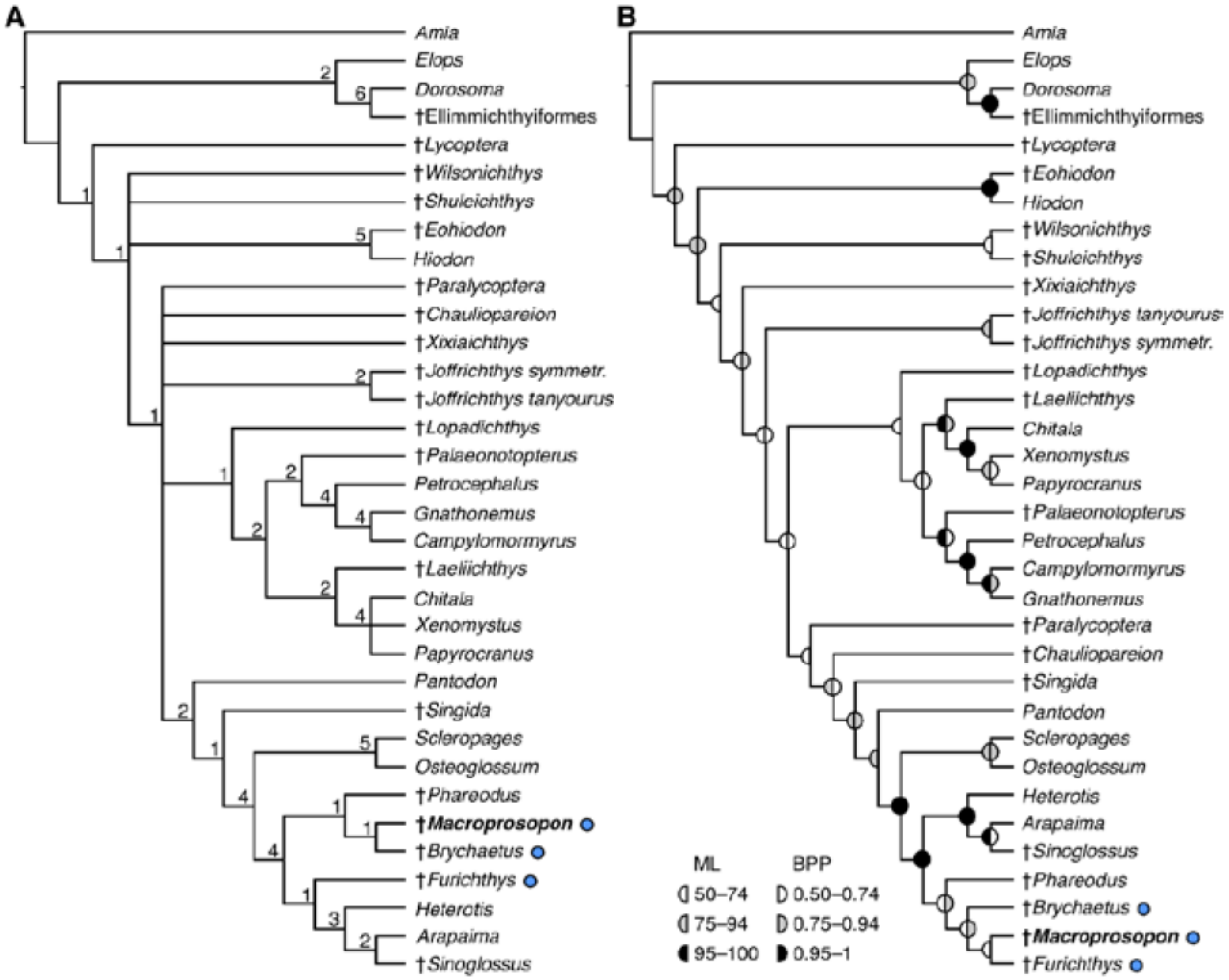

Figure 15. Phylogenetic relationships of Osteoglossomorpha. The position of †*Macroprosopon hiltoni* is highlighted in bold. Marine taxa are marked with a blue dot. A, strict consensus tree of 20 maximum parsimony phylogenies, with Bremer decay indices above nodes; B, tree topology shared by the maximum likelihood and Bayesian consensus trees. Statistical support values for nodes are indicated by shaded semicircles. Maximum likelihood bootstrap percentages (ML) and Bayesian posterior probabilities (BPP) are represented by the left and right semicircles, respectively. Nodes without a right semicircle have less than 0.50 BPP.

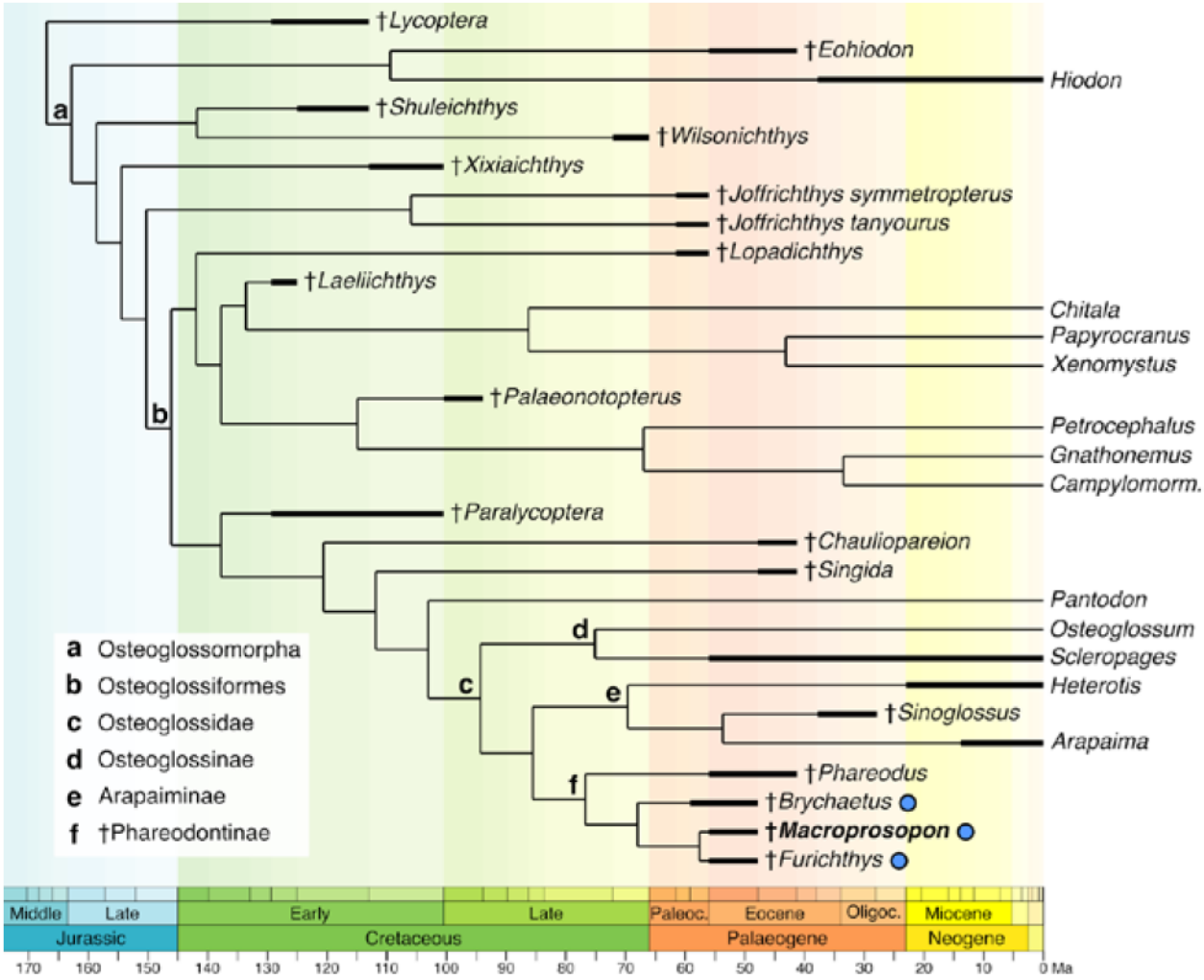

Figure 16. Time-scaled phylogenetic tree of Osteoglossomorpha, based on the topology of the maximum likelihood phylogeny. The position of †*Macroprosopon hiltoni* is highlighted in bold. Marine taxa are marked with a blue dot. Stage-level temporal ranges of taxa with fossil record are indicated by solid black bars. Node ages are plotted with the 'equal' method of *a posteriori* time-scaling with user-defined root age using the DatePhylo function in the R package `strap` (Bell and Lloyd, 2015); these are not analytical estimates under an evolutionary model and serve only a visualization purpose. Root age is fixed to the minimum fossil-based age for total-group Osteoglossomorpha estimated in Capobianco and Friedman (2019).

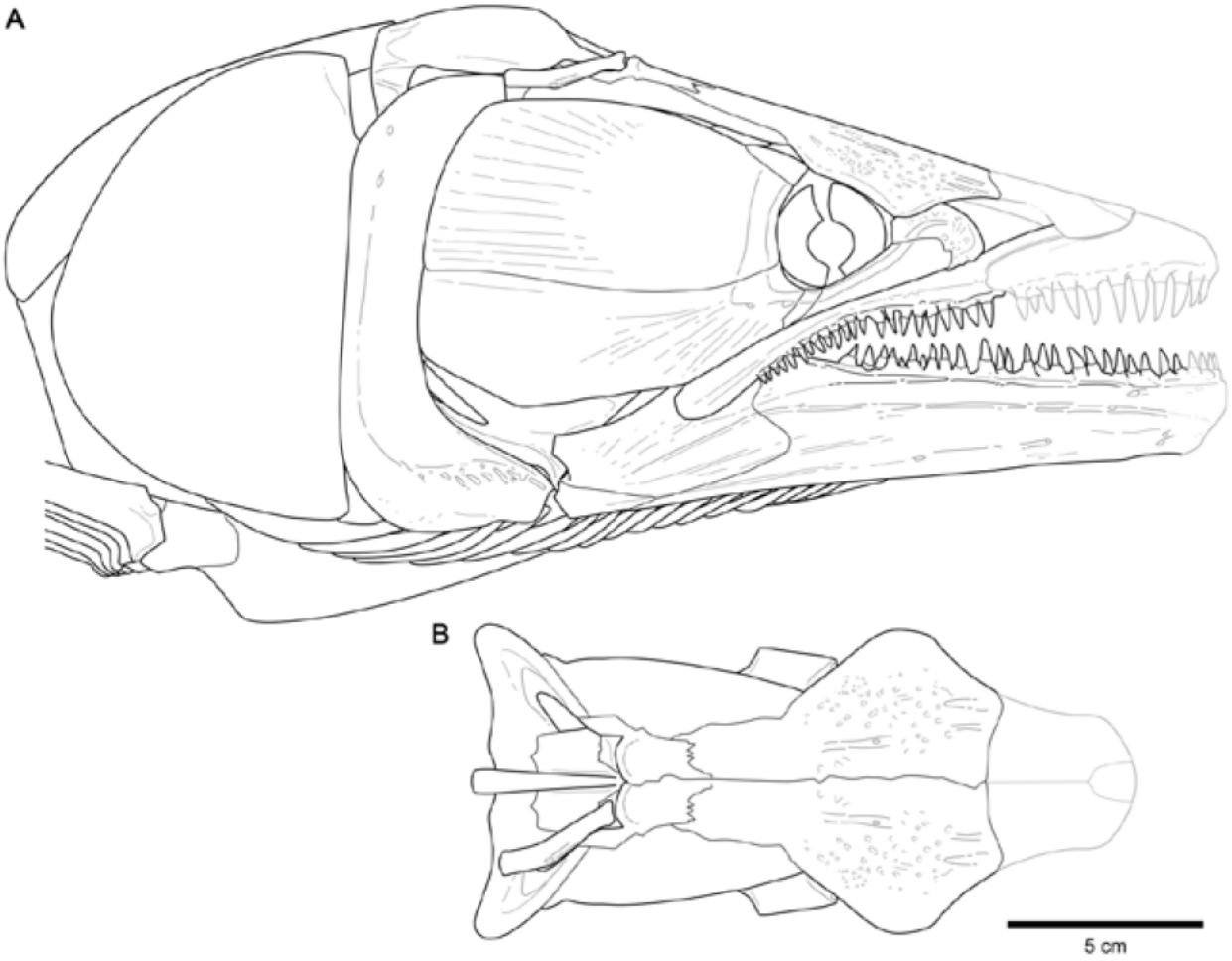

Figure 17. Artistic reconstruction of the long-snouted marine bonytongue †*Macroprosopon hiltoni*. A, skull and pectoral girdle in right lateral view; B, neurocranium in dorsal view. Speculative reconstructed bones are in grey line. Snout length is reconstructed conservatively with the shortest possible length given the preservation of the holotype. The left extrascapular is removed from the neurocranium in dorsal view to reveal the dorso-occipital fossa. Reconstruction by Sky Jung. Scale bar: 50 mm.

SUPPORTING INFORMATION

Character Definitions and Morphological Matrix

Character definitions

This character list is a modification of the Murray *et al*. (2018) character list, with the addition of characters 89–96 and changes to preexisting characters detailed in the main text.

(1) Temporal fossa

0 = absent; 1 = present, with the exoccipital making a contribution to the border; 2 = present, bordered by epioccipital, pterotic and parietal; 3 = present, bordered by epioccipital and pterotic

(2) Shape of extrascapular

0 = expanded; 1 = reduced and irregularly shaped; 2 = reduced and tubular

(3) Shape of frontal bones

0 = anterior margin narrower than posterior margin; 1 = anterior margin about equal in width to posterior margin; 2 = anterior margin wider than posterior margin

(4) Supraorbital shelf of frontal bone

0 = absent; 1 = present

(5) Length of frontal bone

0 = over twice as long as parietal; 1 = less than twice as long as parietal

(6) Relationship of nasal bones

0 = some part separated by anterior portion of frontals; 1 = separated only by ethmoid bones; 2 = meet each other in midline

(7) Nasal bones

0 = tubular but not curved; 1 = tubular and strongly curved; 2 = gutter-like; 3 = flat and broad

(8) Parasphenoid teeth

0 = absent; 1 = small; 2 = large and found along the length of the parasphenoid; 3 = large and restricted to the basal portion of the parasphenoid

(9) Basipterygoid process

0 = absent; 1 = present

(10) Supratemporal commissure passing through the parietals

0 = absent; 1 = present

(11) Supraorbital sensory canal

0 = ending in parietal; 1 = ending in frontal

(12) Orbitosphenoid

0 = present; 1 = absent

(13) Basisphenoid

0 = present; 1 = absent

(14) Basioccipital process of the parasphenoid

0 = divided; 1 = median

(15) Ventral occipital groove

0 = present; 1 = absent

(16) Intercalar

0 = present; 1 = absent

(17) Foramen/foramina for anteroventral lateral line nerve plus cranial nerve V

0 = in the prootic; 1 = straddling the suture between the prootic and pterosphenoid; 2 = straddling the suture between the sphenotic and pterosphenoid; 3 = foramina separate from each other, one straddling the suture between the prootic, sphenotic and the pterosphenoid (dorsally) and one straddling the suture between the prootic, pterosphenoid and parasphenoid (ventrally)

(18) Suture between the parasphenoid and sphenotic

0 = absent; 1 = present

(19) Foramen for cranial nerve VI

0 = opens within the prootic bridge; 1 = opens anterior to the prootic bridge

(20) Supraorbital bone

0 = present; 1 = absent

(21) Otic and supraorbital sensory canal

0 = in bony canals; 1 = partially or completely in grooves

(22) Number of bones in the infraorbital series, not including the dermosphenotic or the antorbital if present

0 = five; 1 = four

(23) First infraorbital

0 = does not contribute or only partially contributes to the anterior margin of the orbit; 1 = is the only bone that contributes to the anterior margin of the orbit

(24) Condition of the infraorbital sensory canal in at least some infraorbitals

0 = enclosed in a bony canal; 1 = open in a gutter

(25) Palatoquadrate area behind and below the orbit

0 = not completely covered by the infraorbitals; 1 = completely covered by infraorbitals

(26) Dermosphenotic

0 = flattened, plate-like; 1 = triradiate; 2 = tubular

(27) Posterior extent of the fossa on the neurocranium for the hyomandibula

0 = formed of pterotic; 1 = formed of pterotic and intercalar; 2 = formed of pterotic and exoccipital; 3 = formed of exoccipital and intercalary

(28) Neurocranial heads of the hyomandibula

0 = one head or two heads but continuous; 1 = two heads, separate; 2 = two heads, bridged

(29) Anterior process (wing) of the hyomandibula that contacts the entopterygoid

0 = absent; 1 = present

(30) Bones of palatoquadrate

0 = two lateral elements; 1 = one lateral element; 2 = one element, laterally and medially

(31) Autopalatine bone

0 = present; 1 = absent

(32) Preopercular sensory canal

0 = opens by pores the entire length of the canal; 1 = opens by pores ventrally and by a groove dorsally; 2 = opens by pores dorsally and a groove ventrally; 3 = opens by a groove the entire length of the canal

(33) Opercle depth to width ratio

0 = less than two; 1 = about two or greater than two

(34) Posterodorsal spine on the opercle

0 = absent; 1 = present

(35) Subopercle bone

0 = large and ventral to the opercle; 1 = small and anterior to the opercle; 2 = absent

(36) Gular bone

0 = present; 1 = absent

(37) Ascending process of the premaxilla

0 = well developed; 1 = only slightly developed if at all

(38) Premaxillae

0 = paired; 1 = median

(39) Posterior portion of maxilla

0 = lies on angular; 1 = lies on dentary

(40) Supramaxillae

0 = present; 1 = absent

(41) Mandibular canal

0 = enclosed in a bony tube; 1 = open in a groove

(42) Posterior bones of the lower jaw

0 = angular and retroarticular bones fused; 1 = angular and articular bones fused; 2 = all separate; 3 = all fused

(43) Retroarticular bone

0 = included in the articulation with the quadrate; 1 = excluded from the articulation with the quadrate

(44) Medial wall of the Meckelian fossa of the lower jaw

0 = present; 1 = absent

(45) Bony elements associated with the second ventral gill arch

0 = absent; 1 = present as autogenous elements; 2 = present as a bony process on the second hypobranchial

(46) Toothplates associated with basibranchial 4

0 = present; 1 = absent

(47) Basihyal toothplate

0 = present; 1 = absent

(48) Basihyal toothplate

0 = flat; 1 = with ventrally directed processes

(49) Basibranchial toothplate and basihyal toothplate

0 = separate; 1 = continuous

(50) Basihyal

0 = present and ossified; 1 = present and cartilaginous; 2 = absent

(51) Hypohyals

0 = two ossified pairs present; 1 = one ossified pair present; 2 = one ossified pair present but greatly reduced in size

(52) Infrapharyngobranchial 3

0 = undivided; 1 = divided into two elements

(53) Infrapharyngobranchial 1

0 = present; 1 = absent

(54) Orientation of infrapharyngobranchial 1

0 = proximal tip anteriorly directed; 1 = proximal tip posteriorly directed

(55) Abdominal scutes

0 = absent; 1 = present as paired structures

(56) Epipleural bones

0 = absent; 1 = only a few bones in anterior caudal region; 2 = present throughout abdominal and caudal region

(57) Dorsal arm of the post-temporal bone

0 = less than 1.5 times as long as the ventral arm; 1 = more than twice as long as the ventral arm

(58) Lateral line that pierces the supracleithrum

0 = present; 1 = absent

(59) Cleithrum

0 = with no or only a slight medial lamina; 1= with a broad medial lamina

(60) Coracoid fenestra

0 = absent; 1 = present

(61) First pectoral fin ray

0 = normal; 1 = greatly expanded

(62) Post-pelvic bone

0 = absent; 1 = present

(63) Pelvic bone

0 = slender; 1 = possesses a thin deep lamella in dorsoventral plane

(64) Posterior end of anal fin

0 = separate from caudal fin; 1 = continuous with caudal fin

(65) Number of principal caudal fin rays

0 = 19 or more; 1 = 18; 2 = 17 or fewer

(66) Uroneurals

0 = three or more; 1 = two or one; 2 = absent

(67) Neural spine on ural centrum 1

0 = absent or rudimentary; 1 = one or more

(68) Epurals

0 = two or three; 1 = one; 2 = absent

(69) Neural spine on the first preural centrum

0 = complete; 1 = rudimentary; 2 = absent

(70) Number of neural spines on the second preural centrum

0 = one; 1 = two

(71) Number of hypurals

0 = seven; 1 = six or fewer

(72) Scales

0 = no reticulate furrows; 1 = both radial and reticulate furrows present; 2 = reticulate furrows only present over entire scale

(73) Pelvic fin ray number

0 = more than seven; 1 = seven; 2 = six or fewer

(74) Swimbladder-ear direct connection

0 = absent; 1 = present

(75) Intestine

0 = coils to right of esophagus and stomach; 1 = coils to left of esophagus and stomach

(76) Opercle shape dorsal to facet for articulation with hyomandibula

0 = rounded; 1 = flattened or truncated; 2 = flattened with posterior recurved process

(77) Upper hypurals and second ural

0 = not fused; 1 = fused

(78) Second infraorbital shape and size

0 = more or less slender or tubular and small in size; 1 = triangular or rectangular and smaller than third infraorbital; 2 = expanded and equivalent in size to or larger than third infraorbital

(79) Dorsal fin shape

0 = base moderately long, fin triangular or falcate; 1 = base very short, much shorter than fin height, or fin absent; 2 = base moderately long to very long, fin with rounded outline anteriorly and posteriorly

(80) Posterior rays of dorsal and anal fin

0 = shorter than anterior ones; 1 = longer than or as long as anterior ones

(81) 'Cheek wall' formed by enlargement of first to third infraorbitals

0 = absent; 1 = present

(82) Ventral part of preopercle

0 = extending anteriorly to beneath orbit or to level of posterior edge of orbit; 1 = anteriorly does not reach level of orbit

(83) Posterior edge of nasal when it is gutter-like or irregularly subrectangular

0 = straight or slightly curved; 1 = strongly curved and extending backward

(84) Angle of jaws

0 = anterior to middle vertical line of orbit; 1 = between middle vertical line and posterior edge of orbit; 2 = behind orbit

(85) Utriculus

0 = connected with sacculus and lagena; 1 = completely separated from sacculus and lagena

(86) Anal fin sexual dimorphism

0 = absent; 1 = present

(87) Ventral margin of opercle

0 = rounded or pointed and narrower than mid-point of opercle; 1 = curved but not greatly narrowed compared to midpoint of opercle; 2 = flattened or only very slightly rounded

(88) Parapophysis on the first centrum

0 = not expanded or hypertrophied; 1 = expanded and rounded, barely reaching below the occiput and not touching the parasphenoid; 2 = greatly hypertrophied and extending anteriorly to touch the parasphenoid, wedge-shaped in lateral view

(89) Dorso-occipital fossa

0 = absent; 1 = present

(90) Contact between dermosphenotic and anteriormost bone of the infraorbital series

0 = absent; 1 = present

(91) Depth of dorsal posterior infraorbital compared to ventral posterior infraorbital

0 = shallower; 1 = equal; 2 = deeper

(92) Scleral ossicles

0 = absent; 1 = present

(93) Postero-dorsal flange of the angular

0 = absent; 1 = present

(94) Posterior process of the hyomandibula

0 = short (less than half the length of the dorsal articulating surface of the hyomandibula); 1 = long (more than half the length of the dorsal articulating surface of the hyomandibula); 2 = absent or extremely reduced

(95) Endopterygoid dentition

0 = patch of shagreen-like fine teeth or small conical teeth; 1 = few rows of large conical teeth; 2 = one or more medio-dorsal rows of large conical teeth, bordered laterally by a patch of shagreen-like fine teeth; 3 = teeth absent or extremely reduced

(96) Number of branchiostegal rays

0 = 8 or less; 1 = between 9 and 13; 2 = 14 or more

Morphological matrix

Amia

0?10123110100000001?10010000000000000010021100???2100000000000000210000000001020012102000(0 1)01001

Ellimmichthyiformes

3?000100111011100000?????0000?0100110000 1????????1??011000000000100101012??00?00?0?0?00?00?100(0 2 3)(0 1)

Dorosoma

2000010001101010000000000000000000001101001111112??10001110100000001001010112?0000000?1?00000110030

Elops

1000000100100000000000000010000000100000000000000000200000000000010000000?00011?2?00000010002

Lycoptera

??00110200000????????000000?0?0?0000000000??1??000????0000??0?0010(0 1)100002??0010000?0?02?00?00001

Paralycoptera 0000(0 1)2321000???????1010010?00??2100100000111??????1???000??01?00201200101???00000001??1?00200101

Sinoglossus

??00?2????10???????1?11??0?????000??0?110??????????????0????????2????0??2??0?1211000??1??010????

Eohiodon

200011120010??00???1010001?200?00101100100 01??010?0???0010000?001001(0

1)0001??2010000?0?12?002?01?(0 1)

Hiodon 2000111200(0

1)000000001010001120010010110010001000100000000100001001001(0 1)(0

1)00111201000 0?001200001010(0 1)

'Joffrichthys_symmetropterus'??100132?1100??0???10110001 0????100?1001021???

????????000?000?001?1200?02??0?10010?1??000?100??0

'Joffrichthys_tanyourus'

20100132?0100??0???10?00001001?2100?1001021???????????000?000?00101200002??00?

0010?1??0?0?0000?0

Lopadichthys

10100002?010???????10?000001????00??100?011???????????000?0?0??01102001 02??001

0010?0??0?00?000?1

Chauliopareion

2010003?1100???????10100000???2101?10110?1???????????0010?110102????0102??0?1

?00000?11??010000(0 1)

Shuleichthys 3010010200100??0?0?11???0?100??(0

1)0001?0?10210??00?01???001??0010010(0 1)100001??00?0000?1??2?0??00001

Wilsonichthys

2?100?00001????????11?0??0??0??0100?10110?????00??????0010??0?00110111001??00??

??0?0?????0?0???0

Xixiaichthys

0?100132??000??????1?1000??00??0102100010 2????0???0???001?0?0?00001200001??001000002??1?0??000?1

Heterotis

22201230111010100001011010011100001110110200211??111000101010000211200122010112110000 2?00201010

Arapaima

32001232111010101011011010011110001100110200201??211000001100000211200122011112111000 01201201101

Phareodus

?2210133101 0?100???10100100 11?02101100010210??001????000??11?002?1?00122??00121011 2?01210201121

Pantodon

22101132101011101001100010000110102101010100200011101?00100110102112001120101110011 2012010000000011

Singida

22101030100 0???????10100100 0???2102???010?1???????????0000?1101021120010 2??001000102?00100100?31

Scleropages 32100233111110000101010010001 1(01)2101110010110210011100000010110102112001220101021011200010110102 2

Osteoglossum

32100233111110000101010010001112101110010110210011100000010110102112001220101021011200 0101000021

Petrocephalus

1000002210100011211111010220021000011111113?021000210010?011000011020011???
??20????????000200230

Gnathonemus

1000102210101011311111010220021000011111113?1211??2200100?011000011020011??1?
??0????????000100230

Campylomormyrus

1000002210101011211111010220021000011111113?1211??2200100?011000011020011????
?20????????000100230

Chitala

1120022101100100101111010030011200210001111011010110 1?10010100012212001 0??1
1?21??1????0000100000

Xenomystus

1110022201100100101111010230011200210001111011010110 1?10010100012212001 0??1
1?21??0????0000200030

Papyrocranus

1110022201101100101111010230011200210001111011010110 0010010100?122120(0
1)10??11?21??0????0000100100

Palaeonotopterus

1000???200100?00110?1?????000????????????????????????????????1????????????????????
?????00??0????

Macroprosopon

?211?????11????????1?10010?1???????1?0010200????????????1???1??????????0???1?0??01?2???210211?2

Furichthys

??????3????????0??????????0?11??2000?10??021???????????0??1?11??????????0???0?????1????2??0???1??

Brychaetus

??2101301??0100000010100101111???10?1100?0???21????????0??????????????????????0????0111??0210(1 2)11102

Laeliichthys

?1100232?1100??????1110110?00??2002100011111???0???????000101100011120010 2??1?20000????0?00000?01

SUPPORTING INFORMATION

Character Definitions and Morphological Matrix

Character definitions

This character list is a modification of the Murray *et al*. (2018) character list, with the addition of characters 89–96 and changes to preexisting characters detailed in the main text.

(1) Temporal fossa

0 = absent; 1 = present, with the exoccipital making a contribution to the border; 2 = present, bordered by epioccipital, pterotic and parietal; 3 = present, bordered by epioccipital and pterotic

(2) Shape of extrascapular

0 = expanded; 1 = reduced and irregularly shaped; 2 = reduced and tubular

(3) Shape of frontal bones

0 = anterior margin narrower than posterior margin; 1 = anterior margin about equal in width to posterior margin; 2 = anterior margin wider than posterior margin

(4) Supraorbital shelf of frontal bone

0 = absent; 1 = present

(5) Length of frontal bone

0 = over twice as long as parietal; 1 = less than twice as long as parietal

(6) Relationship of nasal bones

0 = some part separated by anterior portion of frontals; 1 = separated only by ethmoid bones; 2 = meet each other in midline

(7) Nasal bones

0 = tubular but not curved; 1 = tubular and strongly curved; 2 = gutter-like; 3 = flat and broad

(8) Parasphenoid teeth

0 = absent; 1 = small; 2 = large and found along the length of the parasphenoid; 3 = large and restricted to the basal portion of the parasphenoid

(9) Basipterygoid process

0 = absent; 1 = present

(10) Supratemporal commissure passing through the parietals

0 = absent; 1 = present

(11) Supraorbital sensory canal

0 = ending in parietal; 1 = ending in frontal

(12) Orbitosphenoid

0 = present; 1 = absent

(13) Basisphenoid

0 = present; 1 = absent

(14) Basioccipital process of the parasphenoid

0 = divided; 1 = median

(15) Ventral occipital groove

0 = present; 1 = absent

(16) Intercalar

0 = present; 1 = absent

(17) Foramen/foramina for anteroventral lateral line nerve plus cranial nerve V

0 = in the prootic; 1 = straddling the suture between the prootic and pterosphenoid; 2 = straddling the suture between the sphenotic and pterosphenoid; 3 = foramina separate from each other, one straddling the suture between the prootic, sphenotic and the pterosphenoid (dorsally) and one straddling the suture between the prootic, pterosphenoid and parasphenoid (ventrally)

(18) Suture between the parasphenoid and sphenotic

0 = absent; 1 = present

(19) Foramen for cranial nerve VI

0 = opens within the prootic bridge; 1 = opens anterior to the prootic bridge

(20) Supraorbital bone

0 = present; 1 = absent

(21) Otic and supraorbital sensory canal

0 = in bony canals; 1 = partially or completely in grooves

(22) Number of bones in the infraorbital series, not including the dermosphenotic or the antorbital if present

0 = five; 1 = four

(23) First infraorbital

0 = does not contribute or only partially contributes to the anterior margin of the orbit; 1 = is the only bone that contributes to the anterior margin of the orbit

(24) Condition of the infraorbital sensory canal in at least some infraorbitals

0 = enclosed in a bony canal; 1 = open in a gutter

(25) Palatoquadrate area behind and below the orbit

0 = not completely covered by the infraorbitals; 1 = completely covered by infraorbitals

(26) Dermosphenotic

0 = flattened, plate-like; 1 = triradiate; 2 = tubular

(27) Posterior extent of the fossa on the neurocranium for the hyomandibula

0 = formed of pterotic; 1 = formed of pterotic and intercalar; 2 = formed of pterotic and exoccipital; 3 = formed of exoccipital and intercalary

(28) Neurocranial heads of the hyomandibula

0 = one head or two heads but continuous; 1 = two heads, separate; 2 = two heads, bridged

(29) Anterior process (wing) of the hyomandibula that contacts the entopterygoid

0 = absent; 1 = present

(30) Bones of palatoquadrate

0 = two lateral elements; 1 = one lateral element; 2 = one element, laterally and medially

(31) Autopalatine bone

0 = present; 1 = absent

(32) Preopercular sensory canal

0 = opens by pores the entire length of the canal; 1 = opens by pores ventrally and by a groove dorsally; 2 = opens by pores dorsally and a groove ventrally; 3 = opens by a groove the entire length of the canal

(33) Opercle depth to width ratio

0 = less than two; 1 = about two or greater than two

(34) Posterodorsal spine on the opercle

0 = absent; 1 = present

(35) Subopercle bone

0 = large and ventral to the opercle; 1 = small and anterior to the opercle; 2 = absent

(36) Gular bone

0 = present; 1 = absent

(37) Ascending process of the premaxilla

0 = well developed; 1 = only slightly developed if at all

(38) Premaxillae

0 = paired; 1 = median

(39) Posterior portion of maxilla

0 = lies on angular; 1 = lies on dentary

(40) Supramaxillae

0 = present; 1 = absent

(41) Mandibular canal

0 = enclosed in a bony tube; 1 = open in a groove

(42) Posterior bones of the lower jaw

0 = angular and retroarticular bones fused; 1 = angular and articular bones fused; 2 = all separate; 3 = all fused

(43) Retroarticular bone

0 = included in the articulation with the quadrate; 1 = excluded from the articulation with the quadrate

(44) Medial wall of the Meckelian fossa of the lower jaw

0 = present; 1 = absent

(45) Bony elements associated with the second ventral gill arch

0 = absent; 1 = present as autogenous elements; 2 = present as a bony process on the second hypobranchial

(46) Toothplates associated with basibranchial 4

0 = present; 1 = absent

(47) Basihyal toothplate

0 = present; 1 = absent

(48) Basihyal toothplate

0 = flat; 1 = with ventrally directed processes

(49) Basibranchial toothplate and basihyal toothplate

0 = separate; 1 = continuous

(50) Basihyal

0 = present and ossified; 1 = present and cartilaginous; 2 = absent

(51) Hypohyals

0 = two ossified pairs present; 1 = one ossified pair present; 2 = one ossified pair present but greatly reduced in size

(52) Infrapharyngobranchial 3

0 = undivided; 1 = divided into two elements

(53) Infrapharyngobranchial 1

0 = present; 1 = absent

(54) Orientation of infrapharyngobranchial 1

0 = proximal tip anteriorly directed; 1 = proximal tip posteriorly directed

(55) Abdominal scutes

0 = absent; 1 = present as paired structures

(56) Epipleural bones

0 = absent; 1 = only a few bones in anterior caudal region; 2 = present throughout abdominal and caudal region

(57) Dorsal arm of the post-temporal bone

0 = less than 1.5 times as long as the ventral arm; 1 = more than twice as long as the ventral arm

(58) Lateral line that pierces the supracleithrum

0 = present; 1 = absent

(59) Cleithrum

0 = with no or only a slight medial lamina; 1= with a broad medial lamina

(60) Coracoid fenestra

0 = absent; 1 = present

(61) First pectoral fin ray

0 = normal; 1 = greatly expanded

(62) Post-pelvic bone

0 = absent; 1 = present

(63) Pelvic bone

0 = slender; 1 = possesses a thin deep lamella in dorsoventral plane

(64) Posterior end of anal fin

0 = separate from caudal fin; 1 = continuous with caudal fin

(65) Number of principal caudal fin rays

0 = 19 or more; 1 = 18; 2 = 17 or fewer

(66) Uroneurals

0 = three or more; 1 = two or one; 2 = absent

(67) Neural spine on ural centrum 1

0 = absent or rudimentary; 1 = one or more

(68) Epurals

0 = two or three; 1 = one; 2 = absent

(69) Neural spine on the first preural centrum

0 = complete; 1 = rudimentary; 2 = absent

(70) Number of neural spines on the second preural centrum

0 = one; 1 = two

(71) Number of hypurals

0 = seven; 1 = six or fewer

(72) Scales

0 = no reticulate furrows; 1 = both radial and reticulate furrows present; 2 = reticulate furrows only present over entire scale

(73) Pelvic fin ray number

0 = more than seven; 1 = seven; 2 = six or fewer

(74) Swimbladder-ear direct connection

0 = absent; 1 = present

(75) Intestine

0 = coils to right of esophagus and stomach; 1 = coils to left of esophagus and stomach

(76) Opercle shape dorsal to facet for articulation with hyomandibula

0 = rounded; 1 = flattened or truncated; 2 = flattened with posterior recurved process

(77) Upper hypurals and second ural

0 = not fused; 1 = fused

(78) Second infraorbital shape and size

0 = more or less slender or tubular and small in size; 1 = triangular or rectangular and smaller than third infraorbital; 2 = expanded and equivalent in size to or larger than third infraorbital

(79) Dorsal fin shape

0 = base moderately long, fin triangular or falcate; 1 = base very short, much shorter than fin height, or fin absent; 2 = base moderately long to very long, fin with rounded outline anteriorly and posteriorly

(80) Posterior rays of dorsal and anal fin

0 = shorter than anterior ones; 1 = longer than or as long as anterior ones

(81) 'Cheek wall' formed by enlargement of first to third infraorbitals

0 = absent; 1 = present

(82) Ventral part of preopercle

0 = extending anteriorly to beneath orbit or to level of posterior edge of orbit; 1 = anteriorly does not reach level of orbit

(83) Posterior edge of nasal when it is gutter-like or irregularly subrectangular

0 = straight or slightly curved; 1 = strongly curved and extending backward

(84) Angle of jaws

0 = anterior to middle vertical line of orbit; 1 = between middle vertical line and posterior edge of orbit; 2 = behind orbit

(85) Utriculus

0 = connected with sacculus and lagena; 1 = completely separated from sacculus and lagena

(86) Anal fin sexual dimorphism

0 = absent; 1 = present

(87) Ventral margin of opercle

0 = rounded or pointed and narrower than mid-point of opercle; 1 = curved but not greatly narrowed compared to midpoint of opercle; 2 = flattened or only very slightly rounded

(88) Parapophysis on the first centrum

0 = not expanded or hypertrophied; 1 = expanded and rounded, barely reaching below the occiput and not touching the parasphenoid; 2 = greatly hypertrophied and extending anteriorly to touch the parasphenoid, wedge-shaped in lateral view

(89) Dorso-occipital fossa

0 = absent; 1 = present

(90) Contact between dermosphenotic and anteriormost bone of the infraorbital series

0 = absent; 1 = present

(91) Depth of dorsal posterior infraorbital compared to ventral posterior infraorbital

0 = shallower; 1 = equal; 2 = deeper

(92) Scleral ossicles

0 = absent; 1 = present

(93) Postero-dorsal flange of the angular

0 = absent; 1 = present

(94) Posterior process of the hyomandibula

0 = short (less than half the length of the dorsal articulating surface of the hyomandibula); 1 = long (more than half the length of the dorsal articulating surface of the hyomandibula); 2 = absent or extremely reduced

(95) Endopterygoid dentition

0 = patch of shagreen-like fine teeth or small conical teeth; 1 = few rows of large conical teeth; 2 = one or more medio-dorsal rows of large conical teeth, bordered laterally by a patch of shagreen-like fine teeth; 3 = teeth absent or extremely reduced

(96) Number of branchiostegal rays

0 = 8 or less; 1 = between 9 and 13; 2 = 14 or more

Morphological matrix

Amia

0?10123110100000001?10010000000000000010021100???2100000000000000210000000001020012102000(0 1)01001

Ellimmichthyiformes

3?000100111011100000?????0000?0100110000 1????????1??011000000000100101012??00?00?0?0?00?00?100(0 2 3)(0 1)

Dorosoma

2000010001101010000000000000000000001101001111112??10001110100000001001010112?0000000?1?00000110030

Elops

1000000100100000000000000001000000001000000000000000000020000000000001000000?00011?2?00000010002

Lycoptera

??00110200000????????000000?0?0?0000000000??1??000????0000??0?0010(0 1)100002??0010000?0?02?00?00001

Paralycoptera 0000(0 1)2321000???????1010010?00??2100100000111??????1???000??01?00201200101???000000012??1?00200101

Sinoglossus

??00?2????10???????1?11??0?????000??0?110??????????????0????????2????0??2??0?1211000??1??010????

Eohiodon

2000111200l0??00???1010001?200?00101100l0001??010?0???0010000?001001(0

1)0001??2010000?0?12?002?01?(0 1)

Hiodon 2000111200(0

1)000000001010001120010010110010001000100000000100001001001(0 1)(0

1)00111201000?001200001010(0 1)

'Joffrichthys_symmetropterus'??100132?1100??0???10110001?????100?1001021???

????????000?000?001?1200?02??0?10010?1??000?100??0

'Joffrichthys_tanyourus'

20100132?0100??0???10?00001001?2100?1001021???????????000?000?00101200002??00?

0010?1??0?0?0000?0

Lopadichthys

10100002?010???????10?000001????00??100?011???????????000?0?0??01102001O2??001

0010?0??0?00?000?1

Chauliopareion

2010003?1100???????10100000???2101?10110?1???????????0010?110102????0102??0?1

?00000?11??010000(0 1)

Shuleichthys 30100102001O0??0?0?11???0?100??(0

1)0001?0?10210??00?01???001??0010010(0 1)100001??00?0000?1??2?0??00001

Wilsonichthys

2?100?00001????????11?0??0??0??0100?10110?????00??????0010??0?00110111001??00??

??0?0?????0?0???0

Xixiaichthys

0?100132??000??????1?1000??00??0102100010 2????0???0???001?0?0?00001200001??001000002??1?0??000?1

Heterotis

22201230111010100001011010011100001110110200211??111000101010000211200122010112110000 2?00201010

Arapaima

32001232111010101011011010011110001100110200201??211000001100000211200122011111211100 0012012011 01

Phareodus

?22101331010?100???10100100 11?02101100010210??001?????000??11?002?1?00122??00121011 2?01210201121

Pantodon

22101132101011101001100010000110102101010100200011101?00100110102112001120101110011 2010000000011

Singida

22101030100???????10100100 0???2102???010?1???????????0000?11010211200102??001000102?00100100?31

Scleropages 32100233111110000101010010001 1(01)2101110010110210011100000010110102112001220101021011200010110102 2

Osteoglossum

32100233111110000101010010001 1121011100101102100111000000101101021120012201010210112000101000021

Petrocephalus

1000002210100011211111010220021000011111113?021000210010?01100001102001 1???

??20????????000200230

Gnathonemus

1000102210101011311111010220021000011111113?1211??2200100?01100001102001 1??1?

??0????????000100230

Campylomormyrus

1000002210101011211111010220021000011111113?1211??2200100?01100001102001 1????

?20????????000100230

Chitala

1120022101100100101111010030011200210001111011010110 1?10010100012212001 0??1

1?21??1????0000100000

Xenomystus

1110022201100100101111010230011200210001111011010110 1?10010100012212001 0??1

1?21??0????0000200030

Papyrocranus

1110022201101100101111010230011200210001111011010110 00100100101 00?122120(0

1)10??11?21??0????0000100100

Palaeonotopterus

1000???200100?00110?1?????000????????????????????????????????1????????????????????

?????00??0????

Macroprosopon

?211?????11????????1?10010?1???????1?0010200????????????1???1??????????0???1?0??0

1?2???210211?2

Furichthys

??????3????????0??????????0?11??2000?10??021???????????0??1?11??????????0???0?????1

????2??0???1??

Brychaetus

??2101301??0100000010100101111???10?1100?0???21????????0??????????????????????0????

0111??0210(1 2)11102

Laeliichthys

?1100232?1100??????1110110?00??20021000111???0???????000101100011120010 2??1?

20000????0?00000?01

#NEXUS

[written Sat Dec 05 22:12:42 EST 2020 by Mesquite version 3.61 (build 927) at DESKTOP-3RRJP94/10.255.36.140]

BEGIN TAXA;

TITLE Taxa;

DIMENSIONS NTAX=34;

TAXLABELS

Amia Ellimmichthyiformes Dorosoma Elops Lycoptera Paralycoptera Sinoglossus Eohiodon Hiodon 'Joffrichthys_symmetropterus' 'Joffrichthys_tanyourus' Lopadichthys Chauliopareion Shuleichthys Wilsonichthys Xixiaichthys Heterotis Arapaima Phareodus Pantodon Singida Scleropages Osteoglossum Petrocephalus Gnathonemus Campylomormyrus Chitala Xenomystus Papyrocranus Palaeonotopterus Macroprosopon Furichthys Brychaetus Laeliichthys

;

END;

BEGIN CHARACTERS;

TITLE 'Matrix modified from file "Murrayetal2018_NewmatrixOsteogJune2017"';

DIMENSIONS NCHAR=96;

FORMAT DATATYPE = STANDARD RESPECTCASE GAP = - MISSING = ? SYMBOLS = " 0 1 2 3";

MATRIX

Amia
0?10123110100000001?10010000000000000010021100???2100000000000000210000000001020001?2102000(0 1)01001

Ellimmichthyiformes
3?000100111011100000?????0000?01001100001????????1??011000000000100101012??00?00?0?0?00?00?100(0 2 3)(0 1)

Dorosoma
2000010001101010000000000000000000011010011111??10001110100000001001010112?0000000?1?00000110030

Elops
10000001001000000000000000010000000010000000000000000002000000000000010000000?00011?2?00000010002

Lycoptera
??00110200000????????000000?0?0?0000000000??1??000?????0000??0?0010(01)100002??0010000?0?02?00?00001

Paralycoptera 0000(01)2321000???????1010010?00??2100100000111??????1???000??01?00201200101???00000001??1?00200101

Sinoglossus
??00?2????10????????1?11??0?????000??0?110?????????????????0????????2????0??2??0?1211000??1??010????

Eohiodon
20001112001O??00???1010001?200?00101100100001??010?0???0010000?001001(01)0001??2010000?0?12?002?01?(0 1)

Hiodon 2000111200(01)00000000101000112001001011001000100010000000010000100100 1)(01)00111201000?001200001010(0 1)

'Joffrichthys_symmetropterus'??100132?1100??0???10110001O????100?1001021???????????000?000?001?1200?02??0?10010?1??000?100??0

'Joffrichthys_tanyourus'
20100132?0100??0???10?00001001?2100?1001021???????????000?000?00101200002??00?0010?1??0?0?0000?0

Lopadichthys
10100002?010????????10?000001????00??100?011???????????000?0?0??01102001O2??0010010?0??0?00?000?1

Chauliopareion
2010003?1100????????101000000???2101?10110?1???????????0010?110102????0102??0?1?00000?11??010000(0 1)

Shuleichthys 30100102001O0??0?0?11???0?100??(01)0001?0?10210??00?01???001??0010010(0 1)100001??00?0000?1??2?0??00001

Wilsonichthys
2?100?00001????????11?0??0??0??0100?10110?????00??????0010??0?00110111001??00????0?0?????0?0???0

Xixiaichthys
0?100132??000??????1?1000??00??0102100010O2????0???0???001?0?0?00001200001??0010000O2??1?0??000?1

Heterotis
22201230111010100001011010011100001110110200211??11100010101000021120012201011211000002?00201010

Arapaima
32001232111010101011011010011110001100110200201??21100000110000021120012201111211100001201201101

Phareodus
?2210133101O?100???10100100 11?021011000102 10??001?????000??11?002?1?00122??001210112?01210201121

Pantodon
22101132101011101001100010000110102101010100200011101?00100110102112001120101110011201000000011

Singida
2210103010000???????10100100???2102???010?1???????????0000?11010211200102??0010001 02?00100100?31

Scleropages 32100233111110000101010010001 1(01)2101110010110210011100000010110102112001220101021011200010110102 2

Osteoglossum
32100233111110000101010010001112101110010110210011100000010110102112001220101021011200010000021

Petrocephalus
10000022101000112111110102200210000111111 3?0210002100100?011000011020011?????20???????000200230

Gnathonemus
10001022101010113111110102200210000111111 3?1211??2200100?011000011020011??1???0???????000100230

Campylomormyrus
10000022101010112111110102200210000111111 3?1211??2200100?011000011020011?????20???????000100230

Chitala
11200221011001001011110100300112002100011111011010110 1?10010100012212001 0??11?21??1????0000100000

Xenomystus
11100222011001001011110102300112002100011111011010110 1?10010100012212001 0??11?21??0????0000200030

Papyrocranus
111002220110110010111101023001120021000111101101011000100101001?122120(01)10??11?21??0????0000100100

Palaeonotopterus
1000???200100?00110?1?????000?????????????????????????????1?????????????????????????
????00??0????

Macroprosopon
?211?????11?????????1?10010?1???????1?0010200?????????????1???1??????????0???1?0??01?
2???210211?2

Furichthys
??????3????????0?????????0?11??2000?10??021???????????0??1?11??????????0???0?????1?
???2??0???1??

Brychaetus
??2101301??0100000010100101111???10?1100?0???21????????0?????????????????????0????01
11??0210(1 2)11102

Laeliichthys
?1100232?1100??????1110110?00??2002100011111???0???????000101100011120010 2??1?2000
0????0?00000?01

;

END;